# Activation of Stat3 Signaling in AgRP Neurons Promotes Locomotor Activity

Inaugural-Dissertation

zur

Erlangung des Doktorgrades

der Mathematisch-Naturwissenschaftlichen Fakultät

der Universität zu Köln

vorgelegt von

Andrea Mesaros

aus Bergisch Gladbach

Köln 2007

| | |
|---|---|
| Berichterstatter: | Prof. Dr. Jens Brüning |
| | Prof. Dr. Thomas Langer |
| Tag der mündlichen Prüfung: | 17.04.2008 |

# Figure Index

# Table Index

# Abbrevations

| | |
|---|---|
| A | alanine |
| ACTH | adrenocorticotrophin |
| AgRP | agouti-related peptide |
| Ala | alanine |
| am | ante meridiem |
| ARC | arcuate nucleus |
| Asn | asparagine |
| BAT | brown adipose tissue |
| BMI | body mass index |
| BrdU | 5-bromodeoxyuridine |
| °C | temperature in degree celsius |
| $CaCl_2$ | calcium chloride |
| cDNA | complementary DNA |
| CPu | caudate putamen (striatum) |
| Cre | site specific recombinase from phage P1 (causes recombination) |
| CRH | corticotropin-releasing hormone |
| d | deci |
| Da | Dalton |
| DAPI | 4',6-diamidino-2-phenylindole |
| DIG | digoxigenin |
| DMH | dorsomedial hypothalamic nucleus |
| DMSO | dimethylsulfoxide |
| DNA | deoxyribonucleic acid |
| DNase | deoxyribonuclease |
| dNTP | deoxyribonucleotide-triphosphate |
| *E. coli* | *Escherichia coli* |
| EDTA | ethylendiamine tetraacetate |
| ELISA | enzyme-linked immunosorbent assay |
| EMSA | electromobility-shift assay |
| Erk | extracellular signal-regulated kinase |

| | |
|---|---|
| EtOH | ethanol |
| FCS | fetal calf serum |
| floxed | loxP flanked |
| Flp | site-specific recombinase, product of yeast FLP1 gene |
| FrA | frontal association cortex |
| FRT | Flp recombination target |
| fT3 | free triiodothyronine |
| g | gram |
| GAPDH | glyceraldehyde 3-phosphate dehydrogenase |
| GFP | green fluorescent protein |
| h | hour |
| HCl | hydrochloric acid |
| HCRT | hypocretin |
| HE | hematoxylin/eosin |
| HEPES | 4-(2-hydroxyethyl)-1-piperazineethanesulfonic acid |
| HFD | high fat diet |
| $H_2O_2$ | hydrogen peroxide |
| HPRT | hypoxanthine guanine phosphoribosyl transferase |
| Ht | hypothalamus |
| ICV | intracerebroventricular |
| IRES | internal ribosome entry site |
| IRS | insulin receptor substate |
| Jak | Janus kinase |
| k | kilo |
| KCl | potassium chloride |
| l | liter |
| *LacZ* | gene encoding the enzyme β-galactosidase |
| LB | Luria-Bertani |
| LHA | lateral hypothalamic area |
| loxP | recognition sequence for Cre (locus of x-ing over phage P1) |
| m | meter |
| m | milli |
| M | molar |

| | |
|---|---|
| MCH | melanin-concentrating hormone |
| MCR | melanocortin receptor |
| ME | median eminence |
| $MgCl_2$ | magnesium chloride |
| min | minute |
| MOPS | 3-(N-morpholino)propanesulfonic acid |
| mRNA | messenger RNA |
| MSH | melanocyte-stimulating hormone |
| n | nano |
| N | asparagine |
| N | Normal |
| NaCl | sodium chloride |
| $NaH_2PO_4$ | monosodium phosphate |
| $Na_2HPO_4$ | disodium hydrogen phosphate |
| NCD | normal chow diet |
| $Neo^R$ | neomycine resistance gene |
| NIH | National Institutes of Health |
| NP-40 | Nondiet P-40 |
| NPY | neuropeptide Y |
| ObRb | long isoform of the leptin receptor |
| OD | optical density |
| p | pico |
| PAGE | polyacrylamid gel electrophoresis |
| PBS | phosphate buffered saline |
| PCR | polymerase chain reaction |
| $\alpha$-$^{32}$P-CTP | $^{32}$P-labeled cytidine triphosphate |
| PFA | paraformaldehyde |
| pGK-hyg | hygromycin resistance gene driven by the phosphoglycerate kinase promoter |
| PI3K | phosphatidylinositol-3 kinase |
| pm | post meridiem |
| POMC | proopiomelanocortin |
| PVN | paraventricular nucleus |
| RNA | ribonucleic acid |

| | |
|---|---|
| RNase | ribonuclease |
| SA | splice acceptor |
| SDS | sodiumdodecylsulfate |
| sec | second |
| SEM | standard error of the mean |
| SH | Src homology |
| Shp2 | tyrosine phosphatase 2 |
| Socs | suppressor of cytokine signaling |
| SSC | sodium chloride/sodium acetate buffer |
| Stat | signal transducer and activator of transcription |
| Stat3-C | constitutively active form of Stat3 |
| TAE | Tris-acetate-EDTA |
| TBS | Tris buffered saline |
| TE | Tris-EDTA |
| Thr | threonine |
| TRH | thyrotropin-releasing hormone |
| Tris | trishydroxymethylaminomethan |
| tRNA | transfer RNA |
| Tyr | tyrosine |
| U | unit |
| UCP | uncoupling protein |
| UV | ultraviolet |
| VMH | ventromedial nucleus of the hypothalamus |
| $VO_2$ | volume of consumed oxygen |
| VTA | ventral tegmental area |
| v/v | volume per volume |
| WAT | white adipose tissue |
| WHO | World Health Organisation |
| w/v | weight per volume |
| µ | micro |
| 3’ | three prime end of DNA sequences |
| 5’ | five prime end of DNA sequences |

# 1 Introduction

## 1.1 Obesity

Obesity is a steadily growing health problem in industrialized societies (Figure 1) representing a major risk factor for numerous diseases, including diabetes mellitus type 2, cardiovascular diseases, sleep apnea, hypertension, stroke and certain forms of cancers (Bray, 2004; Haslam and James, 2005; Hill and Peters, 1998). According to the World Health Organization (WHO), the worldwide number of obese adults doubled in the last ten years to more than 400 million. In addition to the high number of obese people, currently more than one billion adults are overweight. Furthermore, the prevalence of obesity and overweight is predicted to rise dramatically within the next years. Projections of the WHO predict more than 700 million obese adults by 2015. However, obesity is not exclusively a problem concerning adults, as also childhood obesity rises rapidly with more than 20 million overweight children under five years of age worldwide (WHO).

The presence of overweight and obesity is commonly assessed by the body mass index (BMI), which is defined by the ratio of body weight to height (body weight/height$^2$) (Mei et al., 2002). While overweight is defined by a BMI of 25 to 29.9 kg/m$^2$, obesity is defined by a BMI of 30 kg/m$^2$ or greater (WHO). Approximately 20 % of all german adults and even 30 % of all adults in the USA exhibit a BMI of greater than 30 kg/m² (Telefonischer Gesundheitssurvey 2003 (GSTel03), Centers for Disease Control and Prevention) (Seidell, 1997). The likelihood of developing diseases like diabetes mellitus type 2 rises with increasing BMI. Consequently, not only the incidence of obesity but also the incidence of obesity associated diseases rises rapidly. Thus, the number of people suffering from diabetes mellitus type 2 is predicted to double by 2030 to at least 360 million (WHO). Even mortality is increased in obesity, with a BMI of over 32 associated with a doubled risk of death (Manson et al., 1995). However, there is evidence that the risk of chronic diseases already increases progressively from a BMI of 21 (WHO). As a consequence of the high prevalence of obesity, at least 6 % of total health care costs are associated with overweight and obesity in several industrialized countries. However, these calculations do not include all obesity-related issues (WHO).

Various genetic conditions that feature obesity, such as Prader-Willi syndrome and leptin and melanocortin receptor mutations have been identified. However, the known single gene mutations have been found in only 5 % of all obese individuals. Therefore, these mutations described in patients with severe obesity cannot explain the epidemic increase of overweight and obesity, but make it possible to relate clinical to experimental findings (Barsh et al., 2000). The huge increase in the prevalence of obesity is rather based on behavioural and environmental changes resulting from technological advances, which are in part amplified by genetic predisposition. Most likely, the combination of an excessive and energy-dense nutrient intake combined with reduced physical activity causes the rapid acceleration of obesity in industrialized societies in the last decades (Hill and Peters, 1998).

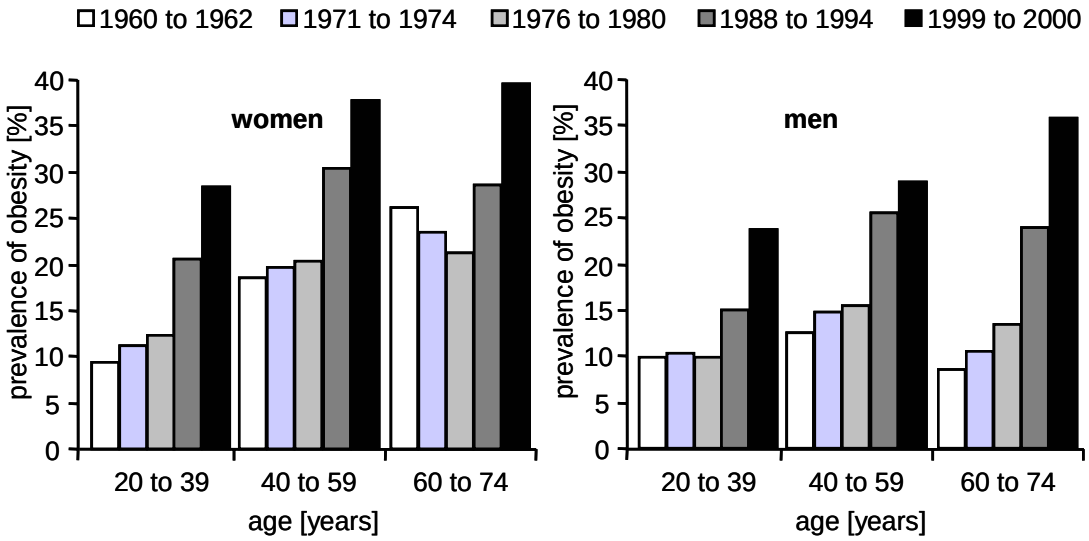


**Figure 1: Prevalence of obesity in the USA**

Trends in the age-specific prevalence of obesity of women (left panel) and man (right panel) in the USA between the years 1960 and 2000 (Flegal et al., 2002).

## 1.2 Energy homeostasis

Body weight is determined by the balance between energy intake and energy expenditure. An imbalance of energy intake over energy expenditure leads to a positive energy balance resulting in calories stored in form of fat. Obesity results from a long-

term positive energy balance. Therefore, the research on mechanisms regulating energy homeostasis, i.e. the balance between caloric intake and energy expenditure is imperative to understand the mechanisms of obesity.

Energy homeostasis is achieved by the integration of peripheral metabolic signals by neural circuits and is predominantly regulated by the central nervous system (for review, see (Schwartz and Porte, 2005)). The brain integrates signals from hormones and nutrients and adjusts feeding behaviour and substrate metabolism to regulate energy homeostasis (Figure 4). In times of sufficient fat stores and food availability, the brain receives signals that lead to the inhibition of food intake and endogenous glucose production and to the increase of energy expenditure and mobilization of fat stores. Conversely, signals on food deficiency and low energy stores result in responses that promote energy intake and hepatic glucose production and in contrast inhibit energy expenditure.

Two major hormones secreted from peripheral organs that are crucial for the regulation of energy homeostasis are the adipocyte-derived hormone leptin and the pancreatic β-cell hormone insulin. They regulate energy balance by directly acting on peripheral organs and by signaling the body's energy stores to the central nervous system.

## 1.3 Leptin

Adipose tissue was considered as an inert energy depot for a long time. Nowadays various functions of adipocytes are known, which are controlled by neuronal and hormonal mechanisms (Ailhaud, 2000; Kahn and Flier, 2000). Adipose tissue serves as an energy reservoir for the body. To expand its capacity, the number of cells can increase and individual adipocytes can alter their volumes up to 1000-fold to be filled with triacylglycerol (Fruhbeck et al., 2001). Leptin is a hormone predominantly secreted from white adipose tissue (from greek: leptos = thin) and at low levels produced in gastric epithelium, placenta and testis (Bado et al., 1998; Herrid et al., 2007; Masuzaki et al., 1997; Zhang et al., 1994). Leptin is the product of the *obese* (*ob*) gene and critically involved in energy homeostasis. The 16 kDa protein was discovered in 1994 by J. Friedman, who found that mutation of the *ob* gene resulted in profound

obesity and type 2 diabetes mellitus (Zhang et al., 1994). For the first time a hormone secreted from adipose tissue was identified that informs the brain about body energy stores. Leptin is secreted in proportion to adipocyte size and number and thus signals energy stores from the periphery to the central nervous system to suppress food intake and stimulate energy expenditure (Campfield et al., 1995; Halaas et al., 1995; Schwartz et al., 1996b; Walker et al., 2002). The importance of leptin in the regulation of energy homeostasis is reflected in *ob/ob* mice, which do not synthesize leptin and in *db/db* mice, which lack the leptin receptor. *Ob/ob* and *db/db* mice show a similar phenotype, both are characterized by hyperphagia and extreme obesity (Li et al., 1998; Licinio et al., 2004). Central and peripheral administration of leptin to *ob/ob* mice reverses the hyperphagia and obesity (Campfield et al., 1995; Pelleymounter et al., 1995). Similarly, chronic peripheral administration of leptin to wild type rodents results in reduced food intake, loss of body weight and fat mass (Halaas et al., 1995). Shortly after the discovery of leptin, the corresponding defects to *ob/ob* and *db/db* mice were also described in patients with forms of severe hyperphagia and obesity (Clement et al., 1998; Montague et al., 1997). As in rodents, also the obesity in humans caused by mutations resulting in the absence of leptin can be ameliorated with recombinant leptin therapy (Farooqi et al., 1999; Licinio et al., 2004).

In addition to the ability for long-term signaling as a reflection of body energy stores, leptin also responds to acute stimuli. Leptin expression decreases during fasting and is restored by refeeding. However, leptin secretion does not increase significantly after a meal and thereby does not by itself lead to the termination of a meal (Considine et al., 1996b; Maffei et al., 1995). Leptin secretion from adipocytes is stimulated by glucose, insulin and increased adipocyte glucose metabolism (Levy et al., 2000; Mizuno et al., 1996; Saladin et al., 1995; Walker et al., 2005). Conversely, the secretion of leptin is inhibited by some fatty acids (Cammisotto et al., 2003; Shintani et al., 2000) and an increased rate of lipolysis in adipocytes (Coppack et al., 1998; Donahoo et al., 1997). Circulating leptin is transported to the brain across the blood-brain barrier via a saturable process (Banks et al., 1996). The transport of leptin is regulated by acute stimuli. Starvation reduces and refeeding increases the transport of leptin across the blood-brain barrier (Kastin and Pan, 2000).

Besides its ability to regulate energy metabolism, leptin plays an important role in the regulation of growth and reproduction, reflected in *ob/ob* and *db/db* mice, which exhibit reduced body length and are infertile (Chehab et al., 1996). Equally, circulating

leptin levels are also correlated with fertility in humans (Mantzoros et al., 1997; Matkovic et al., 1997; Welt et al., 2004). Furthermore, leptin activates the thyroid axis and the sympathetic nervous system and suppresses the production of adrenal corticosteroids (Bornstein et al., 1997; Harris et al., 2001; Pralong et al., 1998; Rahmouni et al., 2002). Moreover, leptin regulates glucose homeostasis both directly and secondary to the regulation of body weight. The direct regulation is partly mediated via the central nervous system, and additionally, leptin also directly regulates pancreatic β-cells and insulin-sensitive tissues (Burcelin et al., 1999; Covey et al., 2006; Kulkarni et al., 1997; Liu et al., 1998) .

### 1.3.1 Mechanisms of leptin receptor signaling

Multiple leptin receptor isoforms are encoded by a single leptin receptor gene (*ObR*), each containing an identical ligand binding domain but differing by the presence or absence of a transmembrane domain or a complete cytosolic domain (Lee et al., 1996; Tartaglia et al., 1995). The function of the short splice variants which lack a complete cytosolic domain (LEPR-A, C, D, E and F) remains undistinct. The secreted isoforms (LEPR-E and proteolytic cleavage products of membrane-bound leptin receptor forms) of the leptin receptor contain only the extracellular leptin-binding domain and are thought to bind circulating leptin thus modulating its biological activity (Ge et al., 2002). LEPR-A is expressed ubiquitously and is the predominant form of the short isoforms (Lollmann et al., 1997). The long form of the leptin receptor LEPR-B is also expressed ubiquitously, but at much lower levels than LEPR-A, except for the hypothalamus, where the LEPR-B isoform represents the predominant form of the leptin receptor transcripts (Hoggard et al., 1997; Luoh et al., 1997). Of all isoforms, only LEPR-B (ObRb) contains the complete cytosolic domain required for modulation of the known intracellular signaling effectors of leptin action. ObRb is a member of the class I cytokine receptor family and functions as a dimer activating the Janus kinase/signal transducer and activator of transcription (Jak/Stat) signaling pathway (Kloek et al., 2002; Tartaglia et al., 1995). Binding of leptin to the long form of the receptor results in activation of constitutively associated Jak2 leading to the autophosphorylation of Jak2 on multiple tyrosine residues and phosphorylation of three tyrosine residues of the receptor, $Tyr_{985}$, $Tyr_{1077}$ and $Tyr_{1138}$ (Figure 2) (Banks et al.,

2000; Tartaglia, 1997; White et al., 1997). Importantly, ObRb is the only leptin receptor isoform that contains intracellular tyrosine residues. The phosphorylation of each of the three tyrosine residues of the receptor leads to activation of different downstream signaling pathways.

Phosphorylation of $Tyr_{985}$ results in binding and phosphorylation of the tyrosine phosphatase Shp2 and thereby in activation of the extracellular signal-regulated kinase (Erk) signaling pathway, which was suggested to play a role in energy balance and metabolism (Figure 2) (Bagnol et al., 1999; Bjorbaek et al., 2001; Zhang et al., 2004). The function of $Tyr_{1077}$ of the leptin receptor is controversial, but it was shown recently, that phosphorylation of $Tyr_{1077}$ recruits and activates the signal transducer and activator of transcription (Stat) 5, presumably contributing to the transcriptional response to leptin (Gong et al., 2007). Phosphorylation of $Tyr_{1138}$ creates a docking site for Stat3, which is activated by tyrosine-phosphorylation upon binding to the receptor (Banks et al., 2000; Vaisse et al., 1996). Phosphorylated Stat3 dimerizes and translocates from the cytoplasm to the nucleus to modulate transcription of multiple target genes via Stat-responsive elements (Lutticken et al., 1994; Stahl and Yancopoulos, 1994). One of the genes activated by Stat3 is the suppressor of cytokine signaling 3 (Socs3) (Endo et al., 1997; Naka et al., 1997; Starr et al., 1997). Expression of Socs3 is induced in hypothalamic regions important for the regulation of feeding by peripheral administration of leptin to *ob/ob* mice (Bjorbaek et al., 1998). Socs3 plays an important role in leptin signaling by inhibiting leptin signaling in a negative feedback loop by multiple mechanisms. Socs3 can bind directly to Jak2, leading to diminished phosphorylation of downstream molecules by Jak2 (Endo et al., 1997; Naka et al., 1997; Yasukawa et al., 1999) and to attenuated leptin-induced tyrosine phosphorylation of Jak2 (Bjorbaek et al., 1999). Moreover, Socs3 directly inhibits the leptin receptor itself by binding to $Tyr_{985}$ and consequently inhibiting the Stat3 signal (Bjorbak et al., 2000). However, binding of Socs3 to $Tyr_{985}$ does not diminish the activation of Erk (Dunn et al., 2005). Inhibition of Erk by Stat3 is rather mediated via inhibition of Jak2 (Dunn et al., 2005).

Additionally, binding of leptin to ObRb mediates tyrosine-phosphorylation of insulin receptor substrate (IRS) proteins and activation of the phosphatidylinositol-3 kinase (PI3K) directly by Jak2, independently of tyrosine phosphorylation sites of the receptor (Figure 2) (Banks et al., 2000; Niswender et al., 2001).

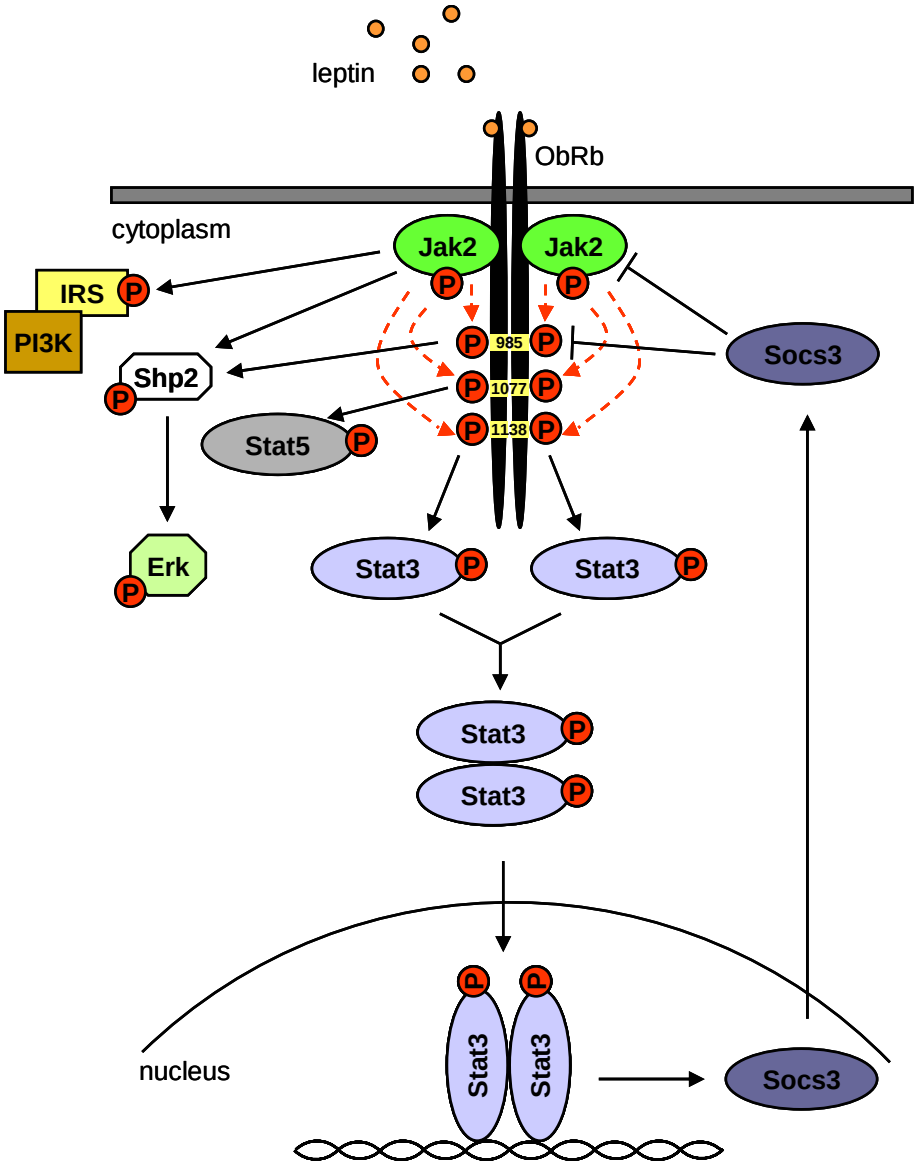


**Figure 2: Leptin receptor signaling**

Binding of leptin to the long form of the leptin receptor leads to activation of Jak2 and subsequently to Jak2-mediated phosphorylation of three different intracellular tyrosine residues of the receptor resulting in different downstream signaling pathways. Phosphorylated Jak2 directly activates the IRS/PI3K and the Shp2/Erk signaling pathway. Furthermore, Jak2-mediated $Tyr_{985}$ phosphorylation of the receptor contributes to the activation of the Shp2/Erk pathway. Phosphorylation of $Tyr_{1077}$ leads to activation of Stat5, whereas phosphorylation of $Tyr_{1138}$ mediates the phosphorylation and thereby activation of Stat3. Activated Stat3 dimerizes, translocates to the nucleus and activates target genes including Socs3, which in turn inhibits leptin signaling in a negative feedback loop by inhibiting Jak2 and the receptor via $Tyr_{985}$. ObRb: long form of the leptin receptor; Jak2: janus kinase 2; Stat3: signal transducer and activator of transcription 3; Socs3: suppressor of cytokine signaling 3; Shp2: protein tyrosine phosphatase 2; Erk: extracellular signal-regulated kinase; IRS: insulin receptor substrate; PI3K: phosphatidylinositol-3 kinase.

## 1.4 Insulin

The peptide-hormone insulin produced by the β-cells of the islets of Langerhans in the pancreas represents a major hormone in the control of energy homeostasis and glucose metabolism. Insulin was discovered in 1921 by Frederick Banting and Charles Best, who were awarded the Nobel Prize in Medicine for their discovery two years later. Insulin is synthesized as the inactive precursor proinsulin, which is then cleaved to insulin by different peptidases (Docherty and Hutton, 1983). Insulin is predominantly secreted upon rising levels of blood glucose and acts on peripheral tissues, particularly on muscle cells and adipocytes via translocation of the glucose transporter to remove the glucose from the blood and store it in form of glycogen (Birnbaum, 1992; Cushman and Wardzala, 1980; Poitout et al., 2006). In addition to glucose clearance from the blood, insulin increases glycolysis and inhibits gluconeogenesis (for review, see (Pilkis and Granner, 1992)). Insulin stimulates anabolic processes like triacylglycerol storage in adipocytes by augmenting adipocyte glucose uptake and by directly stimulating enzymes involved in fatty acid esterification (Cushman et al., 1984; Sul et al., 2000) and inhibits catabolic processes like glycogenolysis and lipolysis. In addition to the effect of insulin on peripheral tissues, it circulates in proportion to fat mass and crosses the blood-brain barrier to act on the central nervous system as an adiposity signal (Bagdade et al., 1967; Polonsky et al., 1988). Neuronal insulin receptor knockout mice demonstrate diet-sensitive obesity and insulin resistance (Bruning et al., 2000). Consistently, central administration of insulin results in reduction of body weight whereas insulin-deficient animals are hyperphagic (Sipols et al., 1995; Strubbe and Mein, 1977). In contrast, central administration of antibodies against insulin and diminished insulin receptor expression increase food intake (Obici et al., 2002a; Woods et al., 1979). Furthermore, the central nervous system is required for insulin's ability to suppress hepatic glucose production (Inoue et al., 2006; Konner et al., 2007).

### 1.4.1 Mechanisms of insulin receptor signaling

The heterotetrameric insulin receptor is ubiquitiously expressed and belongs to the family of ligand-activated receptor tyrosine kinases. Binding of insulin leads to autophosphorylation of the receptor on three intracellular tyrosine residues resulting in complete activation of the intrinsic tyrosine activity of the receptor. Receptor autophosphorylation results in recruitment and binding of intracellular proteins through their phosphotyrosine binding domains. Signaling molecules for the insulin receptor include the insulin receptor substrates (IRS) 1 to 4 which are phosphorylated by the receptor upon binding and thereby serve as a docking platform for other proteins, leading to activation of different downstream signaling pathways. Two major pathways activated by the IRS proteins are the Ras/Raf Mitogen activated protein (MAP) kinase and the PI3K pathway (Backer et al., 1992; Howe et al., 1992).

## 1.5 Central regulation of energy homeostasis

### 1.5.1 The hypothalamus

During the last decades, the research on the central regulation of energy homeostasis has focused on the hypothalamus. The hypothalamus is a part of the diencephalon located in the middle of the base of the brain below the thalamus. It synthesizes and secretes neurohormones and -peptides, many of them involved in the control of feeding and energy balance. The hypothalamus is also involved in the regulation of body temperature, circadian cycles, reproduction and the autonomic nervous system. Histological analysis of the hypothalamus revealed nuclei as clusters of neurons whithin the hypothalamus. Lesion and electrical stimulation studies of different hypothalamic nuclei suggested them to act as satiety or feeding centers. The major hypothalamic nuclei include the arcuate nucleus (ARC), the paraventricular nucleus (PVN), the ventromedial nucleus of the hypothalamus (VMH), the dorsomedial hypothalamic nucleus (DMH) and the lateral hypothalamic area (LHA), which is vaguely defined (Figure 3) (for review, see (Williams et al., 2000)).

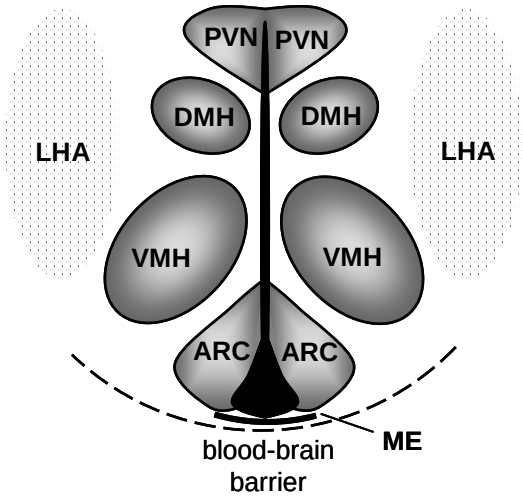


**Figure 3: Basic anatomy of the hypothalamus**

Schematic frontal section of the hypothalamus including main regions implicated in energy homeostasis. PVN, DMH, VMH and ARC surround the third ventricle (black). PVN: paraventricular nucleus; DMH: dorsomedial hypothalamic nucleus; VMH: ventromedial nucleus of the hypothalamus; ARC: arcuate nucleus; ME: median eminence; LHA: lateral hypothalamic area.

The ARC is located in the mediobasal hypothalamus adjacent to the base of the third ventricle and lies above the median eminence. The ARC/median eminence area has a modified blood-brain barrier that allows simplified signaling of circulating molecules, including insulin and leptin (Broadwell and Brightman, 1976; Faouzi et al., 2007). The PVN is located at the dorsal end of the third ventricle and represents the hypothalamic part where numerous neuronal pathways implied in the regulation of energy balance converge, including the major projections from the ARC. Lesions of the PVN and the VMH, which is located directly above the ARC, result in severe hyperphagia and obesity. The DMH is located dorsal of the VMH and was suggested to integrate information from the LHA and other medial hypothalamic nuclei. The LHA contains projections from and to the medial hypothalamus and brainstem structures. The LHA was described as a classical feeding centre, as lesions of the LHA result in hypophagia (Bernardis et al., 1992).

### 1.5.2 The arcuate nucleus of the hypothalamus

Recent research on energy homeostasis has focused on the ARC of the hypothalamus. The ARC senses and integrates signals received following changes in peripheral energy stores. The integrated signals regulate neuropeptides, which modulate feeding and energy expenditure. Two major neuronal populations situated in the ARC responsible for integrating energy signals from the periphery are the orexigenic agouti-related peptide (AgRP)/neuropeptide Y (NPY) producing neurons and the anorexigenic proopiomelanocortin (POMC) producing neurons. AgRP and NPY are orexigenic neuropeptides that stimulate feeding and reduce energy expenditure, while the anorexigenic neuropeptide POMC suppresses feeding and increases energy expenditure (Larhammar, 1996; McMinn et al., 2000; Rossi et al., 1998). Consistently, mutation of the human *AgRP* gene (Ala67Thr) is associated with inherited leanness (Marks et al., 2004), whereas mutations causing a deficiency in POMC or its receptor (melanocortin-3 and -4 receptor (MC3R and MC4R)) are the most common reasons of genetic obesity in humans (Farooqi and O'Rahilly, 2005b). The neurotransmitters AgRP and POMC are part of the melanocortin system which promotes negative energy balance. The melanocortin system is inhibited by AgRP and activated by melanocortins derived from POMC (for review, see (Wilson et al., 2006)).

POMC is a 241 amino acid precursor peptide of the melanocyte-stimulating hormones (MSHs) and adrenocorticotrophin (ACTH) as well as β-endorphin (Chretien et al., 1979). Apart from the ARC, POMC is expressed in the pituitary, the nucleus tractus solitarius of the brainstem and in several peripheral tissues (Harris, 1959; Joseph et al., 1983; Lacaze-Masmonteil et al., 1987). The energy status of the body is reflected by levels of POMC expression, as POMC mRNA is markedly reduced in fasted animals and restored after refeeding (Swart et al., 2002). In the hypothalamus, the most potent melanocortin α-MSH binds MC3R and MC4R, which are G-protein coupled receptors that activate the adenylate cyclase (Jegou et al., 2000; Mountjoy et al., 1994). Intracerebroventricular (ICV) injection of α-MSH reduces food intake and body weight and POMC deficiency is characterized by severe early onset obesity in mice (McMinn et al., 2000; Yaswen et al., 1999).

The orexigenic neurotransmitter AgRP consists of 132 amino acids. It is coexpressed with NPY in a distinct neuronal population of the ARC and functions as a MC3R/MC4R antagonist (Ollmann et al., 1997). Aside from the ARC the only

peripheral tissue with detectable AgRP expression is the adrenal gland (Ollmann et al., 1997). The expression of AgRP mRNA in the ARC is elevated upon fasting (Swart et al., 2002). Transgenic mice with ubiquitous overexpression of AgRP are obese (Ollmann et al., 1997) and ICV injection of AgRP increases food intake and is able to block the reduction of food intake resulting from ICV injection of α-MSH (Rossi et al., 1998). Reduction of hypothalamic AgRP mRNA results in increased metabolic rate and in reduction of body weight without affecting food intake (Makimura et al., 2002). While neonatal ablation of AgRP/NPY neurons has minimal effects on feeding, selective ablation of AgRP/NPY neurons in adult mice results in acute reduction of food intake (Gropp et al., 2005; Luquet et al., 2005).

The orexigenic neuropeptide NPY is a 36 amino acid peptide and one of the most abundant neurotransmitters (Minth et al., 1984). NPY binds to a family of seven-transmembrane-domain G-protein-coupled receptors, Y1 to Y6 to increase food intake and body weight gain and reduce energy expenditure (Larhammar, 1996). NPY is expressed at high levels in several central nervous system regions, however, the major site for NPY expression is the ARC of the hypothalamus (Morris, 1989). NPY is the most potent endogenous orexigenic signal. Like the expression of AgRP, also the expression of hypothalamic NPY mRNA and the release of NPY increase with fasting and decrease after refeeding, but the decrease after refeeding appears earlier than that of AgRP (Chua et al., 1991; Pages et al., 1993; Swart et al., 2002). Central administration of NPY causes obesity as a result of hyperphagia and decreased energy expenditure (Billington et al., 1991; Stanley et al., 1986). As described above, ablation of AgRP/NPY neurons in adult mice causes immediate starvation and drastic weight loss (Gropp et al., 2005; Luquet et al., 2005).

Both AgRP/NPY and POMC neurons originating in the ARC project primarily to the PVN, where numerous feeding-related pathways converge. Moreover, they project to the DMH and VMH and the perifornical part of the LHA, regions known to be important in the control of energy homeostasis (Bagnol et al., 1999; Williams et al., 2000). In the PVN, AgRP, NPY and POMC are secreted from the nerve terminals and bind to their specific receptors, resulting in the regulation of neuropeptides important for energy homeostasis in the PVN, including corticotropin-releasing hormone (CRH) and thyrotropin-releasing hormone (TRH), which were shown to exhibit anorexigenic potential (Fekete et al., 2001; Sainsbury et al., 1997). Moreover, peptides of the perifornical part of the LHA have been shown to act as downstream mediators of ARC

signaling. Melanin-concentrating hormone (MCH) for example is expressed in in the LHA in neurons that receive synaptic input from AgRP/NPY and POMC neurons originating in the ARC (Elias et al., 1998). MCH acts as an orexigenic neuropeptide, reflected in animals lacking MCH which exhibit reduced food intake and body fat stores (Qu et al., 1996; Shimada et al., 1998). Hypothalamic MCH neurons in turn project to diverse forebrain and hindbrain areas also known to be involved in the regulation of food intake. Another group of neurons in the perifornical part of the LHA receiving synaptic input from AgRP/NPY neurons are the hypocretin expressing neurons, which in turn innervate AgRP/NPY and POMC cells in the ARC (Williams et al., 2000). Hypocretin acts as an orexigenic peptide to stimulate food intake and concomitantly increases locomotor activity in mice. Accordingly, hypothalamic hypocretin levels are upregulated during fasting (Sakurai et al., 1998).

#### 1.5.2.1 Regulation of neurons located in the arcuate nucleus

A major target site for leptin signaling is the ARC of the hypothalamus. Aside from the DMH and the VMH, the highest levels of ObRb expression are found in the ARC (Elmquist et al., 1998). Both AgRP/NPY and POMC neurons within the ARC express the long form of the leptin receptor (Cheung et al., 1997; Wilson et al., 1999) and are directly regulated by leptin. While the orexigenic AgRP/NPY-producing neurons are inhibited by leptin (Elias et al., 1999; van den Top et al., 2004), the anorexigenic POMC neurons are activated (Cowley et al., 2001; Elias et al., 1999). Thus, leptin stimulates the production and secretion of anorexigenic neuropeptides and reciprocally suppresses levels of orexigenic peptides. Consistently, *ob/ob* and *db/db* mice exhibit elevated levels of AgRP and NPY mRNA and reduced levels of POMC mRNA (Mizuno and Mobbs, 1999; Schwartz et al., 1997; Shutter et al., 1997). Administration of leptin stimulates expression of POMC (Kitamura et al., 2006; Schwartz et al., 1996c) and inhibits expression of AgRP and NPY (Fekete et al., 2006; Morrison et al., 2005). Moreover, administration of a MC4R antagonist attenuates the anorexigenic response of leptin (Seeley et al., 1997). It has been shown that leptin increases the frequency of action potentials in POMC neurons by depolarization through a nonspecific cation channel and reduced inhibition by local NPY neurons (Cowley et al., 2001).

Both AgRP/NPY and POMC neurons coexpress the insulin receptor and the leptin receptor (Benoit et al., 2002; Schwartz et al., 1992). Insulin signals to the ARC of the hypothalamus to inhibit orexigenic AgRP/NPY neurons and to stimulate anorexigenic POMC neurons (Benoit et al., 2002; Choudhury et al., 2005; Schwartz et al., 2000; Sipols et al., 1995). Central administration of insulin results in increased POMC and decreased NPY expression, without affecting the expression of AgRP (Fekete et al., 2006). Recently, it was shown that insulin signaling in AgRP neurons is required for insulin's ability to suppress hepatic glucose production (Konner et al., 2007).

Besides the ability of the central nervous system to integrate information about the body energy status derived from hormones like insulin and leptin, the hypothalamus can also respond directly to circulating concentrations of nutrients, in particular of glucose and free fatty acids. Central administration of glucose decreases blood glucose levels (Lam et al., 2005) and central administration of oleic acid inhibits food intake by inhibiting NPY gene expression (Obici et al., 2002b). It has been shown that molecular disruption of the hypothalamic nutrient-sensing mechanism via overexpression of malonyl-coenzyme A decarboxylase involved in fatty acid metabolism induces obesity (He et al., 2006). Furthermore, inhibition of hypothalamic lipid oxidation and central inhibition of fatty acid synthase inhibit feeding (Benoit et al., 2002; Clegg et al., 2002; Loftus et al., 2000; Obici et al., 2002b).

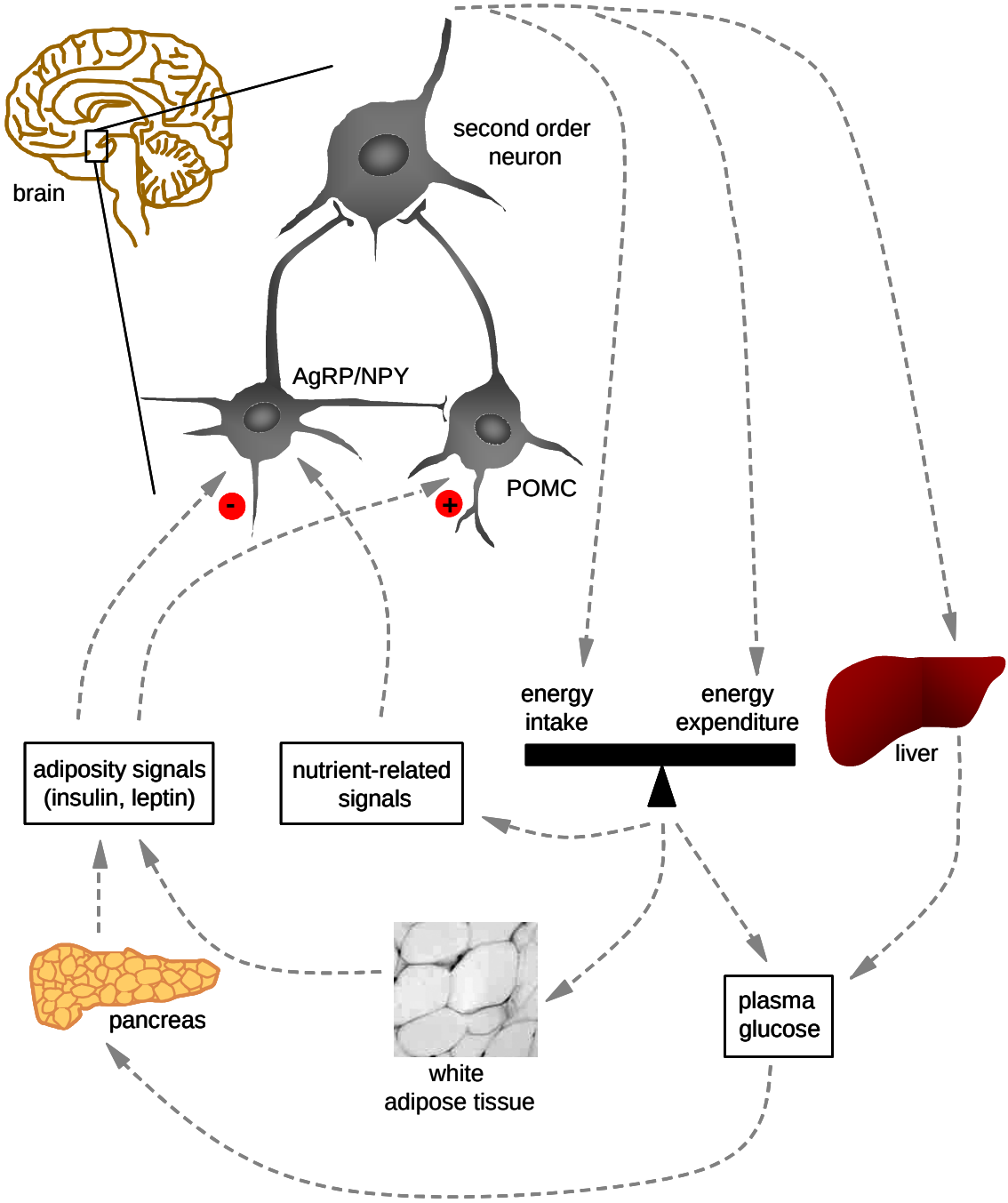


**Figure 4: Regulation of energy homeostasis**

The brain, in particular AgRP/NPY and POMC neurons located in the ARC of the hypothalamus sense and integrate signals on body energy stores such as insulin secreted from the pancreas and leptin secreted from white adipose tissue and signals on circulating nutrients such as glucose and free fatty acids. AgRP/NPY and POMC neurons respond via second order neurons, thus regulating hepatic glucose production and energy balance by the regulation of energy intake and energy expenditure (Schwartz and Porte, 2005).

### 1.5.3 Central regulation of energy homeostasis by leptin *in vivo*

The study of *db/db* mice, which lack the long form of the leptin receptor in all tissues, and of *ob/ob* mice, which do not synthesize leptin, reveals the importance of leptin signaling in the regulation of energy homeostasis. The phenotype observed in *db/db* and *ob/ob* mice resembles abnormalities seen in starved animals, including decreased body core temperature, hyperphagia accompanied by elevated AgRP and NPY and reduced POMC expression, decreased energy expenditure, locomotor activity and immune function and infertility (Coleman, 1978). *Db/db* and *ob/ob* mice develop profound and early-onset obesity weighing three times more than normal mice and exhibiting a fivefold increase in body fat content. Although the leptin receptor is widely expressed in many tissues, the absence of central leptin receptor signaling accounts for most of the defects observed in *db/db* mice. Accordingly, mice exclusively lacking neuronal leptin receptors show defects similar to *db/db* mice, which lack peripheral leptin receptors additionally (Cohen et al., 2001). Furthermore, expression of a neuron-specific leptin receptor transgene in *db/db* mice leads to a complete rescue of obesity, diabetes and infertility along with improved expression of AgRP, NPY and POMC mRNA (de Luca et al., 2005).

Mutation of $Tyr_{985}$ of the leptin receptor *in vivo* leads to the absence of inhibitory leptin signals. Leptin activates autoinhibitory signals via $Tyr_{985}$ of its receptor to attenuate the anti-obesity effects. According to this, mice carrying the $Tyr_{985}$ mutation exhibit increased leptin sensitivity, reduced adiposity, hypophagia and decreased AgRP and NPY but normal POMC expression. (Bjornholm et al., 2007). On the other hand, deletion of neuronal Shp2 leads to development of early-onset obesity due to alterations of energy metabolism in the absence of hyperphagia in spite of increased NPY expression (Zhang et al., 2004).

The involvement of the IRS/PI3K signaling pathway in ObRb-mediated leptin signaling is reflected in IRS2 deficient mice, which display increased feeding and decreased metabolic rate in the presence of increased adiposity and circulating leptin, suggesting leptin resistance (Burks et al., 2000; Tobe et al., 2001). Leptin-evoked activation of PI3K regulates the membrane potential of hypothalamic neurons *in vivo* (Harvey et al., 2000; Plum et al., 2006; Spanswick et al., 1997). Pharmacological inhibition of hypothalamic PI3K blocks the anorectic effect of leptin (Niswender et al.,

2001). Moreover, PI3K is also involved in the regulation of sympathetic nervous system function by leptin (Rahmouni et al., 2002).

The contribution of Stat3 signaling to leptin action was studied in mice with mutated $Tyr_{1138}$ of the leptin receptor leading to a selective disruption of the leptin receptor-Stat3 signal. Mice with mutated $Tyr_{1138}$ are obese, hyperphagic, exhibit reduced energy expenditure including reduced locomotor activity but show no growth impairment or infertility. While hypothalamic NPY expression is not increased as observed in *db/db* mice, the melanocortin signaling pathway is suppressed indicated by reduced POMC and elevated AgRP mRNA expression (Bates et al., 2003). Consistent with those mice, pan-neuronal Stat3 knockout mice are also obese, hyperphagic with reduced energy expenditure and exhibit elevated expression of AgRP mRNA (Gao et al., 2004). Thus, leptin receptor mediated activation of Stat3 mediates the effect of leptin on melanocortin signaling and thereby on energy homeostasis. On the other hand, leptin-regulated expression of NPY is regulated by signals other than Stat3 (Bates et al., 2003).

The role of leptin signaling in POMC neurons *in vivo* was investigated in mice with selective deletion of the leptin receptor in POMC neurons. These mice are mildly obese, hyperleptinemic and exhibit reduced expression of POMC mRNA (Balthasar et al., 2004). Mice with deletion of Stat3 selectively in POMC neurons demonstrate that POMC expression is directly activated by Stat3 (Xu et al., 2007).

Several observations indicate that inhibition of AgRP by leptin is independent of Stat3 *in vivo*, although Stat-responsive elements exist in the 5' region of *AgRP* and overexpression of Stat3 caused inhibtion of AgRP in reporter gene assays (Brown et al., 2001; Kitamura et al., 2006). On the other hand, it was shown that leptin requires intact PI3K signaling for inhibition of AgRP expression and that activation of Stat3 by leptin is not required for the regulation of AgRP neurons (Morrison et al., 2005). Most importantly, mice lacking Stat3 in AgRP neurons exhibit normal levels of AgRP mRNA (Kaelin et al., 2006). However, the exact molecular mechanism by which leptin inhibits AgRP expression is still unclear.

Besides the regulation of food intake, leptin also regulates locomotor activity, as *ob/ob* mice are hypoactive and leptin treatment normalizes this defect in locomotor activity (Pelleymounter et al., 1995). One study has implicated leptin action in the ARC in the regulation of locomotor activity, since selective unilateral restoration of leptin signaling in the ARC of leptin receptor deficient mice leads to a decrease of food intake and body weight and also normalizes locomotor activity (Coppari et al., 2005).

Nevertheless, the exact neuronal population in the ARC responsible for leptin-evoked locomotor activity has not been identified and the molecular mechanisms involved still remain unknown.

## 1.6 Objectives

The role of leptin signaling and in particular the role of leptin-evoked Stat3 signaling in the regulation of AgRP neurons remains a controversial issue. To address the role of Stat3 signaling directly in AgRP expressing neurons of the ARC *in vivo*, mice expressing a constitutively active version of Stat3 selectively in AgRP neurons upon Cre-mediated recombination were generated (Stat3-$C^{AgRP}$ mice). Characterization of Stat3-$C^{AgRP}$ mice elucidated the physiological role of Stat3 signaling in AgRP neurons, particularly on the regulation of energy homeostasis and neuropeptide expression. Additionally, Stat3-$C^{AgRP}$ mice were crossed with leptin-deficient *ob/ob* mice to further analyze the role of leptin evoked Stat3 signaling *in vivo*.

# 2 Materials and Methods

## 2.1 Chemicals and biological material

All chemicals used in this work are listed in table 1 and all enzymes used in this work are listed in table 2. Solutions were prepared with double distilled water. Bacterial media were autoclaved prior to use.

**Table 1: Chemicals**

| Chemicals | Supplier |
|---|---|
| Agarose | Peqlab, Erlangen, Germany |
| Agarose Ultra Pure | Invitrogen, Karlsruhe, Germany |
| Ascorbic acid | Sigma, Steinheim, Germany |
| 5-bromodeoxyuridine (BrdU) | Sigma, Steinheim, Germany |
| Calcium chloride | Merck, Darmstadt, Germany |
| Carbon dioxide (solid) | Hans Berrenrat GmbH, Köln, Germany |
| Chloroform | Applichem, Darmstadt, Germany |
| Dimethylsulfoxide (DMSO) | Sigma, Steinheim, Germany |
| Formaldehyde | Merck, Darmstadt, Germany |
| Formamide | Applichem, Darmstadt, Germany |
| Denhardt's | Applichem, Darmstadt, Germany |
| di-sodium hydrogen phosphate | Merck, Darmstadt, Germany |
| dNTPs | Amersham, Freiburg, Germany |
| Ethanol, absolute | Roth, Karlsruhe, Germany |
| Ethidium bromide | Applichem, Darmstadt, Germany |
| Ethylendiamine tetraacetate (EDTA) | Applichem, Darmstadt, Germany |
| Fetal calf serum (FCS) | Invitrogen, Karlsruhe, Germany |
| Gene Ruler DNA Ladder Mix | Fermentas, St. Leon-Rot, Germany |
| Glucose, 20 % | DeltaSelect, Dreieich, Germany |
| Glycerol | Applichem, Darmstadt, Germany |
| Glycine | Sigma, Steinheim, Germany |
| Hepes | Applichem, Darmstadt, Germany |

| | |
|---|---|
| Hydrochloric acid (37 %) | KMF Laborchemie, Lohmar, Germany |
| Hydrogen peroxide | Sigma, Steinheim, Germany |
| Isopropanol (2-Propanol) | Roth, Karlsruhe, Germany |
| Lithium chloride | Applichem, Darmstadt, Germany |
| Luria-Bertani (LB) Agar | Sigma, Steinheim, Germany |
| Luria-Bertani (LB) Medium | Applichem, Darmstadt, Germany |
| Magnesium chloride | Merck, Darmstadt, Germany |
| β-Mercaptoethanol | Merck, Darmstadt, Germany |
| Nitrogen (liquid) | Linde, Pullach, Germany |
| NP-40 | Applichem, Darmstadt, Germany |
| α-$^{32}$P-CTP | Amersham, Freiburg, Germany |
| Paraformaldehyde (PFA) | Sigma, Steinheim, Germany |
| PBS | Gibco, Karlsruhe, Germany |
| Potassium chloride | Merck, Darmstadt, Germany |
| Sodium acetate | Merck, Darmstadt, Germany |
| Sodium chloride | Applichem, Darmstadt, Germany |
| Sodium cholide solution, 0.9 % | Berlin-Chemie, Berlin, Germany |
| Sodium citrate | Merck, Darmstadt, Germany |
| Sodium di-hydrogen phosphate | Merck, Darmstadt, Germany |
| Sodiumdodecylsulfate (SDS) | Applichem, Darmstadt, Germany |
| Sucrose | Sigma, Steinheim, Germany |
| Trishydroxymethylaminomethan (Tris) | Applichem, Darmstadt, Germany |
| Triton X-100 | Sigma, Steinheim, Germany |
| Tween | Applichem, Darmstadt, Germany |

**Table 2: Enzymes**

| Enzymes | Supplier |
|---|---|
| *Dde*I | New England Biolabs, Schwalbach, Germany |
| DNase, RNase-free | Promega, Madison, WI, USA |
| EuroScript Reverse Transcriptase | Eurogentec, Seraing, Belgium |
| *Nco*I | Fermentas, St. Leon-Rot, Germany |
| Proteinase K | Roche, Basel, Switzerland |
| REDTaq® DNA Polymerase | Sigma, Steinheim, Germany |
| RNase A, DNase-free | Fermentas, St. Leon-Rot, Germany |
| RNase inhibitor | Roche, Basel, Switzerland |
| *Sac*I | Fermentas, St. Leon-Rot, Germany |
| T7 polymerase | Roche, Basel, Switzerland |

## 2.2 Molecular biology

Standard methods of molecular biology were performed according to protocols described by J. Sambrook (Sambrook et al., 1989), if not stated otherwise.

### 2.2.1 Competent cells and isolation of plasmid DNA

Competent *Escherichia coli (E. coli)* DH5α cells were prepared according to a standard protocol (Inoue et al., 1990) and used in heat shock transformation of plasmid DNA. Isolation of plasmid DNA was performed using an alkaline lysis method (E.Z.N.A.® Plasmid Miniprep Kit 1, Peqlab, Erlangen, Germany) according to manufacturer's instructions.

### 2.2.2 Isolation of genomic DNA from mouse tissue

For isolation of genomic DNA, mouse tail biopsies were incubated in lysis buffer (10 mM Tris/HCl [pH 8]; 10 mM EDTA; 150 mM NaCl; 0.2 % (w/v) SDS; 400

mg/ml proteinase K) at 55 °C for several hours. DNA was precipitated by adding an equal volume of isopropanol, mixed and pelleted by centrifugation. After washing with 70 % (v/v) EtOH, the pellet was dried at room temperature and resuspended in TE-buffer (10 mM Tris/HCl [pH 8]; 1 mM EDTA).

### 2.2.3 Agarose gel electrophoresis and DNA gel extraction

Amplified and digested DNA fragments were separated by size using agarose gel electrophoresis (1 to 3 % (w/v) agarose (depending on fragment size); 1 x TAE; 0.5 mg/ml ethidiumbromide; 1 x TAE electrophoresis buffer). To elute DNA fragments, the fragments were excised and the DNA was eluted using the QIAEX II kit (Qiagen, Hilden, Germany) according to manufacturer's instructions.

Quality of RNA was assessed by electrophoresis on denaturing agarose gels (1.2 % (w/v) agarose; 1 x MOPS; 1 % (v/v) formaldehyde; 1 x MOPS electrophoresis buffer).

### 2.2.4 Construction of a vector for *in situ* hybridization probe synthesis

To clone a vector for *in situ* hybridization probe synthesis, a PCR fragment was amplified *in vitro* from mouse hypothalamic cDNA using the High Fidelity PCR Master Kit (Roche, Basel, Switzerland) and primers containg NPY specific sequences (listed in table 3). The PCR fragment was cloned into the pGEM®-T Vector using the pGEM®-T Vector System (Promega, Madison, WI, USA) according to manufacturer's instructions. Finally, the construct was verified by *Sac*I and *Nco*I endonuclease digestion.

**Table 3: Primers used for amplification of NPY cDNA**

| Name of primer | Sequence (5'-3') |
|---|---|
| NPY-5' | ATG CTA GGT AAC AAG CGA ATG G |
| NPY-3' | TCA CCA CAT GGA AGG GTC TTC |

### 2.2.5 Quantification of DNA and RNA

Concentration of nucleic acids was quantified using a spectrophotometer (NanoDrop ND-1000, NanoDrop Technologies, Wilmington, DE, USA). Absorption of samples was measured at 260 nm, which is the highest absorption wavelength for nucleic acids. An $OD_{260}$ (optical density) of 1 corresponds to 50 µg/ml for double-stranded DNA and to 40 µg/ml for RNA. To assess purity of nucleic acids, the ratio of absorptions at 260 nm versus 280 nm was calculated, as proteins absorb maximum at 280 nm. An $OD_{260}/OD_{280}$ ratio of 2 refers to pure nucleic acids, lower values display protein contaminations.

After eluting DNA from agarose gels using the QIAEX II kit, the concentration was assessed by comparing the intensity of the DNA fragment with the band intensity of a standard marker on an agarose gel, as the glassmilk used in the kit for the elution of DNA interferes with UV absorption.

### 2.2.6 Polymerase chain reaction (PCR)

The polymerase chain reaction was performed to amplify a cDNA fragment *in vitro* for *in situ* hybridization probe synthesis, and to detect targeted alleles or transgenes for genotyping of mice (Saiki et al., 1986; Saiki et al., 1985).

To amplify cDNA fragments, the High Fidelity PCR Master Kit (Roche, Basel, Switzerland) containing a polymerase with proofreading activity was used according to manufacturer's guidlines with 500 ng template cDNA and 25 pmol of each primer (listed in table 4). After an initial denaturation step at 94 °C for 2 min, 13 cycles of denaturation at 94 °C for 15 sec, annealing at 54 °C for 30 sec and elongation at 72 °C for 1 min were followed by another 17 cycles of denaturation at 94 °C for 20 sec, annealing at 54 °C for 30 sec and elongation at 72 °C for 1.5 min. The PCR was finished with a final extension step at 72 °C for 10 min.

Genotyping of mice was performed with 500 ng DNA isolated from tail biopsies in a total volume of 25 µl containing 25 pmol of each primer (listed in table 8), 25 µmol dNTPS, 2 to 6 % (v/v) DMSO, 0.625 to 1.2 U REDTaq® DNA Polymerase and 1 x REDTaq® PCR Reaction Buffer (Sigma, Steinheim, Germany). Again, the different

PCRs started with an initial denaturation step at 95 °C for 5 min, followed by 35 to 40 cycles of denaturation at 95 °C for 30 sec, annealing at 54 to 63 °C for 30 to 45 sec and elongation at 72 °C for 30 to 90 sec. The elongation was finished with a final extension step at 72 °C for 10 min.

All PCR reactions were carried out either in an iCycler Thermocycler (Bio-Rad, Hercules, CA, USA) or in a PTC-200 Peltier Thermal Cycler (MJ Research, Waltham, MA, USA).

### 2.2.7 RT-PCR

Different mouse tissues were dissected and homogenized using an Ultra Turrax homogenizer (IKA, Staufen, Germany). RNA isolation was performed using the RNeasy system (Qiagen, Hilden, Germany) according to the manufacturer's instructions. Total RNA was treated with RNase-free DNase and 200 ng RNA were reverse transcribed with EuroScript Reverse Transcriptase according to manufacturer's guidelines. Fragments of Stat3-C, endogenous Stat3 and GAPDH were amplified using specific primers (listed in table 4).

**Table 4: Primers used for amplification of cDNA fragments**

| amplified cDNA fragment | Name of primer | Sequence (5'-3') |
|---|---|---|
| Stat3-C | Rosa512 | GCC GTT CTG TGA GAC AG |
| | 3StatRT | AGG ACA TTG GAC TCT TGC AG |
| endogenous Stat | 5StatRT | CAG TCG GGC CTC AGC CC |
| | 3StatRT | AGG ACA TTG GAC TCT TGC AG |
| GAPDH | GAPDH-5' | ACC ACA GTC CAT GCC ATC AC |
| | GAPDH-3' | TCC ACC ACC CTG TTG CTG TA |

### 2.2.8 Analysis of RNA expression

Expression of mRNA was analyzed using quantitative RT-PCR. cDNA was obtained from hypothalamic tissue, white and brown adipose tissue as well as skeletal muscle as described above and amplified using TaqMan$^{R}$ Universal PCR-Master Mix, No AmpErase® UNG with TaqMan® Assay on demand kits for AgRP (agouti related protein), HCRT (hypocretin (orexin)), HPRT (hypoxanthine guanine phosphoribosyl transferase 1), MCH (pro-melanin-concentrating hormone), NPY (neuropeptide Y), Socs3 (suppressor of cytokine signaling 3), Stat3 (signal transducer and activator of transcription 3), UCP-1 (uncoupling protein 1), UCP-2 (uncoupling protein 2) and UCP-3 (uncoupling protein 3) (Applied Biosystems, Foster City, CA, USA) . Analysis of POMC mRNA expression was performed with customized primers listed in table 5. Standard curves were used based on hypothalamic cDNA, white or brown adipose tissue and skeletal muscle cDNA. Relative expression of samples was adjusted for total RNA content by HPRT RNA quantitative PCR. Calculations were performed by a comparative method (2-ddCT). Quantitative PCR was performed on an ABI-PRISM 7700 Sequence Detector (Applied Biosystems, Foster City, CA, USA). Assays were linear over at least 4 orders of magnitude.

**Table 5: Primers used for analysis of POMC mRNA expression**

| Name of primer | Sequence (5'-3') |
|---|---|
| POMC sense | GAC ACG TGG AAG ATG CCG AG |
| POMC anti-sense | CAG CGA GAG GTC GAG TTT GC |
| probe sequence | FAM-CAA CCT GCT GGC TTG CAT CCG G-TAMRA |

## 2.3 Biochemistry

### 2.3.1 Electromobility-Shift Assay (EMSA)

Mice were intraperitoneally injected with either saline or leptin (5 µg/g body weight) (Sigma, Steinheim, Germany) after an over night (16 h) fast and sacrificed after 20 min. Hypothalamic tissue was homogenized in hypotonic solution (10 mM HEPES [pH 7.6]; 10 mM KCl; 2 mM $MgCl_2$; 0.1 mM EDTA; completed with protease inhibitor cocktail (Roche, Basel, Switzerland)) using an Ultra Turrax homogenizer (IKA, Staufen, Germany) and NP-40 was added to 1 % (v/v) after 10 min incubation on ice. After centrifugation, the nuclear pellet was washed in hypotonic buffer and resuspended in extraction buffer (50 mM HEPES [pH 7.8]; 50 mM KCl; 300 mM NaCl; 0.1 mM EDTA; 10 % (v/v) glycerol). Protein concentration was determined using a photometer (BioPhotometer, Eppendorf, Hamburg, Germany) and the Christian Warburg formula. 4 µg of hypothalamic nuclear extracts were incubated at room temperature for 30 min with 2 µg poly(dI-dC) (Amersham Pharmacia Biotec, Uppsala, Sweden) and 0.5 ng of $^{32}$P-labeled Stat3 probe (Santa Cruz Biotechnology, Inc., Santa Cruz, CA, USA). Samples were fractionated on a 5 % (w/v) PAGE over night and visualized by autoradiography. Density of bands was determined using Quantity One software (Bio-Rad, Hercules, CA, USA).

### 2.3.2 Enzyme-linked Immunosorbent Assay (ELISA)

Serum insulin, leptin and free triiodothyronine (fT3) levels, as well as plasma catecholamine concentrations were measured by ELISA according to manufacturer's guidelines (Mouse Leptin ELISA, Mouse/Rat Insulin ELISA, Crystal Chem, Downers Grove, IL, USA; free triiodothyronine (fT3) ELISA, Alpha Diagnostic Intl. Inc., San Antonio, TX, USA; CatCombi ELISA for Epinephrine and Norepinephrine, IBL, Hamburg, Germany).

Brain catecholamine and serotonin concentrations were measured by ELISA (TriCat ELISA and Serotonin ELISA, DRG, Marburg, Germany). Brain areas of interest (hypothalamus, ventral tegmental area, frontal association cortex and striatum) were

dissected with the aid of a mouse brain atlas (Franklin and Paxinos, 1997) using a coronal acrylic brain matrix (Braintree Scientific, Inc., Braintree, MA, USA) (hypothalamus: 0 to 2 mm posterior relative to bregma; ventral tegmental area: 2 mm to 4 mm posterior relative to bregma; frontal association cortex: 2 mm to 4 mm anterior relative to bregma; striatum: 0 to 1 mm anterior relative to bregma). The brain areas were then dissected from the coronal sections using a scalpel. Brain tissue was homogenized in 0.05 N HCl using the Ultra Turrax homogenizer (IKA, Staufen, Germany) and after centrifugation the supernatant was used to determine catecholamine concentrations according to the manufacturer's guidelines. For determination of serotonin concentrations, ascorbic acid was added to the supernatant to a final concentration of 1 mg/ml, and serotonin concentrations were measured according to the manufacturer's guidelines.

## 2.3.3 Staining of hypothalamic sections

### 2.3.3.1 Immunohistochemistry

AgRPCre$^{+/-}$ mice were mated with *RosaArte1* reporter mice (Seibler et al., 2003). Mice double-positive for AgRPCre and LacZ (LacZ$^{+/-}$AgRPCre$^{+/-}$) were anesthetized intraperitoneally with Avertin (240 mg/kg) (2,2,2-tribromoethanol, Sigma, Steinheim, Germany) and transcardially perfused with saline followed by 4 % (w/v) paraformaldehyde (PFA) in 0.1 M phosphate buffered saline (PBS [pH 7.4]). The brains were dissected and frozen in tissue freezing medium (Jung Tissue Freezing Medium; Leica Microsystems, Wetzlar, Germany) after post-fixation in 4 % (w/v) PFA at 4 °C over night and soaking in 20 % (w/v) sucrose for 6 h. 25 µm thick free-floating coronal sections were cut through the ARC using a freezing microtome (Leica Microsystems, Wetzlar, Germany). Then, the sections were washed extensively in PBS to remove cryoprotectant. Afterwards, the sections were treated with 0.3 % (v/v) $H_2O_2$ in PBS for 20 minutes to quench endogenous peroxidase activity. Following pretreatments, the sections were stained using the Renaissance® TSA™ Fluorescence Systems Tyramide Signal Amplification Kit (PerkinElmer™, Waltham, MA, USA) according to manufacturer's guidelines (primary antibody: rabbit anti-lacZ; secondary antibody: goat anti-rabbit peroxidase labeled; see table 7). The stained sections were embedded in

Vectashield Mounting Medium containing DAPI (Vector Laboratories Burlingame, CA, USA).

#### 2.3.3.2 Combined *in situ* hybridization and immunohistochemistry

For NPY probe synthesis, the NPY-pGEM-T Vector described in 2.2.4 was used as a template to amplify a NPY fragment including an upstream T7 promoter sequence by PCR using primers containing a T7 promoter sequence and NPY-specific sequences (listed in table 6). The fragment was purified and transcribed into digoxigenin (DIG)-labeled RNA *in vitro* using 200 ng of the T7 promoter-NPY-fragment, 1 x DIG RNA labeling mix, 4 U T7 polmyerase, 1 x transcription buffer and 40 U RNase inhibitor in a total volume of 20 µl (all reagents were obtained from Roche, Basel, Switzerland). After incubation at 37 °C for 2 h, the transcribed RNA was *DNase*I-digested, ethanol-precipitated, and the quality of the RNA was assessed by electrophoresis on an agarose gel after quantification of RNA concentration.

**Table 6: Primers used to amplify a T7-promoter-NPY fragment for *in vitro* transcription**

| Name of primer | Sequence (5'-3') |
|---|---|
| NPY-5' | ATG CTA GGT AAC AAG CGA ATG G |
| T7-promoter-NPY-3' | TAA TAC GAC TCA CTA TAG GGT CAC CAC ATG GAA GGG TCT TC |

For NPY *in situ* hybridization, mice were fasted for 48 h to stimulate NPY expression, anesthetized with Avertin and transcardially perfused as described above. After dissection, the brains were post-fixed in 4 % (w/v) PFA for 4 h and soaked in 20 % (w/v) sucrose over night at 4 °C. 8 µm thick coronal sections containing the ARC were dried at room temperature, washed with PBS and treated with proteinase K (0.25 µg/ml) for 10 min at 37 °C. The sections were rinsed with glycine (2 mg/ml), placed into 4 % (w/v) PFA, washed with PBS, and then washed with 2 x SSC. Prehybridization was carried out for 5 h at 55 °C in prehybridization buffer containing 50 % (v/v) formamide, 5 x SSC, 1 x Denhardt's and 0.1 % (v/v) Tween 20. Hybridization was

performed at 55 °C over night in prehybridization buffer containing 2 ng/µl digoxigenin-labeled RNA probe and 360 ng/µl competitor tRNA. After washing with 2 x SSC the sections were RNase-digested for 1 h at 37 °C and afterwards washed with 0.1 x SSC for 1 h at 55 °C, cooled to room temperature and treated with hydrogen peroxide (1 % (v/v)) for 1 h. The sections were blocked for 1 h in Roti®- ImmunoBlock (Roth, Karlsruhe, Germany) and incubated with anti-DIG antibody coupled to alkaline phosphatase (see table 7) for 1 h. After washing, NPY *in situ* hybridization was detected using Vector® Blue Alkaline Phosphatase Substrate Kit III (Vector Laboratories, Burlingame, CA, USA). Determination of mean NPY neuron size was carried out in NPY-stained hypothalamic sections using Zeiss AxioVision 4.2 software (Carl Zeiss Microlmaging, Göttingen, Germany).

For combined Stat3 immunohistochemistry, the sections were incubated with Stat3 antibody together with anti-DIG antibody (see table 7). Stat3 immunostaining was developed prior to the detection of alkaline phosphatase using the Tyramide Signal Amplification Kit as described above (secondary antibody: goat anti-rabbit peroxidase labeled; see table 7).

For combined BrdU immunohistochemistry, the NPY-stained sections were treated with HCl (2 N) for 1 h and incubated with anti-BrdU antibody over night at 4 °C after blocking. BrdU immunostaining was visualized with the Tyramide Signal Amplification Kit as described above (secondary antibody: goat anti-rat peroxidase labeled; see table 7).

After staining, the sections were embedded in Vectashield Mounting Medium containing DAPI (Vector Laboratories Burlingame, CA, USA).

**Table 7: Antibodies used for staining of hypothalamic sections**

| Antibody | Supplier | Working Dilution |
|---|---|---|
| sheep anti-digoxigenin coupled to alkaline phosphatase | Roche, Basel, Switzerland | 1:100 |
| rabbit anti-Stat3 | Santa Cruz Biotechnology, Inc., Santa Cruz, CA, USA | 1:25 |
| goat anti-rabbit peroxidase labeled | Vector Laboratories Burlingame, CA, USA | 1:1000 |
| rat anti-BrdU | Accurate Chemical & Scientific, Westbury, NY, USA | 1:400 |
| goat anti-rat peroxidase labeled | Jackson ImmunoResearch Laboratories, Inc., West Grove, PA, USA | 1:500 |
| rabbit anti-lacZ | Cappel, Durham, NC, USA | 1:200 |

All antibodies were diluted in TBS containing 0.5 % (v/v) FCS and 0.1 % (v/v) Triton X-100.

### 2.3.4 Histomorphology

Dissected white adipose tissue samples were incubated in fixation solution containing 4 % (w/v) PFA at 4 °C over night and embedded in paraffin according to a standard protocol (Plum et al., 2006). 7 µm sections were mounted onto gelatin-coated slides and hematoxylin/eosin-stained (HE) (Sigma, St. Louis, MO, USA) after deparaffinization as previously described (Plum et al., 2006). The determination of mean adipocyte size and adipocyte size distribution was carried out in HE-stained tissues using Zeiss AxioVision 4.2 software (Carl Zeiss Microlmaging, Göttingen, Germany).

## 2.4 Mouse experiments

### 2.4.1 Animal care

Care of all animals was within institutional animal care committee guidelines and all procedures were approved by local government authorities (Bezirksregierung Köln) and were in accordance with NIH guidelines. Mice were housed in groups of 3 to 5 or individually if required for an experiment as indicated. Animals were kept at 22 to 24 °C and were exposed to a 12 hours light/dark cycle with lights on at 7 am. Mice were either fed normal chow diet (Teklad Global Rodent # T.2018.R12; Harlan, Borchen, Germany) containing 53.5 % of carbohydrates, 18.5 % of protein, and 5.5 % of fat (12 % of calories from fat) or a high fat containing diet (# C1057; Altromin, Lage, Germany) containing 32.7 %, 20 % and 35.5 % of carbohydrates, protein and fat (55.2 % of calories from fat), respectively. The animals had access to water *ad libitum* and food was only withdrawn if required for an experiment. Body weight was measured once a week.

### 2.4.2 Mice

Breeding colonies were maintained by mating Stat3-$C^{stoplox/stoplox}$ mice (Casola et al., 2006) with $AgRPCre^{+/-}$ mice (Kaelin et al., 2004) to analyze Stat3-$C^{AgRP}$ animals and *ob*/+Stat3-$C^{stoplox/stoplox}$ mice with *ob*/+$AgRPCre^{+/-}$ mice to analyze *ob/ob*Stat3-$C^{AgRP}$ animals (*ob*/+ mice were obtained from Charles River Laboratories, Wilmington, MA, USA) (Coleman, 1978). Stat3-$C^{AgRP}$ mice were fed either normal chow or high fat diet, *ob/ob*Stat3-$C^{AgRP}$ mice were fed normal chow diet. Only animals from the same mixed background strain generation were compared. Mice were genotyped by PCR using genomic DNA isolated from tail tips. Germline deletion was detected using the NeoRT primer located in the floxed neomycine cassette. Animals with germline deletion (approximately 1 %) were excluded from the experiments. The genotyping strategy for the *ob/ob* mice was based on the fact that the *ob* mutation generates a *Dde*I restriction site. Therefore, the *ob*-PCR product spanning the *ob* mutation was digested with the *Dde*I restriction enzyme.

**Table 8: Primers used for genotyping of mice**

| targeted allele /transgene | Name of primer | Sequence (5'-3') |
|---|---|---|
| AgRPCre | AgRPCre-5' | CCC TAA GGA TGA GGA GAG AC |
| | Cre-intern-rev-3' | ATG TTT AGC TGG CCC AAA TGT |
| | AgRP-Intron | ACT TGG TGC ATG GTG GGT GT |
| POMCCre | POMCCre-5' | TGG CTC AAT GTC CTT CTT GG |
| | Cre-intern-rev-3' | GAG ATA TCT TTA ACC CTG ATC |
| | POMC-Intron | CAC ATA AGC TGC ATC GTT AAG |
| Stat3-C | Typ_forward | AAA GTC GCT CTG AGT TGT TAT C |
| | NeoRT | GCA TCG CCT TCT ATC GCC T |
| | Typ_reverse | GAT ATG AAG TAC TGG GCT CTT |
| ob | ob-3' | TGT CCA AGA TGG ACC AGA CTC |
| | ob-5' | ACT GGT CTG AGG CAG GGA GCA |

### 2.4.3 Intracerebroventricular BrdU injection

Detection of 5-bromodeoxyuridine (BrdU) incorporation was performed on intracerebroventricularly BrdU-injected mice as described before (Kokoeva et al., 2005). Briefly, twenty week old mice were anesthetized intraperitoneally with Avertin as described in 2.3.3.1 and received an subcutaneous injection of the analgesic Tramal (15 mg/kg) (Grünenthal, Aachen, Germany), additionally. Anesthetized mice were placed into a stereotactic device and a sterile cannula (Brain Infusion Kit 3, Alzet, Cupertino, CA, USA) was implanted into the right lateral brain ventricle (0.2 mm posterior and 1 mm lateral relative to bregma and 2.3 mm below the surface of the skull) and connected to an osmotic minipump (model 1002, flow rate 0.25 µl/h, 14 days, Alzet, Cupertino, CA, USA) filled with 2 µg/µl BrdU (Sigma, St. Louis, MO, USA) in artificial cerebrospinal fluid (148 mM NaCl; 3 mM KCl; 1.4 mM $CaCl_2$; 0.8 mM $MgCl_2$; 0.8 mM $Na_2HPO_4$; 0.2 mM $NaH_2PO_4$). The mice were infused with 12 µg BrdU per day for 7 days.

### 2.4.4 Body composition

Body fat content was measured *in vivo* by nuclear magnetic resonance using the minispec mq 7.5 (Bruker Optics, The Woodlands, TX, USA).

### 2.4.5 Collection of blood samples and determination of blood glucose levels

Tail bleeding of mice was performed according to Hogan (Hogan et al., 1987) and Silver (Silver 1995). Blood glucose values were determined from whole venous blood using an automatic glucose monitor (GlucoMen$^{R}$ *GlycÓ*; A. Menarini Diagnostics, Florence, Italy). Determination of blood glucose levels and collection of blood samples were performed in the morning to avoid deviations due to circadian variations.

### 2.4.6 Food intake, indirect calorimetry and physical activity

Food intake was measured over a two week period, during which mice were housed individually in regular cages using food racks. To minimize handling of the animals, food racks were weighed once a week and daily food intake was calculated as the average daily intake of chow within the time stated. Indirect calorimetry was measured in a Calorimetry Module (CaloSys V2.1, TSE Systems, Bad Homburg, Germany and CLAMS, Oximax Windows 4.00, Columbus Instruments, Columbus, OH, USA). After two hours of acclimatization, parameters of indirect calorimetry were measured for at least 48 hours. For the measurement of physical activity, transmitters (PDT-4000 E-Mitter, VitalView Data Acquisition System 4.1; Mini Mitter, Bend, OR, USA) were implanted into the peritoneal cavity of Avertin-anesthetized mice. After 7 days mice that reached at least 90 % of their preoperative body weight were placed into 3.0 l chambers of a Comprehensive Laboratory Animal Monitoring System (CLAMS, Oximax Windows 4.00, Columbus Instruments, Columbus, OH, USA). For the measurement of basal locomotor activity, food and water were provided *ad libitum*. Mice were allowed to acclimatize in the chambers for 2 hours. Physical activity was measured for at least the following 48 hours. For the measurement of fasting-induced

locomotor activity, food was withdrawn and activity was measured for the following 24 hours.

### 2.4.7 Insulin tolerance test

After determination of basal blood glucose levels each animal received an intraperitoneal injection of insulin (0.75 U/kg body weight) (Novo Nordisk, Bagsværd, Denmark). Blood glucose levels were measured 15, 30 and 60 min after insulin injection.

### 2.4.8 Glucose tolerance test

Glucose tolerance tests were performed in the morning with animals after a 16 h fast. After determination of fasted blood glucose levels each animal received an intraperitoneal injection of 20 % (w/v) glucose (10 ml/kg body weight). Blood glucose levels were measured 15, 30, 60 and 120 min after glucose injection.

## 2.5 Statistical methods

Statistical analysis of data was performed using SPSS 12.0 software (SPSS Inc., Chicago, IL, USA). All data were normally distributed. Data were analyzed for statistical significance using a two-tailed unpaired student's t-Test. Prior to performing t-tests, homogeneity of variances was tested and accordingly homoscedastic or heteroscedastic t-Test was performed. All displayed values are means ± SEM. * $p \leq 0.05$ ; ** $p \leq 0.01$ ; *** $p \leq 0.001$ versus control.

# 3 Results

## 3.1 Generation of AgRP neuron specific Stat3-C mice

To investigate the role of Stat3-dependent signaling in AgRP-expressing neurons, a constitutively active version of Stat3 was expressed specifically in this cell type. Therefore, mice carrying a transgene encoding a constitutively active form of the Stat3 protein (Stat3-C) including an upstream loxP-flanked stop sequence in the ubiquitously expressed *Rosa26* locus (Casola et al., 2006) were crossed with mice expressing the Cre recombinase under control of the *AgRP* promoter (Figure 5a and b) (Kaelin et al., 2004).

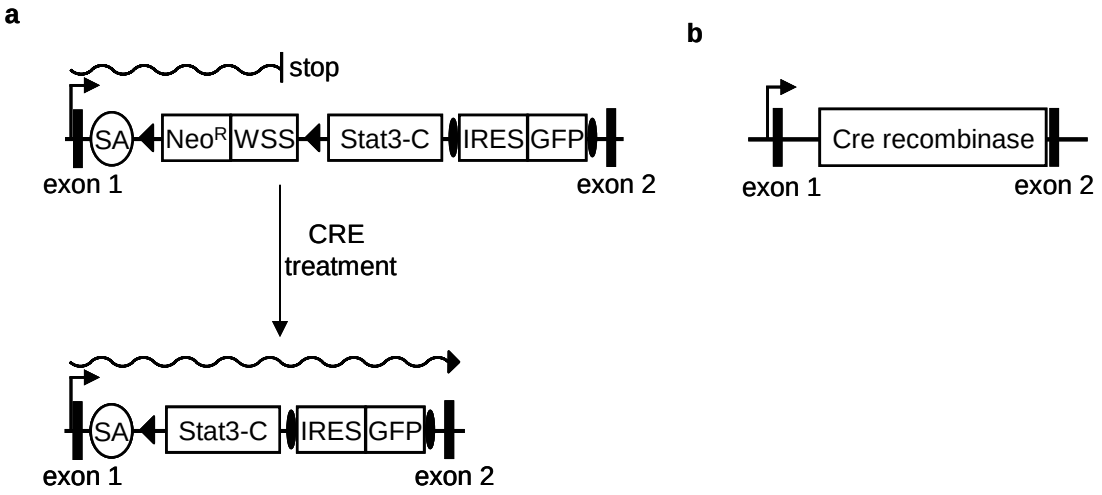


**Figure 5: AgRP neuron-restricted expression of a constitutively active Stat3 transgene**
**(a)** Map of the Stat3-C transgene for Cre-mediated, conditional expression from the *Rosa26* locus. In this configuration Cre-mediated recombination removes the loxP-flanked $Neo^R$ and Westphal stop sequence only in cell types expressing Cre, thus allowing transcription of the bicistronic Stat3-C, GFP mRNA. SA: adenoviral splice acceptor; filled triangles: loxP sites; $Neo^R$: neomycine resistance gene driven by the *pGK* promoter; WSS: Westphal stop sequence; Stat3-C: constitutively active form of Stat3; closed ellipses: FRT sites; IRES: internal ribosome entry site; GFP: *GFP* gene. **(b)** Map of the AgRPCre transgene. The Cre recombinase cassette is located upstream of the normal *AgRP* translational initiation site in exon 2.

In Stat-C AgRPCre double positive mice ($Stat3\text{-}C^{+/-}AgRPCre^{+/-}$), the loxP-flanked stop sequence is removed upon Cre-mediated recombination, leading to the transcription of Stat3-C selectively in AgRP neurons. In the Stat3-C protein,

substitution of two cystein residues for A661 and N663 in the SH2 domain, which is responsible for protein-protein interaction, allows to form sulfhydryl bonds between Stat3 monomers. Thus, dimerization of Stat3 is allowed by formation of disulfide-bonds between the two substituted cysteines independent of signal-dependent tyrosine phosphorylation. The dimerized Stat3-C protein was shown to be able to bind DNA and activate transcription (Bromberg et al., 1999).

To confirm the specificity of transgene expression, total RNA from a variety of tissues of control (Stat3-C$^{+/-}$) and Stat3-C$^{AgRP}$ (Stat3-C$^{+/-}$AgRPCre$^{+/-}$) mice was isolated and the expression of Stat3-C, endogenous Stat3 and GAPDH was determined by RT-PCR. Since AgRP is selectively expressed in neurons of the ARC of the hypothalamus, Cre-dependent Stat3-C transgene expression in Stat3-C$^{AgRP}$ mice should be detectable only in the hypothalamus. Indeed, RT-PCR with transgene-specific primers detected Stat3-C expression only in the hypothalamus and not in other brain regions or peripheral organs isolated from Stat3-C$^{AgRP}$ mice. However, expression of endogenous Stat3 was detected to a similar extent in all tissues analyzed from control and Stat3-C$^{AgRP}$ mice (Figure 6).

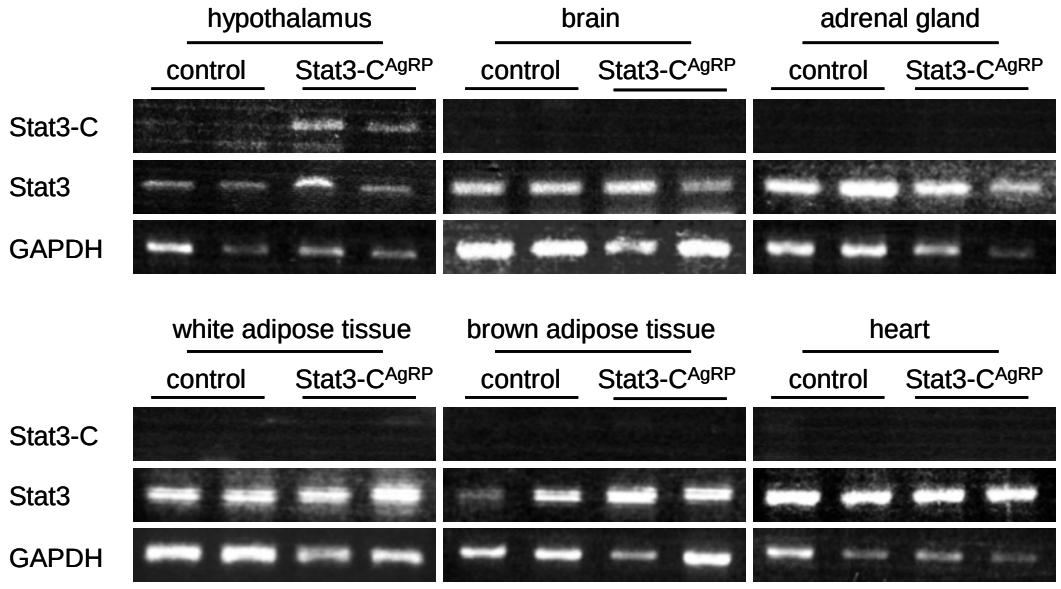


**Figure 6: Expression of Stat3-C is restricted to the hypothalamus of Stat3-C$^{AgRP}$ mice**

Expression of Stat3-C, endogenous Stat3 and GAPDH in different tissues of control and Stat3-C$^{AgRP}$ mice shown by RT-PCR.

To investigate whether the mutant Stat3-C acts as a constitutively active DNA-binding transcription factor, DNA-binding capacity of the transgenically expressed Stat3-C was assessed. To this end, control and Stat3-C$^{AgRP}$ mice were treated with either saline or leptin. Subsequent electromobility shift assay (EMSA) using isolated nuclear hypothalamic extracts revealed a 3-fold enhancement of Stat3 binding activity in the hypothalamus of control mice following *in vivo* leptin treatment (Figure 7a and b). By contrast, hypothalamic nuclear extracts of Stat3-C$^{AgRP}$ mice exhibited high Stat3 binding activity even under basal conditions and this was not further enhanced by leptin treatment (Figure 7a and b), indicating that the mutant Stat3-C indeed acts as a constitutively active DNA-binding transcription factor.

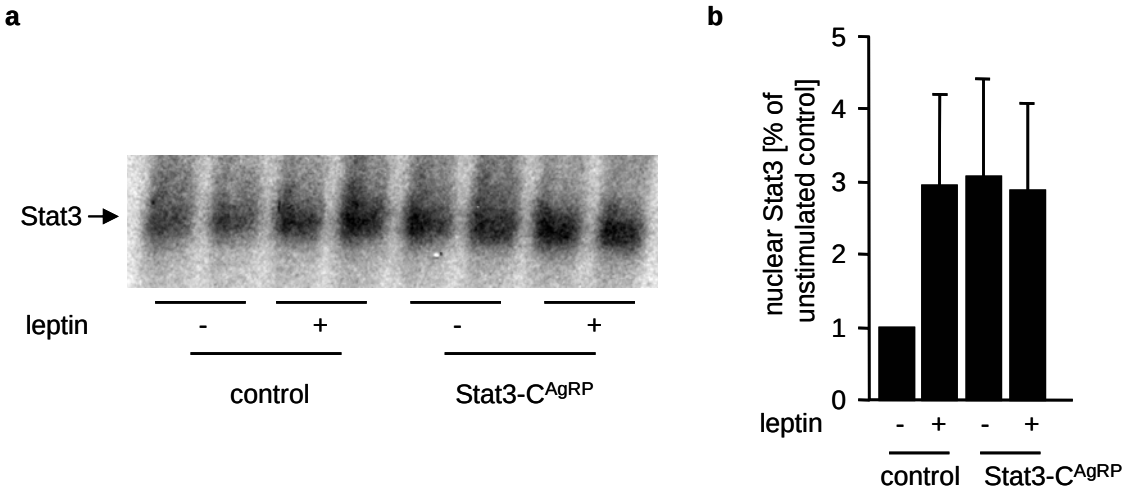


**Figure 7: High Stat3 DNA-binding activity in Stat3-C$^{AgRP}$ mice**

**(a)** Nuclear binding activity to a Stat3 consensus probe in hypothalamic extracts of saline or leptin stimulated control and Stat3-C$^{AgRP}$ mice demonstrated by EMSA. **(b)** Densitometrical analysis of nuclear Stat3 in control and Stat3-C$^{AgRP}$ mice compared to unstimulated controls (n = 8 of each genotype and condition).

To analyze if expression of overall hypothalamic Stat3 was increased in Stat3-C$^{AgRP}$ mice, primers were used recognizing both endogenous and transgenic Stat3 mRNA. In fact, hypothalamic Stat3 expression was 40 to 70 % higher in Stat3-C$^{AgRP}$ animals compared to controls (Figure 8a). Then, expression of the Stat3 target gene suppressor of cytokine signaling 3 (Socs3) was determined to analyze, if the increase in Stat3 expression resulted in elevated Socs3 levels. Hypothalamic Socs3 mRNA

expression in Stat3-C$^{AgRP}$ mice appeared to be 80 to 150 % higher than in control animals, although this difference did not reach statistical significance (Figure 8b).

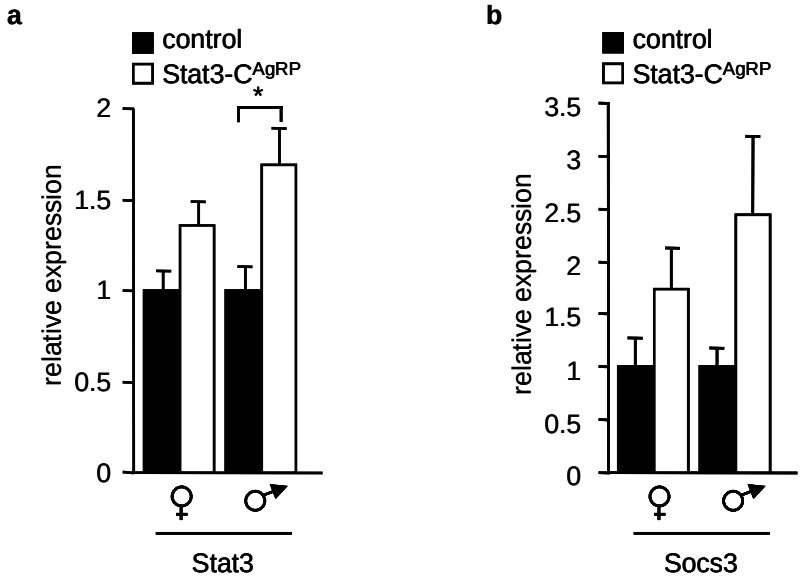


**Figure 8: Enhanced expression of hypothalamic Stat3 and Socs3 in Stat3-C$^{AgRP}$ mice**
Hypothalamic expression of **(a)** Stat3 and **(b)** Socs3 of control and Stat3-C$^{AgRP}$ mice under fasted conditions (n = 7 of each genotype).

To analyze the cell type-specific restriction of Stat3-C expression further, Cre-mediated recombination was verified by crossing AgRPCre mice with a reporter mouse strain (*RosaArte1*) in which transcription of the β-galactosidase gene (*LacZ*) under control of the *Rosa26*-promoter is prevented by a floxed hygromycin resistance gene, thus leading to a β-galactosidase expression only in cell types expressing the Cre recombinase (Figure 9a) (Seibler et al., 2003). In this reporter mouse strain (LacZ$^{+/-}$ AgRPCre) a β-galactosidase expression pattern was observed reflecting the described expression of endogenously expressed AgRP (Figure 9b), consistent with the previously demonstrated colocalization of endogenous AgRP and Cre recombinase activity in this line of Cre-transgenic mice (Kaelin et al., 2006; Kaelin et al., 2004).

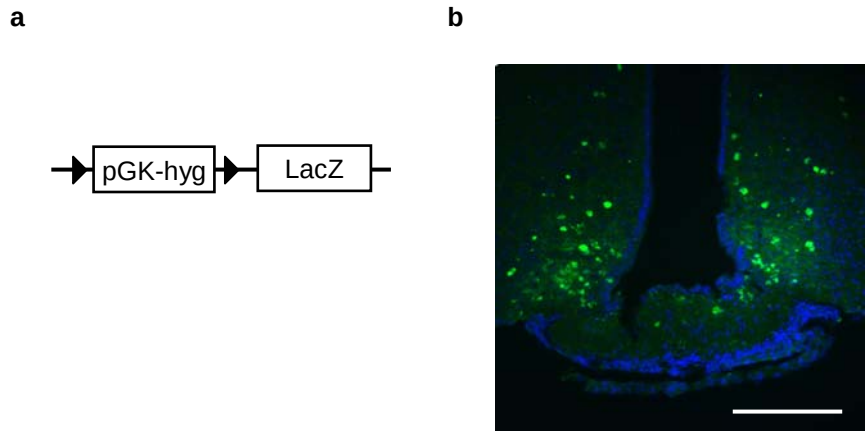


**Figure 9: Verification of Cre-mediated recombination in AgRPCre mice**

**(a)** Map of the *LacZ* transgene for Cre-mediated, conditional expression from the *Rosa26* locus. Filled triangles: loxP sites; pGK-hyg: hygromycin resistance gene driven by the *pGK* promoter. In this configuration Cre-mediated recombination removes the loxP-flanked hygromycin resistance gene only in cell types expressing Cre, resulting in transcription of β-galactosidase. **(b)** Immunohistochemistry for β-galactosidase (β-gal) in brains of double heterozygous reporter mice ($LacZ^{+/-}$AgRPCre) at the age of ten weeks. Blue (DAPI), DNA; green: (β-gal), AgRP neurons. Magnification: 100 x. Scale bar: 200 µm.

To further confirm the expression of the transgene selectively in AgRP/NPY neurons, combined NPY *in situ* hybridization and Stat3 immunohistochemistry was performed on hypothalamic sections of fasted control and Stat3-$C^{AgRP}$ mice. In fasted control animals, Stat3 expression was predominantly located in the cytoplasm of NPY neurons. In contrast, Stat3 was also located in the nuclei of NPY neurons of transgenic mice. Moreover, the amount of Stat3 in NPY neurons of Stat3-$C^{AgRP}$ mice appeared to be higher than in those of control animals (Figure 10).

Taken together, these data demonstrate that the transgenic approach results in AgRP neuron-restricted activation of Stat3-C transcription and thus to enhanced basal Stat3 binding activity in the hypothalamus of these mice, independent of leptin-stimulation.

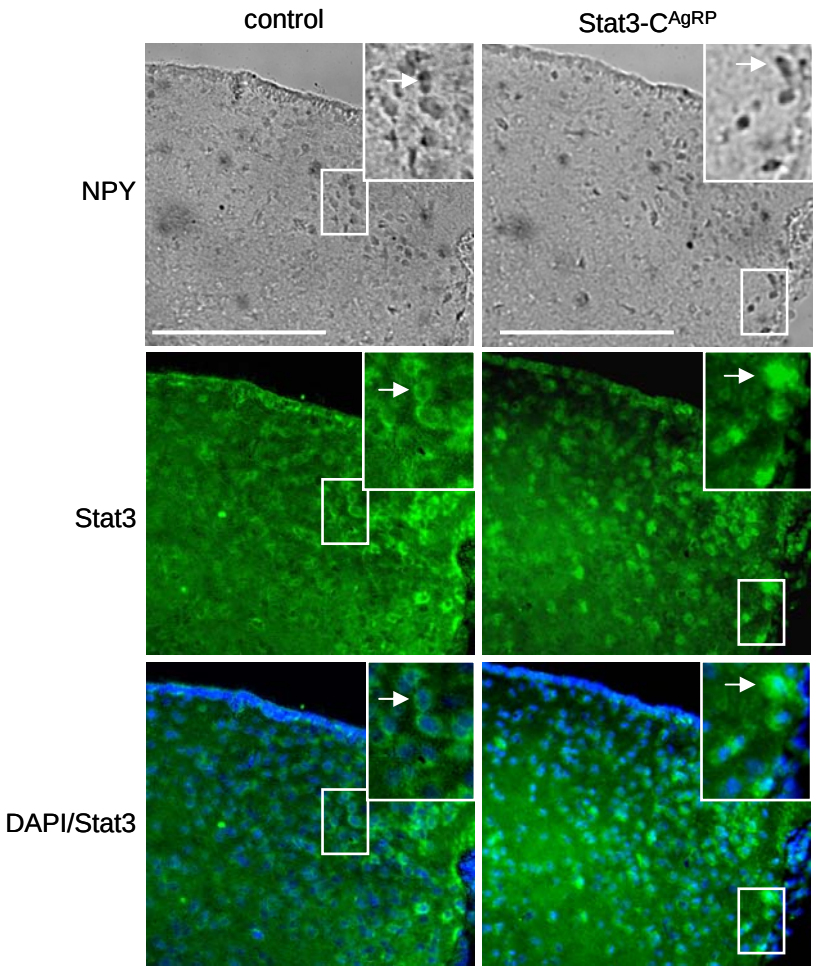


**Figure 10: Increased nuclear Stat3 expression in AgRP/NPY neurons of Stat3-C$^{AgRP}$ mice**

Combined NPY *in situ* hybridization and Stat3 immunohistochemistry of hypothalamic sections of fasted control and Stat3-C$^{AgRP}$ mice at the age of 12 weeks. In control animals, Stat3 is mainly located in the cytoplasm of NPY neurons, whereas expression of the transgene leads to high Stat3 accumulation in the nuclei of NPY neurons in Stat3-C$^{AgRP}$ mice. (Examples are depicted with arrows, respectively). Magnification: 100 x. Scale bar: 200 µm.

As Stat3 was described to exhibit oncogenic potential (Bromberg et al., 1999), the morphology of NPY-positive AgRP neurons of control and Stat3-C$^{AgRP}$ mice was analyzed. First, the size of NPY-positive neurons was determined using NPY-stained hypothalamic sections, but there was no difference detectable between the neurons of control and Stat3-C$^{AgRP}$ animals (Figure 11a). Furthermore, control and Stat3-C$^{AgRP}$ mice were injected intracerebroventricularly with the cell proliferation marker bromodeoxyuridine (BrdU). BrdU is a synthetic analogue of thymidine which is incorporated into the DNA during replication and can afterwards be detected using

specific antibodies. Combined NPY *in situ* hybridization and BrdU immunohistochemistry of hypothalamic sections revealed only a few BrdU-positive cells in both control and transgenic animals, and no BrdU incorporation into the DNA of NPY-positive neurons was detectable (Figure 11b).

Thus, expression of Stat3-C in AgRP neurons appears not to affect neuron size or induce proliferation/transformation of these neurons in Stat3-C$^{AgRP}$ mice.

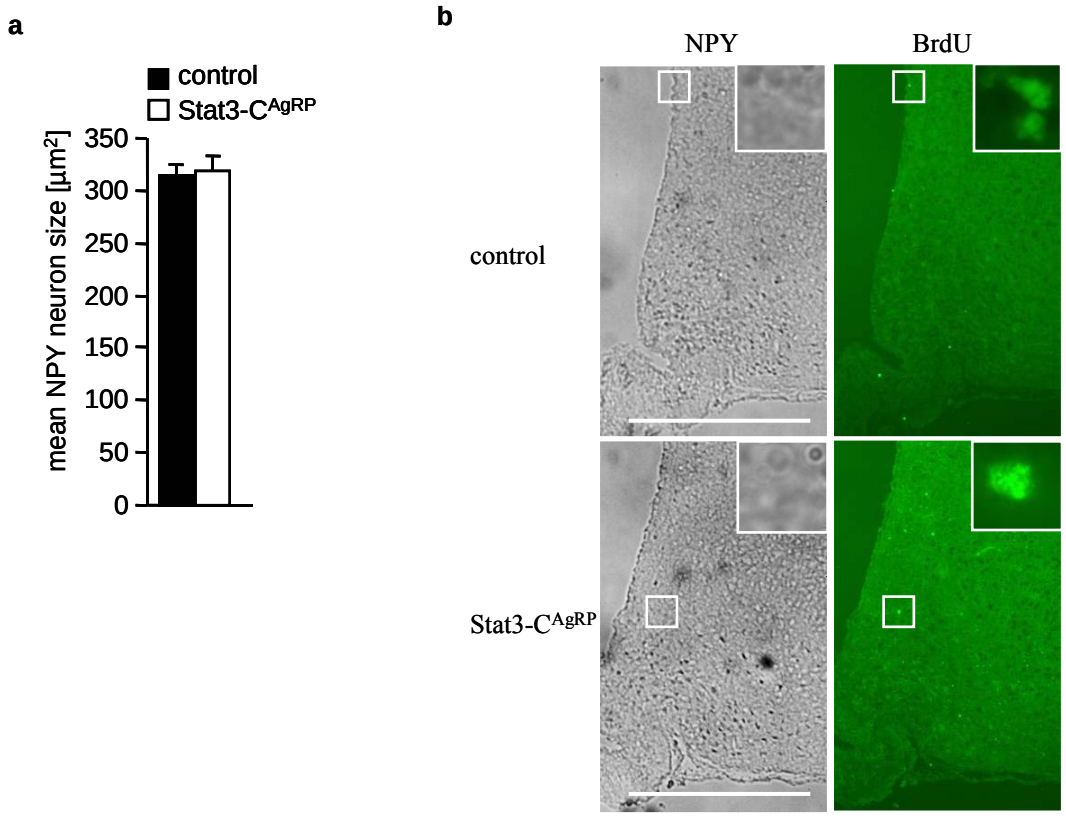


**Figure 11: AgRP/NPY neurons of Stat3-C$^{AgRP}$ mice display normal morphology**

**(a)** Mean NPY neuron size of control and Stat3-C$^{AgRP}$ mice at the age of 12 weeks measured on hypothalamic sections stained for NPY (n = 3 mice per genotype). 80 to 120 neurons per mouse were measured. **(b)** Representative photographs of hypothalamic sections of fasted control and Stat3-C$^{AgRP}$ mice at the age of 20 weeks double-stained for NPY and BrdU. No neurons positive for both NPY and BrdU were detected (n = 4 mice per genotype). Magnification: 100 x. Scale bar: 200 µm.

## 3.2 Leanness in Stat3-C$^{AgRP}$ mice

To investigate the impact of constitutively active Stat3 signaling in AgRP neurons on the regulation of energy homeostasis, body weight of female and male

control and Stat3-C$^{AgRP}$ mice was monitored from weaning until 20 weeks of age under normal chow diet (NCD) and high fat diet (HFD) conditions. Under NCD both female and male Stat3-C$^{AgRP}$ mice exhibited an approximately 10 % reduction in body weight compared to control mice (Figure 12). This difference was more pronounced under HFD conditions, under which Stat3-C$^{AgRP}$ mice gained 15 to 20 % less body weight until the age of 20 weeks. This reduction in body weight was similar in female and male Stat3-C$^{AgRP}$ mice (Figure 12).

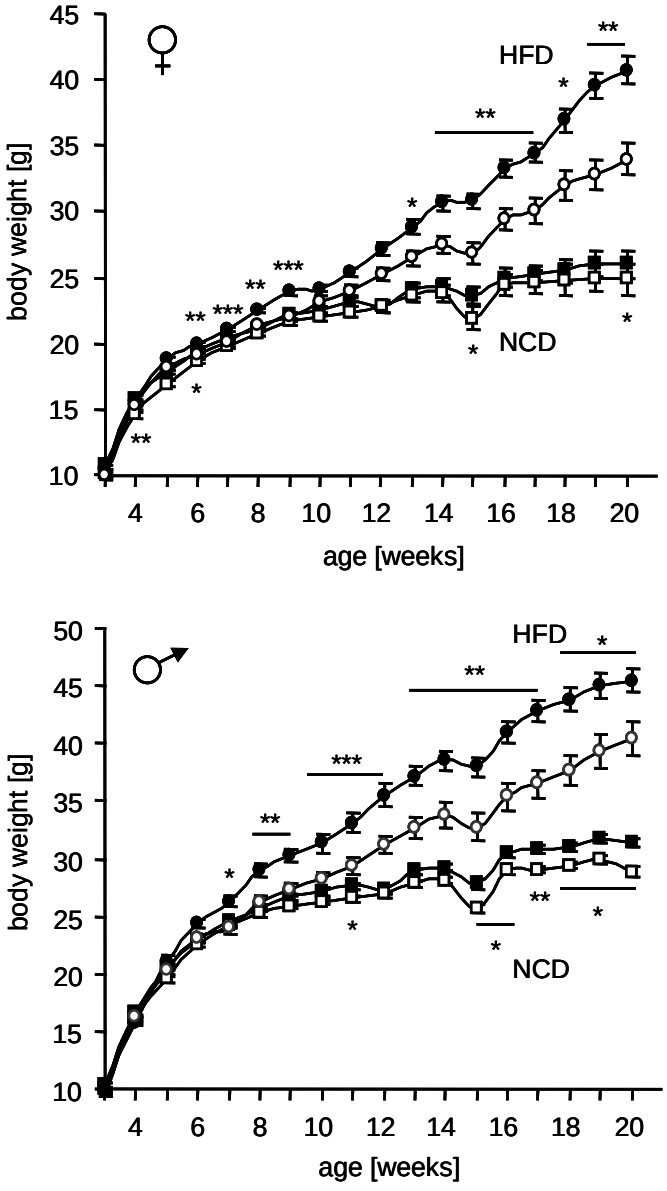


**Figure 12: Reduced body weight of Stat3-C$^{AgRP}$ mice**

Average body weight of female (upper panel) and male (lower panel) control and Stat3-C$^{AgRP}$ mice under NCD and HFD conditions (n = 18 to 53 of each genotype and condition). ■ NCD-fed control mice; □ NCD-fed Stat3-C$^{AgRP}$ mice; ● HFD-fed control mice, ○ HFD-fed Stat3-C$^{AgRP}$ mice.

To investigate, whether reduced body weight in Stat3-$C^{AgRP}$ mice resulted from a decrease in fat mass, the amount of epigonadal fat was examined in female and male control and Stat3-$C^{AgRP}$ mice both under NCD and HFD feeding conditions. Consistent with the growth curves, female and male Stat3-$C^{AgRP}$ mice displayed significantly reduced epigonadal fat pad mass at the age of 20 weeks compared to controls (Figure 13a and b). The difference in fat pad mass of Stat3-$C^{AgRP}$ and control mice increased upon HFD feeding, in that NCD-fed Stat3-$C^{AgRP}$ mice displayed a 30 % reduction in epigonadal fat pad weight and HFD-fed mice showed a 40 to 60 % reduction (Figure 13a and b).

To further confirm reduced adiposity in Stat3-$C^{AgRP}$ mice, also body fat content of 20 week old mice was determined by *in vivo* magnetic resonance spectrometry. Mean body fat content was 20 to 30 % decreased in Stat3-$C^{AgRP}$ mice under NCD and HFD conditions (Figure 13c). Leanness was accompanied by reduced concentrations of circulating leptin. Here, female Stat3-$C^{AgRP}$ mice exhibited the clearest (40 %) reduction, reflecting the most pronounced reduction in fat mass of this group of mice (Figure 13d).

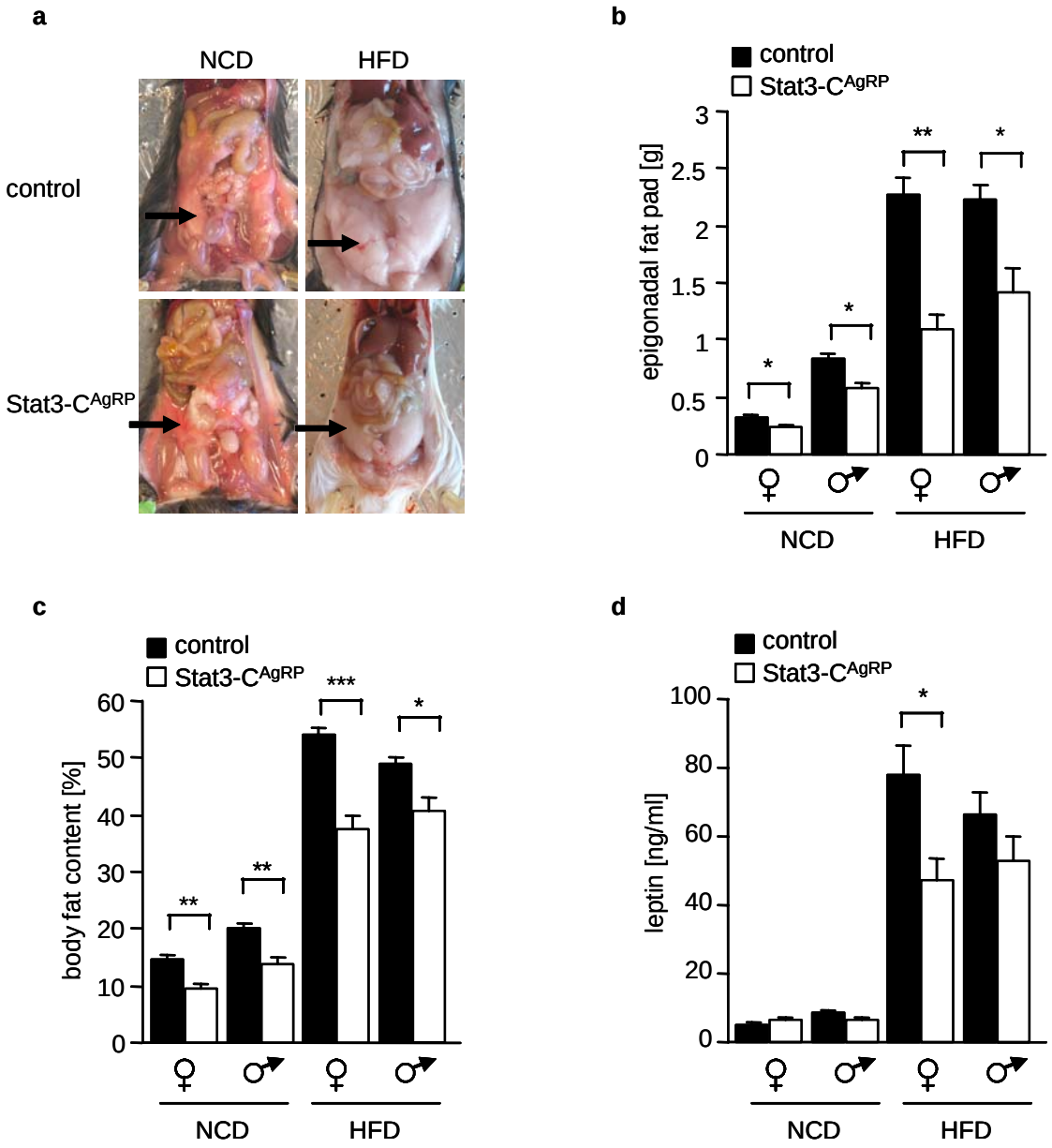


**Figure 13: Reduced adiposity of Stat3-C$^{AgRP}$ mice**

**(a)** Photographs of representative epigonadal fat pads *in situ* of male control and Stat3-C$^{AgRP}$ mice on NCD and female mice on HFD at the age of 20 weeks. **(b)** Epigonadal fat pad weights of control and Stat3-C$^{AgRP}$ mice on NCD and HFD at the age of 20 weeks (n = 5 to 16 of each genotype and condition). **(c)** Average body fat content of control and Stat3-C$^{AgRP}$ mice on NCD and on HFD at the age of 20 weeks measured by nuclear magnetic resonance (n = 7 to 11 of each genotype and condition). **(d)** Serum leptin concentrations of control and Stat3-C$^{AgRP}$ mice on NCD and HFD at the age of 20 weeks (n = 13 to 20 of each genotype and condition).

To investigate whether the reduction in white adipose tissue mass in Stat3-$C^{AgRP}$ mice was accompanied by altered adipocyte characteristics, the histomorphology of white adipose tissue in control and Stat3-$C^{AgRP}$ mice was assessed by histological analysis, which revealed a significant reduction of adipocyte size in Stat3-$C^{AgRP}$ mice compared to control mice (Figure 14a). Quantitative assessment of adipocyte size revealed a 70 % reduction in the mean adipocyte size in Stat3-$C^{AgRP}$ mice compared to control mice under NCD conditions (Figure 14b). Similarly, mean adipocyte size in Stat3-$C^{AgRP}$ mice exposed to HFD was reduced by 80 % compared to control mice fed the same diet (Figure 14b). Analysis of adipocyte size distribution revealed an increased number of small adipocytes and an absence of large adipocytes in epigonadal white adipose tissue of Stat3-$C^{AgRP}$ mice both under NCD and HFD conditions (Figure 14c).

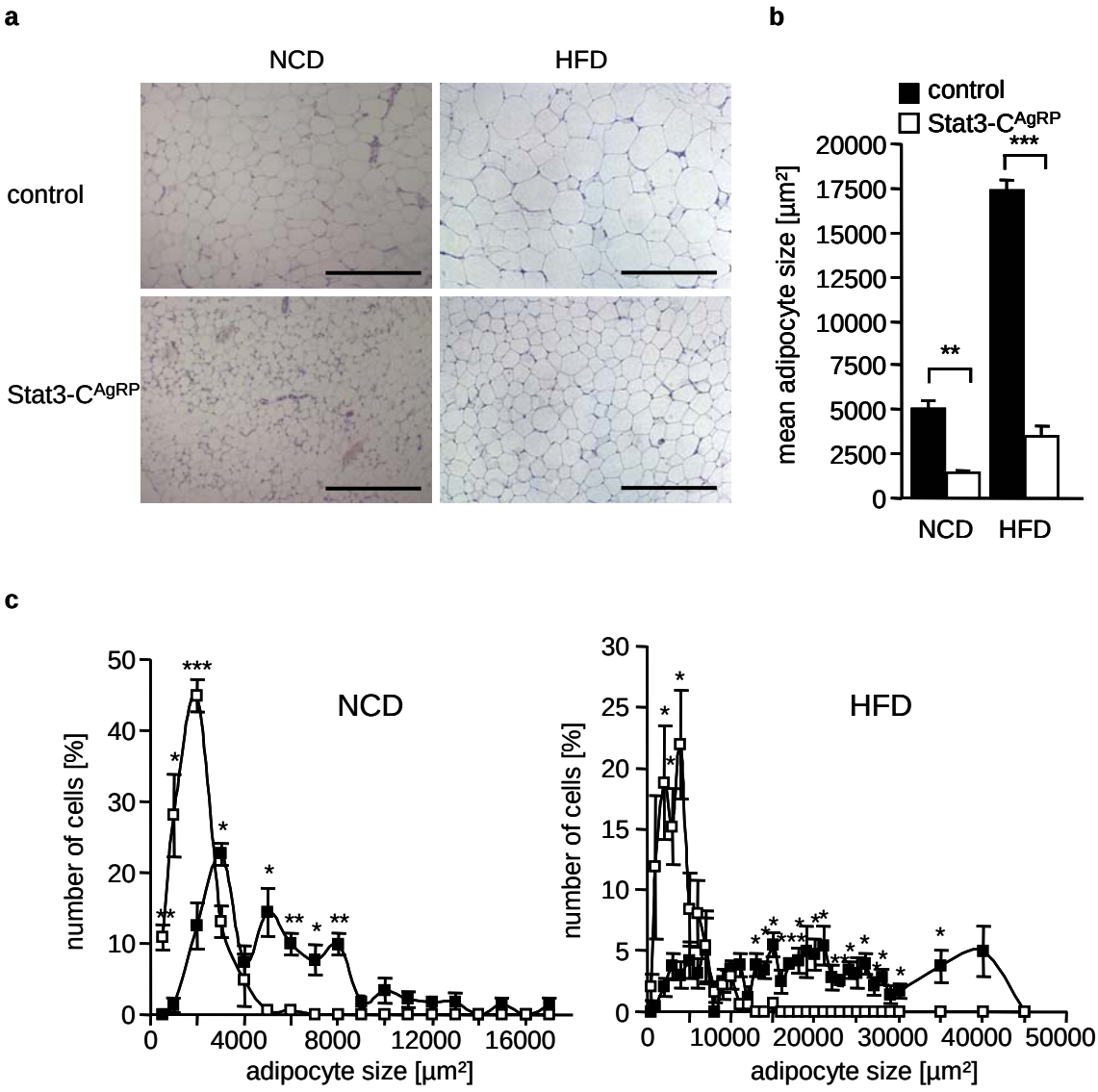


**Figure 14: Reduction of adipocyte size in Stat3-C$^{AgRP}$ mice**

**(a)** Representative hematoxylin/eosin-stained epigonadal fat pad sections from male control and Stat3-C$^{AgRP}$ mice on NCD and HFD at the age of 20 weeks. Magnification: 100 x. Scale bar: 500 µm. **(b)** Mean adipocyte size of epigonadal fat of control and Stat3-C$^{AgRP}$ mice on NCD and HFD at the age of 20 weeks (n = 4 to 5 mice per condition). 28 to 49 adipocytes per mouse were measured. **(c)** Adipocyte size distribution of control and Stat3-C$^{AgRP}$ mice under NCD (left panel) and HFD conditions (right panel) (n = 4 to 5 mice per condition). 28 to 49 adipocytes per mouse were measured. ■ control mice; □ Stat3-C$^{AgRP}$ mice.

To analyze the onset and development of reduced adiposity, body fat content of Stat3-C$^{AgRP}$ mice was determined at different postnatal ages. While at the age of 3 weeks, there was no difference in body fat content between control and Stat3-C$^{AgRP}$ mice, 13 and 20 week old female and male Stat3-C$^{AgRP}$ mice both under NCD and HFD

conditions showed 20 to 40 % reduced fat contents (Figure 15). Thus, leanness in Stat3-$C^{AgRP}$ mice progressively develops after weaning.

Taken together, these results indicate that constitutive activation of Stat3-dependent signaling in AgRP-expressing neurons results in a reduction of body weight and fat mass.

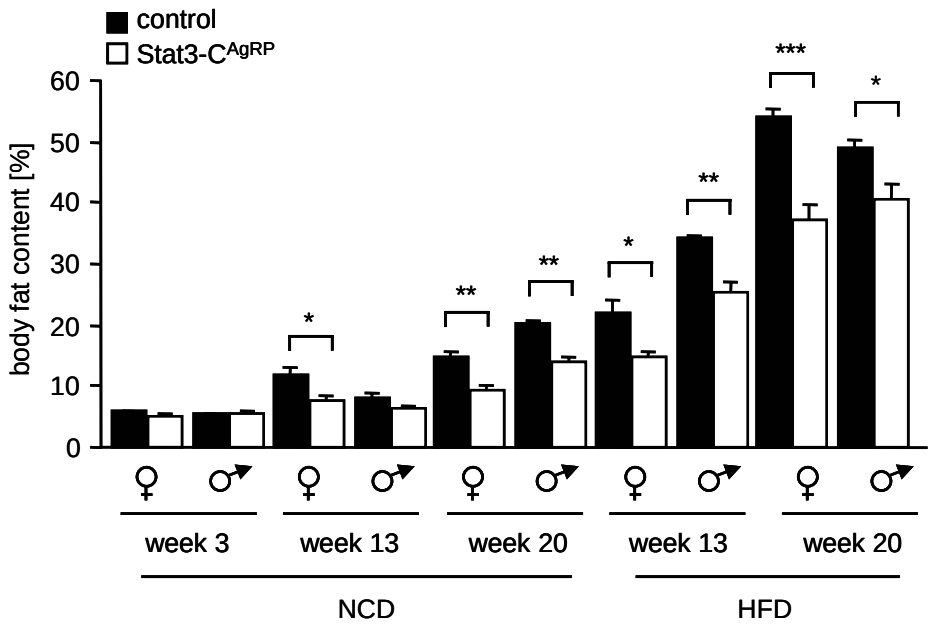


**Figure 15: Stat3-$C^{AgRP}$ mice develop reduced adiposity after the postweaning age**

Average body fat content of control and Stat3-$C^{AgRP}$ mice under NCD and HFD conditions at the indicated ages measured by nuclear magnetic resonance (n = 7 to 11 of each genotype and condition).

## 3.3 Improved glucose metabolism in Stat3-$C^{AgRP}$ mice

Next, glucose metabolism was compared in control and Stat3-$C^{AgRP}$ mice to analyze whether activation of Stat3 signaling in AgRP neurons of Stat3-$C^{AgRP}$ mice leads to alterations in glucose metabolism. First, blood glucose of control and Stat3-$C^{AgRP}$ mice was measured. NCD- and HFD-fed Stat3-$C^{AgRP}$ mice exhibited normal blood glucose levels in the fed condition (Figure 16). A 16 h fast resulted in significantly lower blood glucose concentrations in female and male Stat3-$C^{AgRP}$ mice on HFD compared to controls, whereas Stat3-$C^{AgRP}$ mice on NCD displayed normal blood glucose concentrations upon fasting (Figure 16).

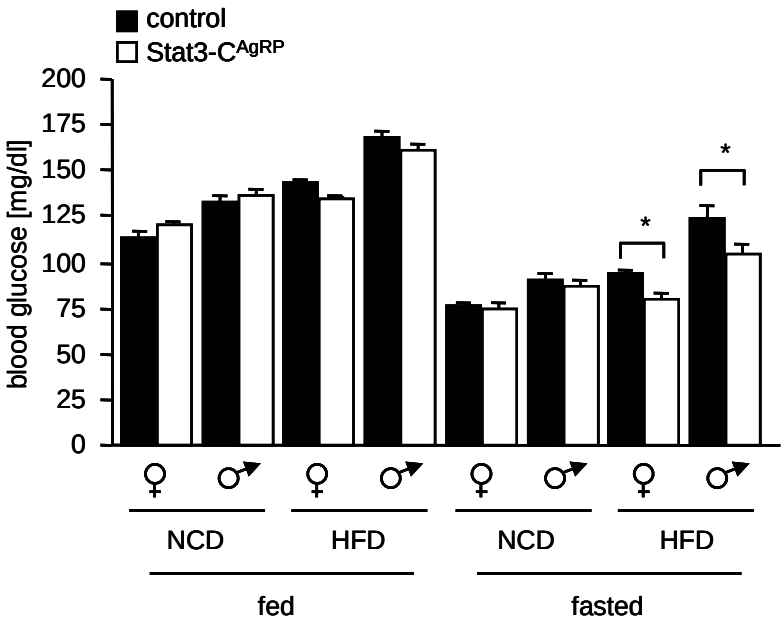


**Figure 16: Improved fasted blood glucose in HFD-fed Stat3-C$^{AgRP}$ mice**

Fed and fasted blood glucose concentrations of control and Stat3-C$^{AgRP}$ mice under NCD and HFD conditions at the age of 14 to 15 weeks (n = 15 to 27 of each genotype and condition).

Moreover, glucose homeostasis of female and male Stat3-C$^{AgRP}$ mice was investigated by insulin and glucose tolerance tests. Insulin tolerance tests revealed no difference between insulin sensitivity of control and Stat3-C$^{AgRP}$ mice, neither under NCD nor under HFD conditions (Figure 17a). However, glucose tolerance tests demonstrate that both female and male HFD-fed Stat3-C$^{AgRP}$ mice were significantly more glucose tolerant than controls, while Stat3-C$^{AgRP}$ mice under NCD conditions exhibited unaltered glucose tolerance (Figure 17b).

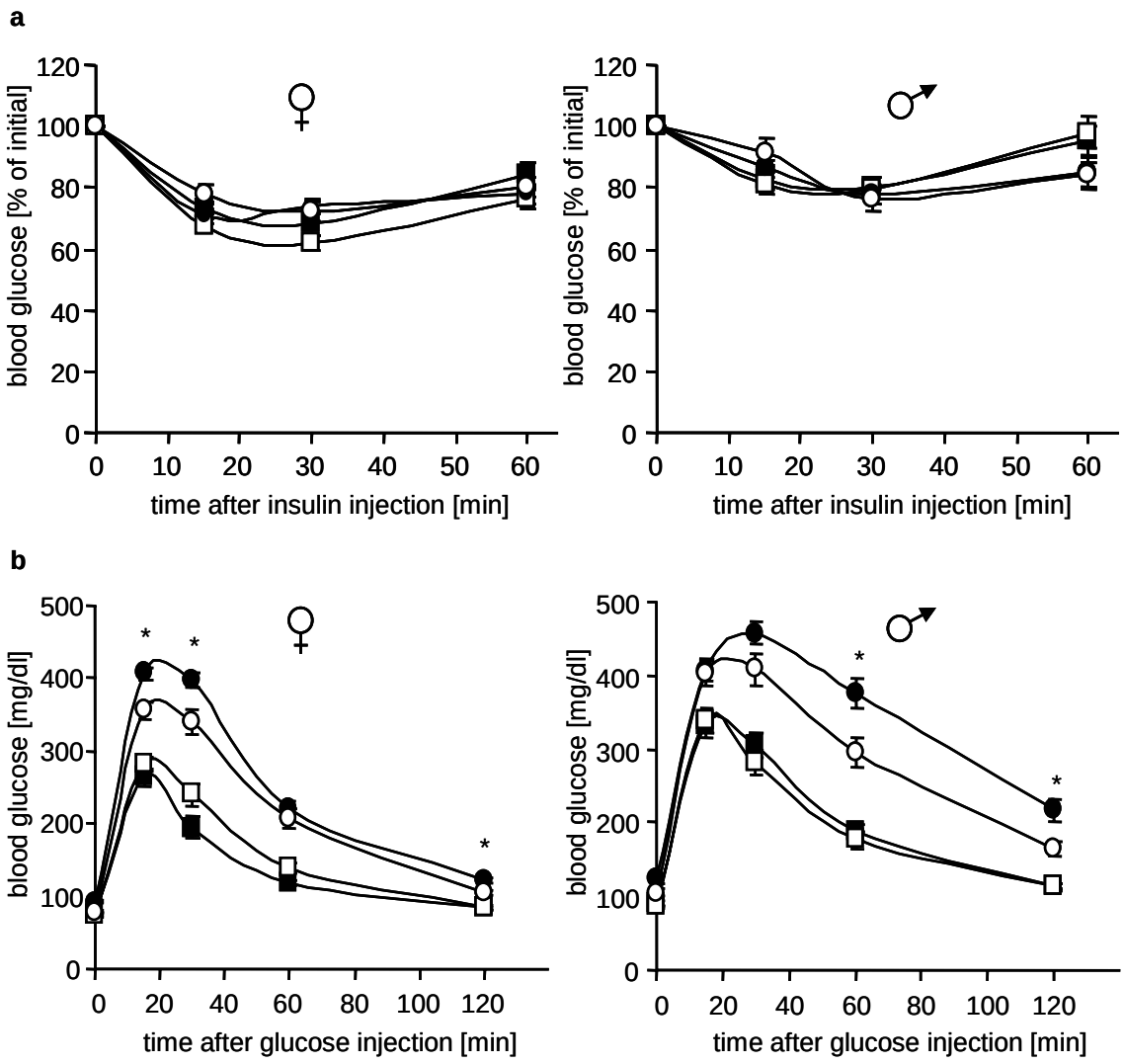


**Figure 17: Unaltered insulin sensitivity and improved glucose tolerance in Stat3-C$^{AgRP}$ mice**

**(a)** Insulin tolerance tests and **(b)** glucose tolerance tests of female (left panel) and male (right panel) control and Stat3-C$^{AgRP}$ mice under NCD and HFD conditions at the age of 13 and 14 weeks, respectively (n = 15 to 22 of each genotype and condition). ■ NCD-fed control mice; □ NCD-fed Stat3-C$^{AgRP}$ mice; ● HFD-fed control mice, ○ HFD-fed Stat3-C$^{AgRP}$ mice.

Consistent with these findings, serum insulin concentrations of Stat3-C$^{AgRP}$ mice under NCD conditions were not altered, but serum levels of Stat3-C$^{AgRP}$ mice on HFD were slightly decreased (Figure 18).

The increased glucose tolerance displayed by Stat3-C$^{AgRP}$ mice compared to controls indicates that activation of Stat3 in AgRP neurons results in improved glucose metabolism.

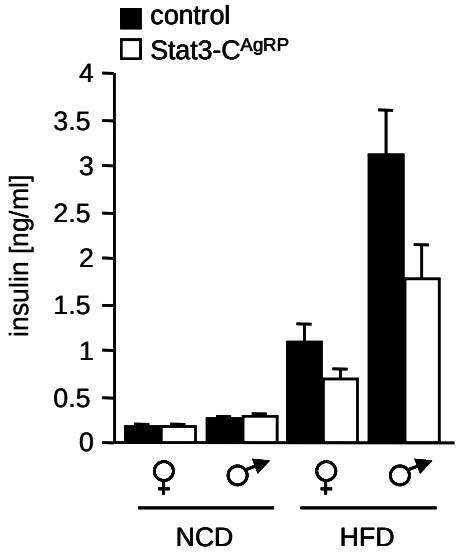


**Figure 18: Slightly decreased serum insulin concentrations in HFD-fed Stat3-C$^{AgRP}$ mice**
Serum insulin concentrations of control and Stat3-C$^{AgRP}$ mice under NCD and HFD conditions at the age of 20 weeks (n = 13 to 20 of each genotype and condition).

## 3.4 Stat3 activation in AgRP neurons does not alter food intake but results in increased energy expenditure

To further analyze the mechanisms resulting in the leanness of Stat3-C$^{AgRP}$ mice, energy intake and energy expenditure in these mice were measured. Stat3-C$^{AgRP}$ mice showed a food intake comparable to control mice despite their lower body and fat mass (Figure 19a). This unaltered food intake was consistent during development both under NCD and HFD conditions. However, when food intake was corrected for body weight, 9 and 13 week old Stat3-C$^{AgRP}$ mice exhibited a relative hyperphagia (Figure 19b). This relative hyperphagia was present in female and male Stat3-C$^{AgRP}$ mice under both NCD and HFD conditions. In contrast, the relative food intake of 3 week old mice did not differ from that of control animals, neither under NCD, nor under HFD conditions (Figure 19b).

Taken together, Stat3-C$^{AgRP}$ mice develop a relative hyperphagia after the postweaning age. Thus, decreased body and fat mass in Stat3-C$^{AgRP}$ mice is clearly not the result of reduced caloric intake.

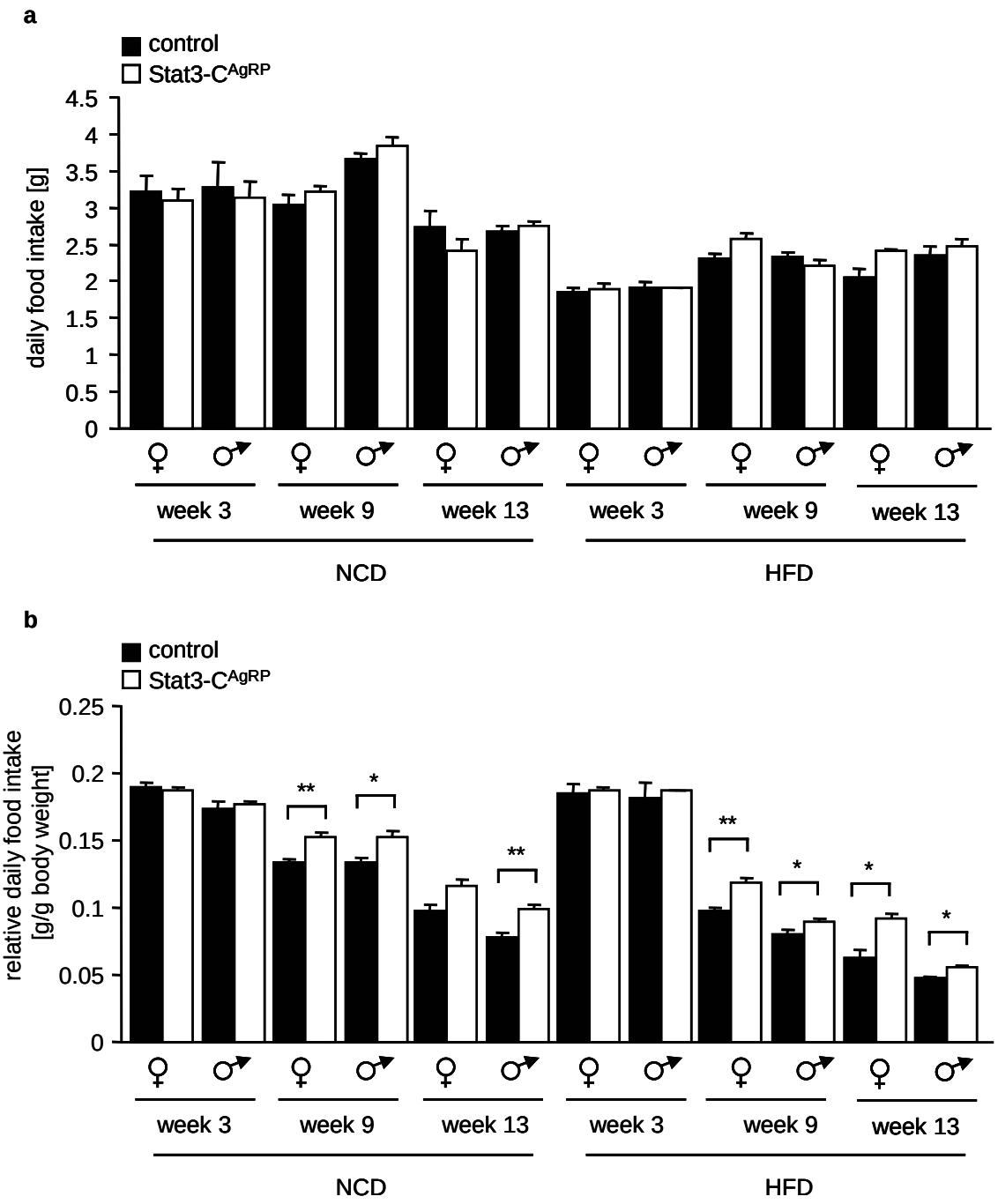


**Figure 19: Relative hyperphagia of Stat3-C$^{AgRP}$ mice**

**(a)** Absolute and **(b)** relative (corrected for body weight) daily food intake of NCD- and HFD-fed control and Stat3-C$^{AgRP}$ mice at the indicated ages (n = 6 to 15 of each genotype and condition).

Then, energy expenditure of Stat3-C$^{AgRP}$ mice at different ages was determined by indirect calorimetrical analysis. This analysis revealed an increase in oxygen consumption of Stat3-C$^{AgRP}$ mice compared to control mice (Figure 20). While 5 week

old Stat3-C$^{AgRP}$ mice showed only a slight tendency for higher oxygen consumption than control animals, 9 week old mice consumed 15 to 20 % more oxygen during both day and night phases (Figure 20a and b). Oxygen consumption of older Stat3-C$^{AgRP}$ mice at the age of 13 weeks was increased by more than 30 % during the light phase, and by even more than 40 % during the dark phase (Figure 20c).

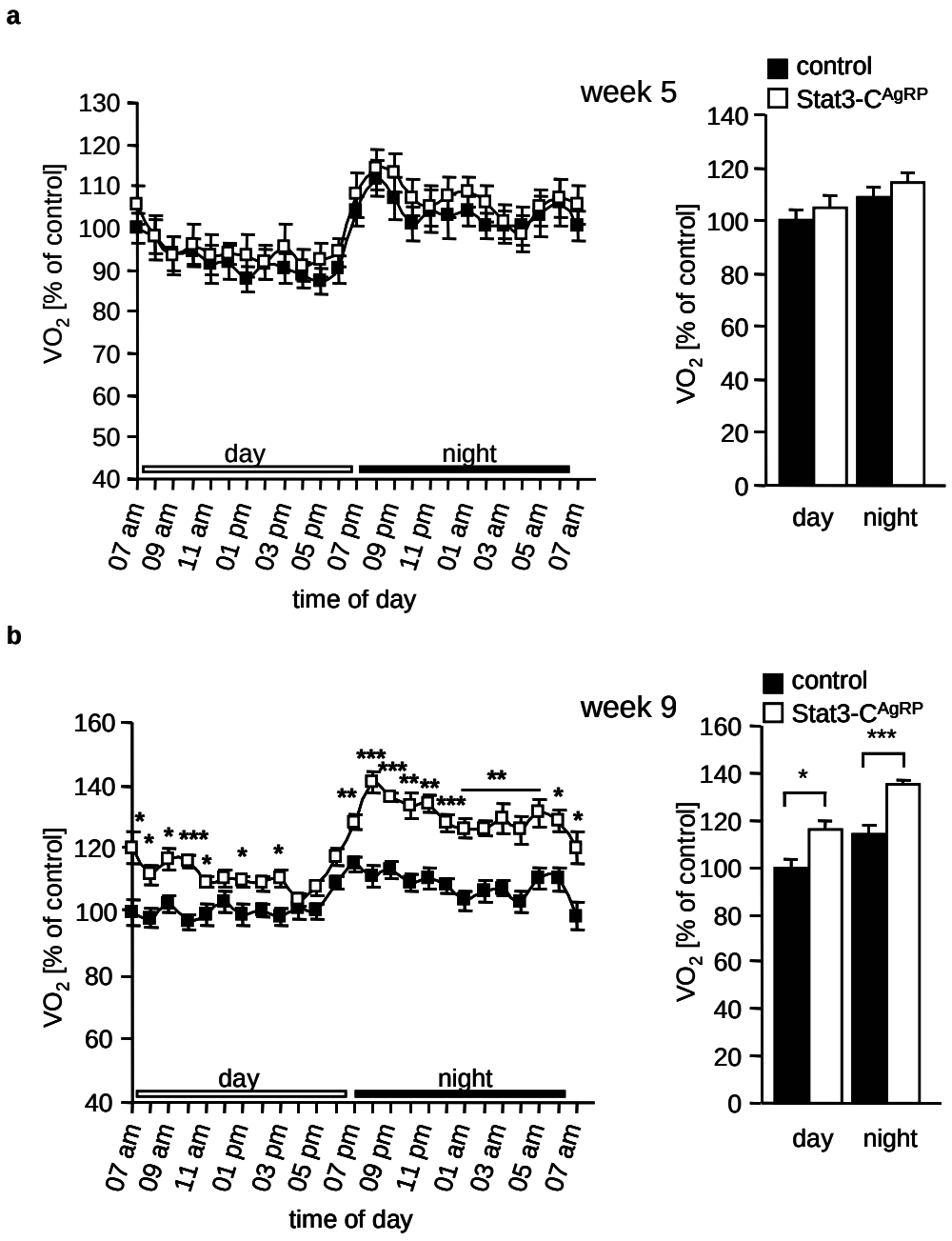

**c**

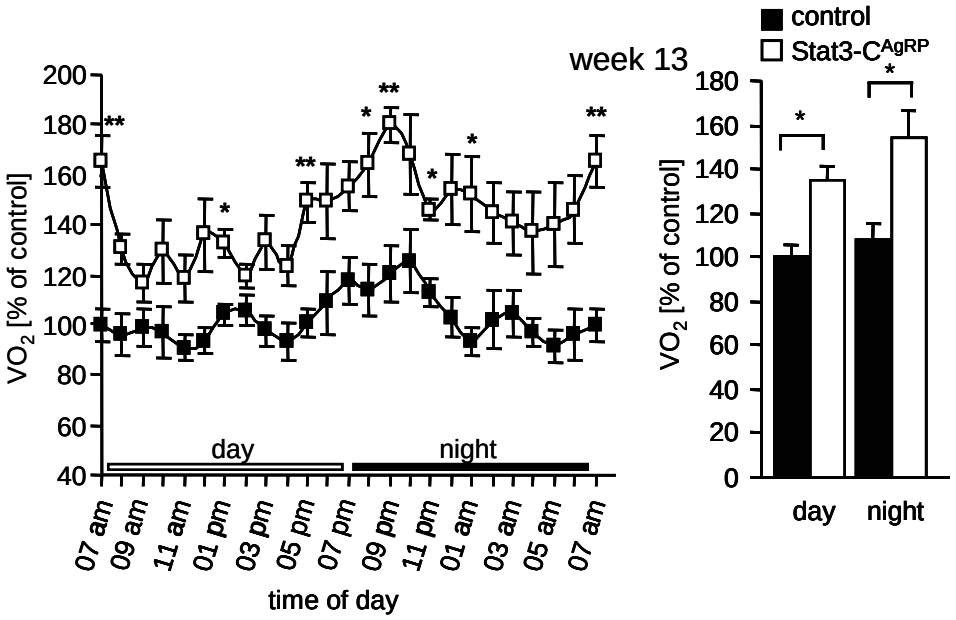


**Figure 20: Increased basal metabolic rate in Stat3-C$^{AgRP}$ mice**

Oxygen consumption of control and Stat3-C$^{AgRP}$ mice on HFD over time (left panel) and mean oxygen consumption of control and Stat3-C$^{AgRP}$ mice (right panel) of **(a)** 5 week old, **(b)** 9 week old and **(c)** 13 week old mice. ■ control mice; □ Stat3-C$^{AgRP}$ mice.

Interestingly, the respiratory exchange ratio, which is the ratio between produced carbon dioxide and consumed oxygen, remained unaltered in Stat3-C$^{AgRP}$ mice compared to control mice, indicating that control and Stat3-C$^{AgRP}$ mice utilize the same substrates for oxidative metabolism (Figure 21).

Taken together, these data indicate that leanness in Stat3-C$^{AgRP}$ mice is the consequence of increased energy expenditure.

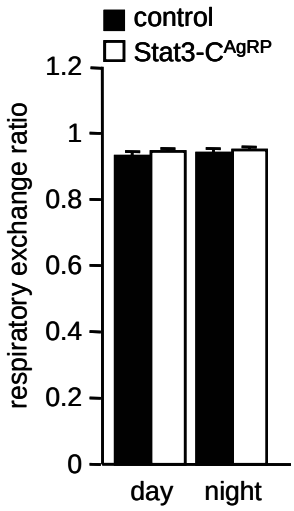


**Figure 21: Unaltered respiratory exchange ratio of Stat3-C$^{AgRP}$ mice**

Mean respiratory exchange ratio of control and Stat3-C$^{AgRP}$ mice under HFD conditions at the age of 13 weeks (n = 6 of each genotype).

## 3.5 Unaltered AgRP expression in Stat3-C$^{AgRP}$ mice

Next, the expression of different neuropeptides critically involved in the regulation of energy homeostasis was determined, particularly the expression of AgRP. Basal and fasting-induced AgRP expression in female and male Stat3-C$^{AgRP}$ mice under NCD conditions were indistinguishable from AgRP expression in control mice (Figure 22a). After 48 h of fasting, AgRP mRNA levels were equally elevated in control and Stat3-C$^{AgRP}$ mice. This confirms that activation of Stat3 does not alter fasting-induced transcription of AgRP mRNA (Kaelin et al., 2006). Analysis of NPY and POMC mRNA expression revealed no difference between Stat3-C$^{AgRP}$ and control mice (Figure 22b).

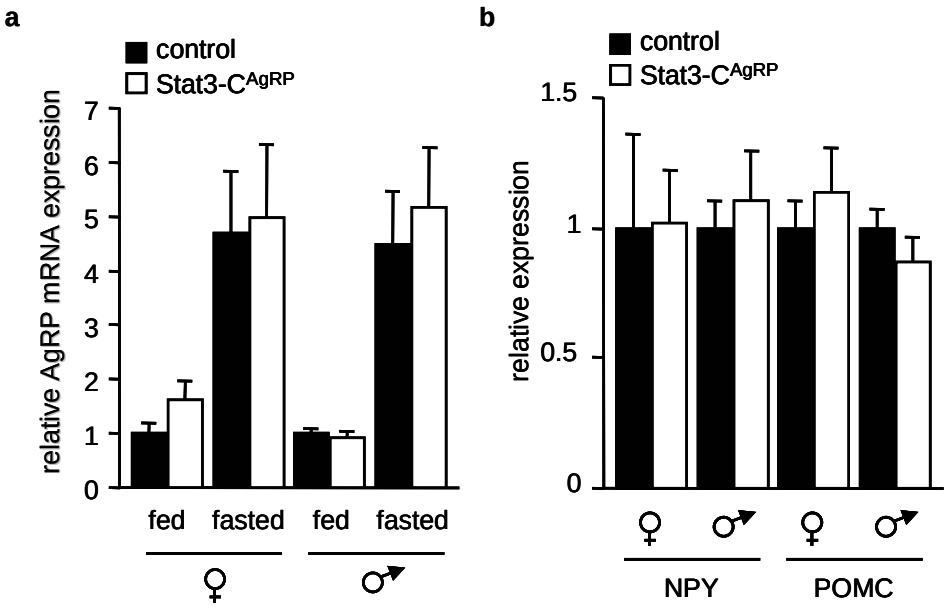


**Figure 22: Unaltered hypothalamic neuropeptide expression of Stat3-C$^{AgRP}$ mice**

**(a)** Fasting-induced AgRP expression of NCD-fed control and Stat3-C$^{AgRP}$ mice (n = 7 to 9 of each genotype). **(b)** Hypothalamic expression of NPY and POMC of control and Stat3-C$^{AgRP}$ mice on NCD (n = 7 of each genotype).

As leanness in Stat3-C$^{AgRP}$ mice is a consequence of increased energy expenditure, mRNA expression of uncoupling protein (UCP) was determined in white adipose tissue, skeletal muscle, and brown adipose tissue of female and male control and Stat3-C$^{AgRP}$ mice exposed to HFD. UCPs are mitochondrial proteins involved in energy metabolism, thermogenesis and obesity. Whereas UCP-1 is uniquely expressed in brown adipose tissue, UCP-2 is expressed in many organs, and UCP-3 is predominantly expressed in skeletal muscle. However, this analysis revealed unaltered UCP mRNA expression in the analyzed tissues (Figure 23a, b, c). Since energy expenditure is also controlled by thyroid function, free triiodothyronine (fT3) levels were tested as an indicator of thyroid function in the different groups of mice. Serum fT3 levels were not altered in female and male Stat3-C$^{AgRP}$ mice either under NCD or under HFD conditions (Figure 23d).

Thus, increased energy expenditure occurs in the presence of unaltered uncoupling protein expression and normal thyroid function.

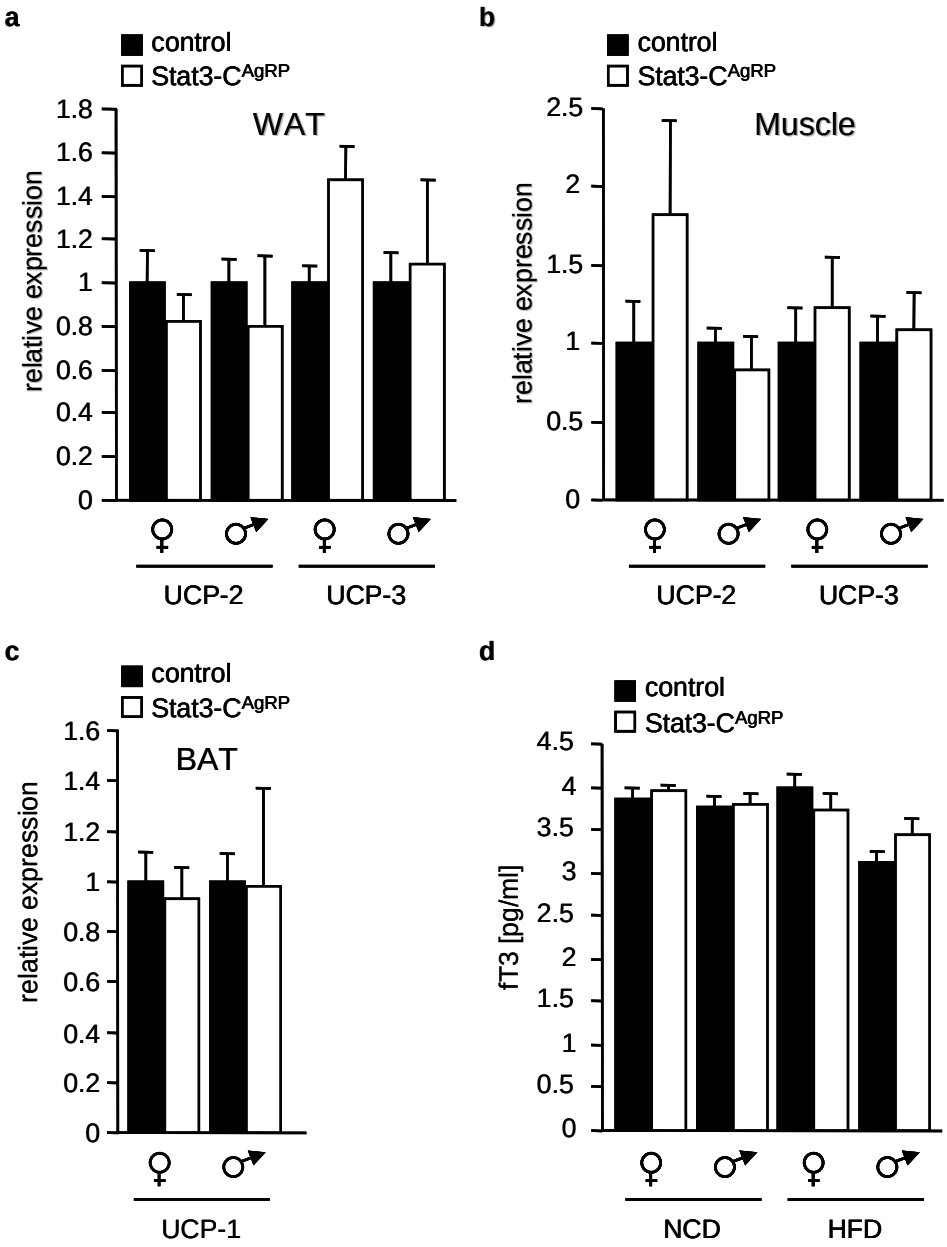


**Figure 23: Unaltered UCP expression and thyroid function of Stat3-C$^{AgRP}$ mice**

**(a)** Expression of UCP-2 and UCP-3 in white adipose tissue (WAT) of female and male control and Stat3-C$^{AgRP}$ mice (n = 6 to 9 of each genotype). **(b)** Expression of UCP-2 and UCP-3 in skeletal muscle of female and male control and Stat3-C$^{AgRP}$ mice (n = 5 to 7 of each genotype). **(c)** Expression of UCP-1 in brown adipose tissue (BAT) of control and Stat3-C$^{AgRP}$ mice (n = 6 to 9 of each genotype). **(d)** FT3 levels in serum of control and Stat3-C$^{AgRP}$ mice under NCD and HFD conditions (n = 13 to 20 of each genotype and condition). All experiments were performed on mice under HFD conditions at the age of 20 weeks, if not stated otherwise.

## 3.6 Stat3-C$^{AgRP}$ mice exhibit increased locomotor activity

To investigate whether the leanness and the increase in energy expenditure of Stat3-C$^{AgRP}$ mice resulted from enhanced locomotor activity, basal locomotor activity of control and Stat3-C$^{AgRP}$ mice was analyzed. At 5 weeks of age Stat3-C$^{AgRP}$ mice exhibited a mild tendency to higher locomotor activity than their control littermates, consistent with the absent tendency towards higher energy expenditure (Figure 24a). At 9 weeks of age, however, Stat3-C$^{AgRP}$ mice exhibited a drastic increase of basal locomotor activity, by 40 % during the light phase and by 60 % during the dark phase, compared to control mice, correlating with the observed significant increase of energy expenditure at this age (Figure 24b). Stat3-C$^{AgRP}$ mice exhibited highest locomotor activity in the beginning of the dark phase, being more than twice as active as their control littermates (Figure 24b).

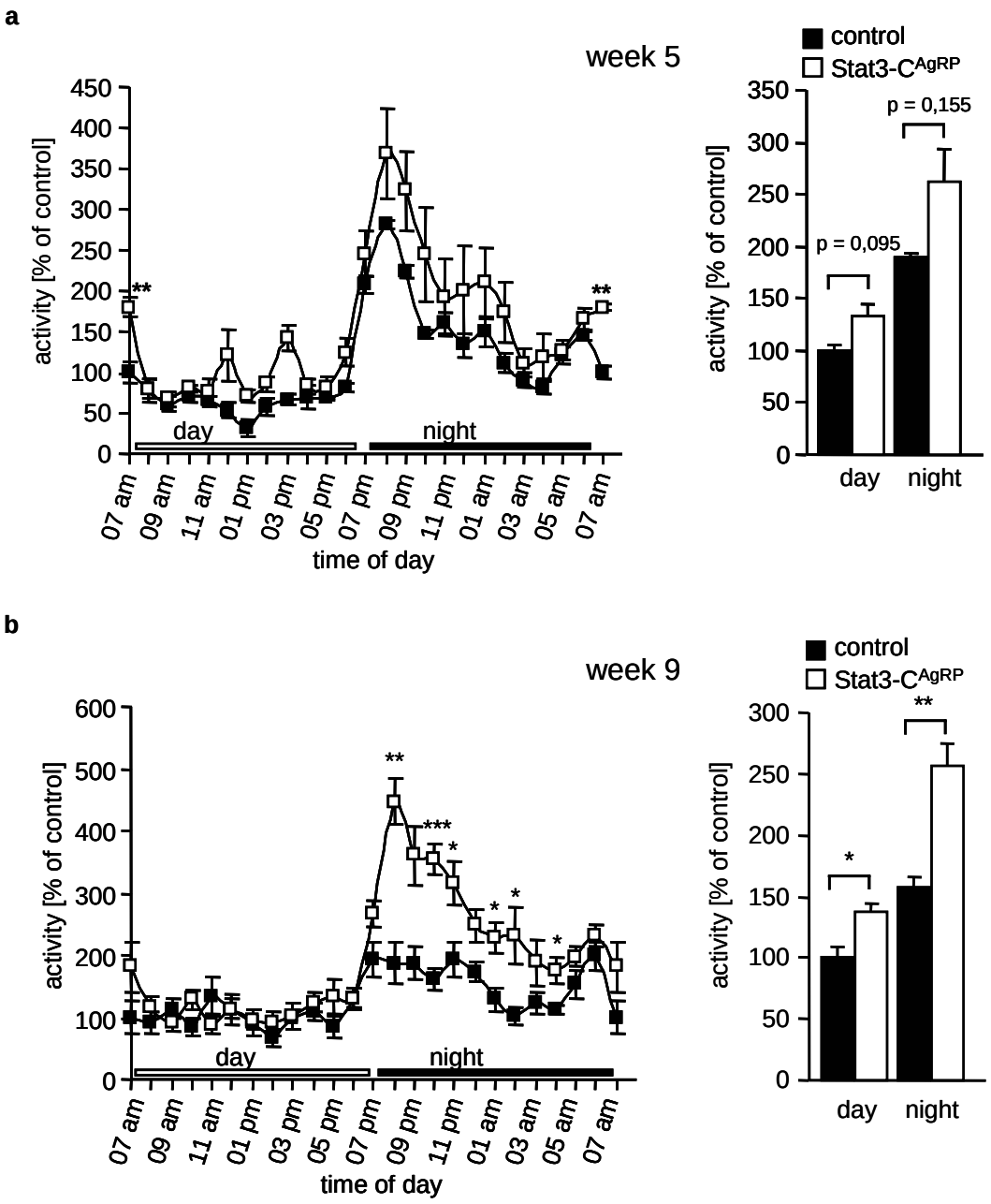


**Figure 24: Increased basal locomotor activity of Stat3-C$^{AgRP}$ mice**

Basal locomotor activity of control and Stat3-C$^{AgRP}$ mice on HFD over time and mean basal locomotor activity of **(a)** 5 week old and **(b)** 9 week old control and Stat3-C$^{AgRP}$ mice (n = 7 to 8 of each genotype). ■ control mice; □ Stat3-C$^{AgRP}$ mice.

As fasting increases light and dark phase locomotor activity (Overton and Williams, 2004; Williams et al., 2003), fasting-induced locomotor activity was analyzed next, to investigate whether locomotor activity of Stat3-C$^{AgRP}$ mice remained higher than that of control animals upon fasting. Both control and Stat3-C$^{AgRP}$ mice showed

increased locomotor activity upon food deprivation in the light and dark phases (Figure 25). Again, the fasting-induced locomotor activity of Stat3-C$^{AgRP}$ mice was also significantly higher than that of control animals. While the locomotor activity of Stat3-C$^{AgRP}$ mice was increased by 60 % during the light phase, it was even 70 % higher during the dark phase compared to control littermates (Figure 25).

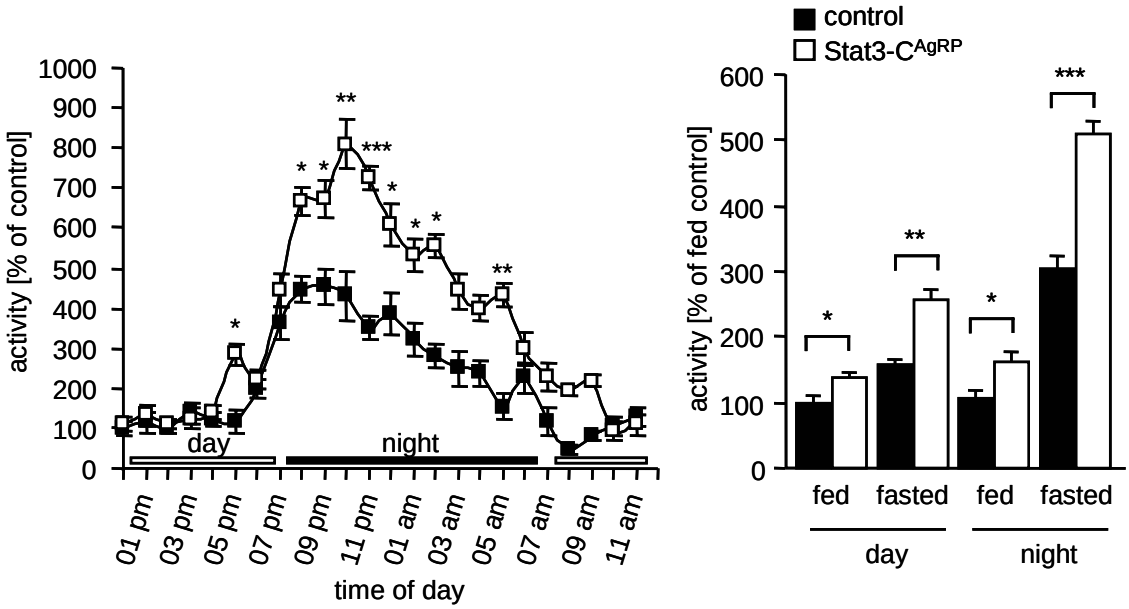


**Figure 25: Increased fasting-induced locomotor activity of Stat3-C$^{AgRP}$ mice**

Fasting-induced locomotor activity of control and Stat3-C$^{AgRP}$ mice under HFD conditions over time and mean basal and fasting-induced locomotor activity of control and Stat3-C$^{AgRP}$ mice at the age of 9 weeks (n = 7 to 8 of each genotype) . ■ control mice; □ Stat3-C$^{AgRP}$ mice.

To further address whether activating Stat3 signaling specifically in AgRP neurons accounts for the observed increase in locomotor activity, mice were generated expressing Stat3-C specifically in neighbouring POMC neurons in the ARC of the hypothalamus. In contrast to Stat3-C$^{AgRP}$ mice, Stat3-C$^{POMC}$ mice exhibited unaltered locomotor activity and energy expenditure at an age, where both parameters are altered in Stat3-C$^{AgRP}$ mice, further supporting the specificity of the observed phenotype in Stat3-C$^{AgRP}$ mice (Figure 26a and b).

Taken together, leanness and increased energy expenditure in Stat3-C$^{AgRP}$ mice are the result of a markedly increased locomotor activity of these mice.

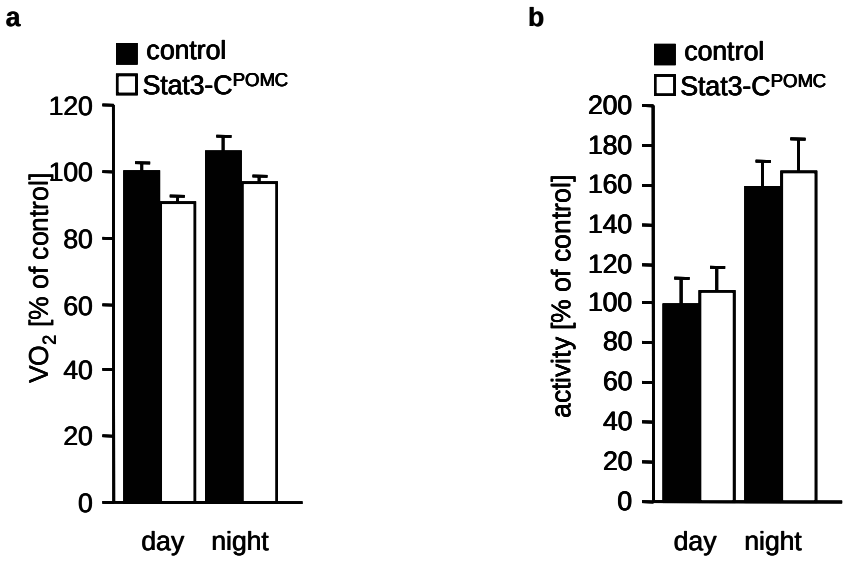


**Figure 26: Unaltered metabolic rate and activity of Stat3-C$^{POMC}$ mice**

Mean **(a)** oxygen consumption and **(b)** locomotor activity of control and Stat3-C$^{POMC}$ mice at the age of 8 weeks (n = 5 of each genotype).

To gain insight into the mechanism underlying the increase in locomotor activity of Stat3-C$^{AgRP}$ mice, circulating plasma catecholamine concentrations were measured in control and Stat3-C$^{AgRP}$ mice to analyze sympathetic nerve activity. Under both NCD and HFD conditions, epinephrine and norepinephrine concentrations tended to be lower in female and male Stat3-C$^{AgRP}$ mice compared to control mice, while only the difference of plasma epinephrine and norepinephrine of NCD-fed male animals reached statistical significance (Figure 27a and b).

Thus, increased locomotor activity does not result from increased peripheral sympathetic nerve activity.

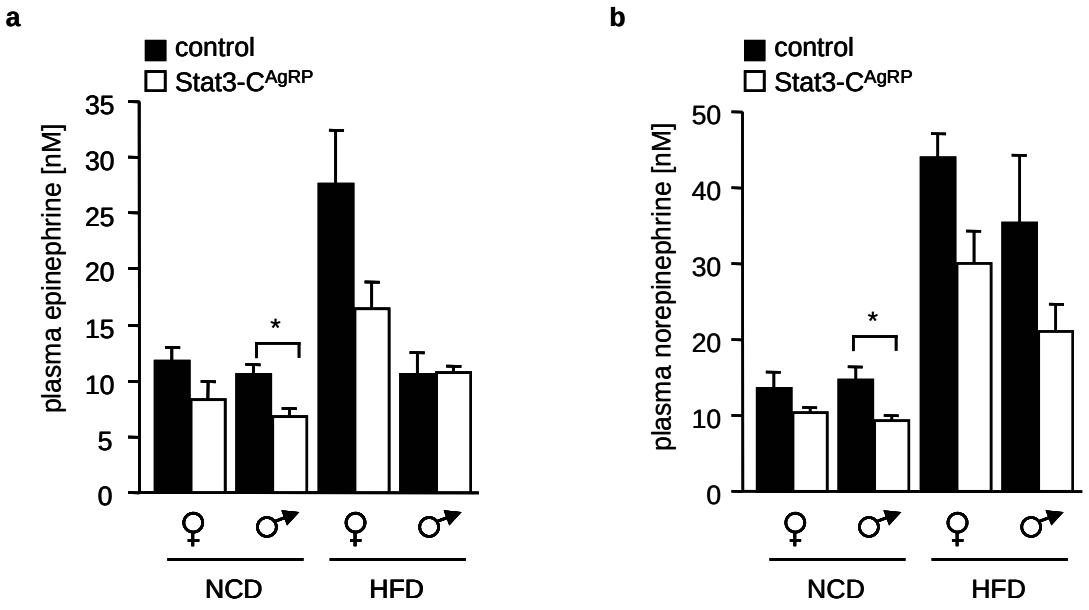


**Figure 27: Plasma catecholamine concentrations of Stat3-C$^{AgRP}$ mice**

Plasma **(a)** epinephrine and **(b)** norepinephrine concentrations of female and male control and Stat3-C$^{AgRP}$ mice on NCD and HFD at the age of 16 to 18 weeks (n = 8 to 14 of each genotype and condition).

Next, catecholamine and serotonin contents in different brain areas critically implicated in the regulation of locomotor activity were determined, but this analysis revealed no significant differences between control and Stat3-C$^{AgRP}$ mice in the examined brain areas (Figure 28a, b, c and d). Nevertheless, Stat3-C$^{AgRP}$ mice exhibited a tendency for higher dopamine and serotonin content in the striatum and for higher dopamine content in the frontal cortex (Figure 28c and d).

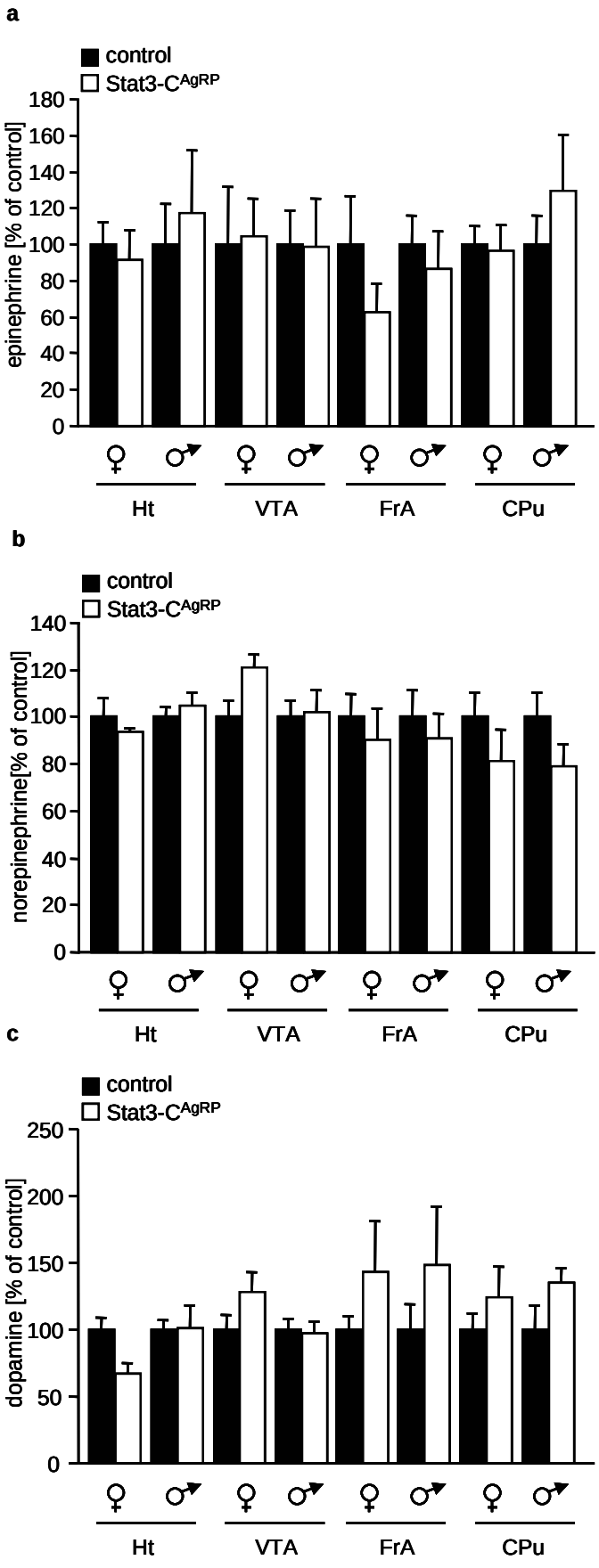
a
control
Stat3-C^AgRP
epinephrine [% of control]
180
160
140
120
100
80
60
40
20
0
♀ ♂ ♀ ♂ ♀ ♂ ♀ ♂
Ht
VTA
FrA
CPu
b
control
Stat3-C^AgRP
norepinephrine[% of control]
140
120
100
80
60
40
20
0
♀ ♂ ♀ ♂ ♀ ♂ ♀ ♂
Ht
VTA
FrA
CPu
c
control
Stat3-C^AgRP
dopamine [% of control]
250
200
150
100
50
0
♀ ♂ ♀ ♂ ♀ ♂ ♀ ♂
Ht
VTA
FrA
CPu

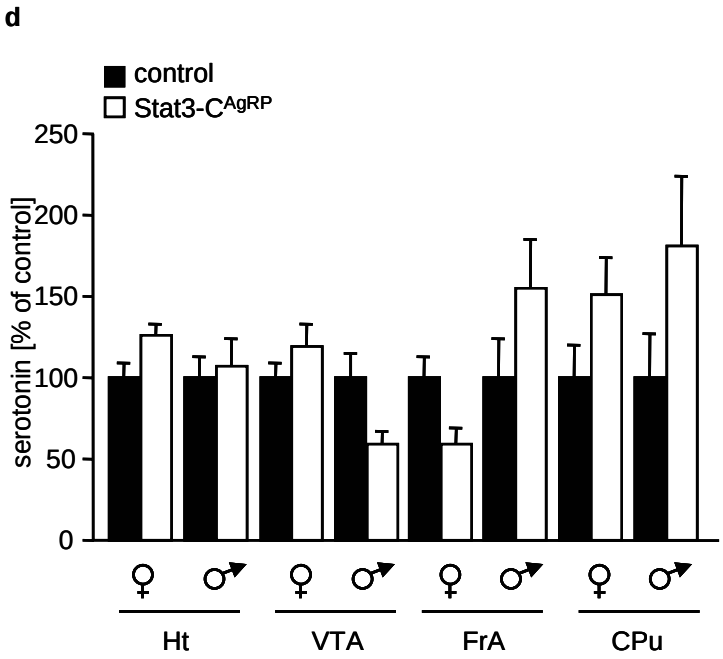


**Figure 28: Brain monoamine content of Stat3-C$^{AgRP}$ mice**

Relative brain **(a)** epinephrine, **(b)** norepinephrine, **(c)** dopamine and **(d)** serotonin content of control and Stat3-C$^{AgRP}$ mice (n = 7 to 10 of each genotype). All experiments were performed on tissues obtained from HFD-fed mice of the indicated genotype and gender at the age of 16 to 20 weeks. Ht: hypothalamus; VTA: ventral tegmental area; FrA: frontal association cortex; CPu: caudate putamen (striatum).

Moreover, hypothalamic expression of hypocretin and MCH were determined, since both neuropeptides are critically involved in the regulation of locomotor activity and since AgRP neurons have been demonstrated to project into the lateral hypothalamus, where both hypocretin- and MCH-expressing neurons reside (Broberger et al., 1998; Hagan et al., 1999). Nevertheless, Stat3-C$^{AgRP}$ mice showed no difference in the expression of both hypothalamic hypocretin and MCH compared to control animals (Figure 29a and b).

Taken together, Stat3-C$^{AgRP}$ mice do not exhibit significantly altered brain catecholamine and serotonin concentrations or hypothalamic MCH and hypocretin expression. Nevertheless, Stat3-C$^{AgRP}$ mice display a tendency for higher dopamine concentration in the striatum and the frontal cortex and for higher serotonin concentrations in the frontal cortex, potentially accounting for the increased locomotor activity in those mice.

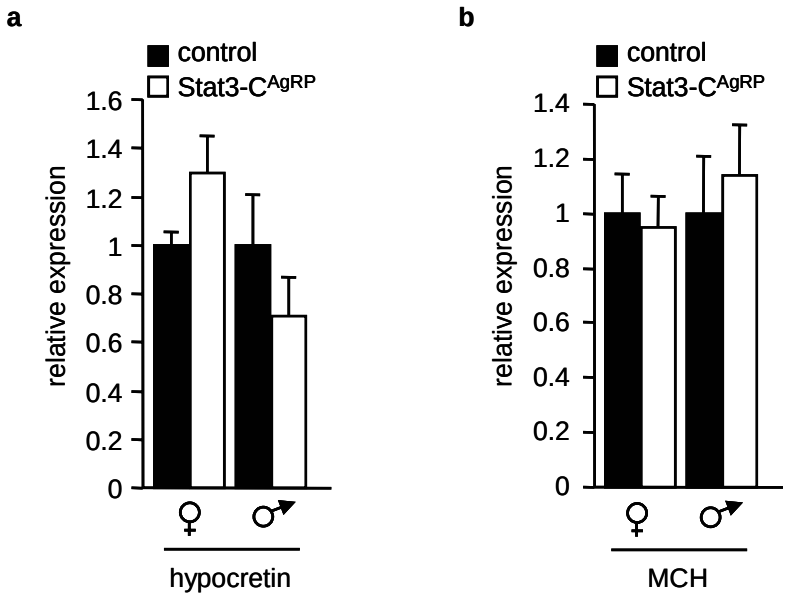


**Figure 29: Unaltered hypothalamic expression of hypocretin and MCH of Stat3-C$^{AgRP}$ mice**
Hypothalamic expression of **(a)** hypocretin and **(b)** MCH of control and Stat3-C$^{AgRP}$ mice under NCD conditions at the age of 20 weeks (n = 7 of each genotype).

## 3.7. Expression of the Stat3-C transgene selectively in AgRP neurons of *ob/ob* mice ameliorates the obese phenotype

To investigate if expression of a constitutively active Stat3 protein selectively in AgRP neurons of *ob/ob* mice leads to an amelioration of the obese phenotype, Stat3-C$^{AgRP}$ mice were crossed with *ob/ob* mice. First, body weight of control *ob/ob* (*ob/ob*Stat3-C$^{+/-}$) and *ob/ob*Stat3-C$^{AgRP}$ (*ob/ob*Stat3-C$^{+/-}$AgRPCre$^{+/-}$) mice under NCD conditions was monitored from weaning until the age of 16 weeks to analyze if expression of Stat3-C in AgRP neurons of *ob/ob* mice has an impact on body weight. *Ob/ob*Stat3-C$^{AgRP}$ mice exhibited an approximately 10 % reduction in body weight from weaning until the age of 16 weeks compared to control mice (Figure 30). This reduction in body weight was similar in female and male *ob/ob*Stat3-C$^{AgRP}$ mice (Figure 30).

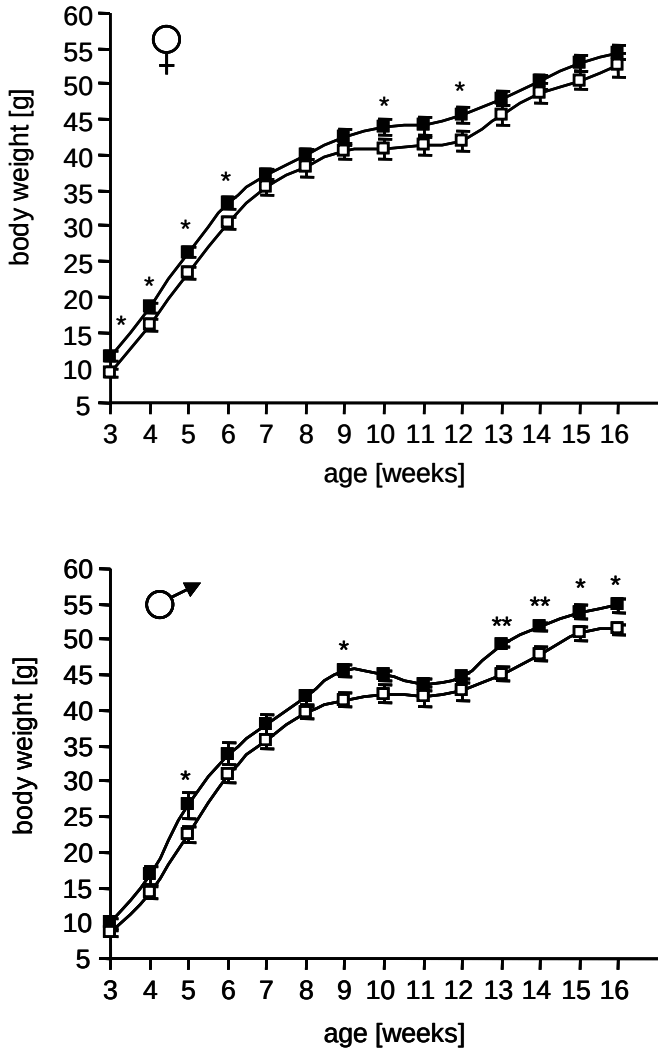


**Figure 30: Reduced body weight of *ob/ob*Stat3-C$^{AgRP}$ mice**

Average body weight of NCD-fed female (upper pannel) and male (lower panel) control (*ob/ob)* and *ob/ob*Stat3-C$^{AgRP}$ mice (n = 8 to 15 of each genotype). ■ control *(ob/ob)* mice; □ *ob/ob*Stat3-C$^{AgRP}$ mice.

To investigate whether the reduction in body weight observed in *ob/ob*Stat3-C$^{AgRP}$ mice resulted from a decrease in fat mass, the amount of epigonadal fat of 16 week old mice was examined. There was no significant difference between the fat pad weights of *ob/ob*Stat3-C$^{AgRP}$ and control mice, however, the fat pads of *ob/ob*Stat3-C$^{AgRP}$ mice showed the tendency to be slightly reduced (Figure 31a).

To further investigate the adiposity of *ob/ob*Stat3-C$^{AgRP}$ mice, total body fat content of 16 week old mice was determined by *in vivo* magnetic resonance spectrometry. Body fat content of 16 week old *ob/ob*Stat3-C$^{AgRP}$ mice was comparable to that of control mice (Figure 31b).

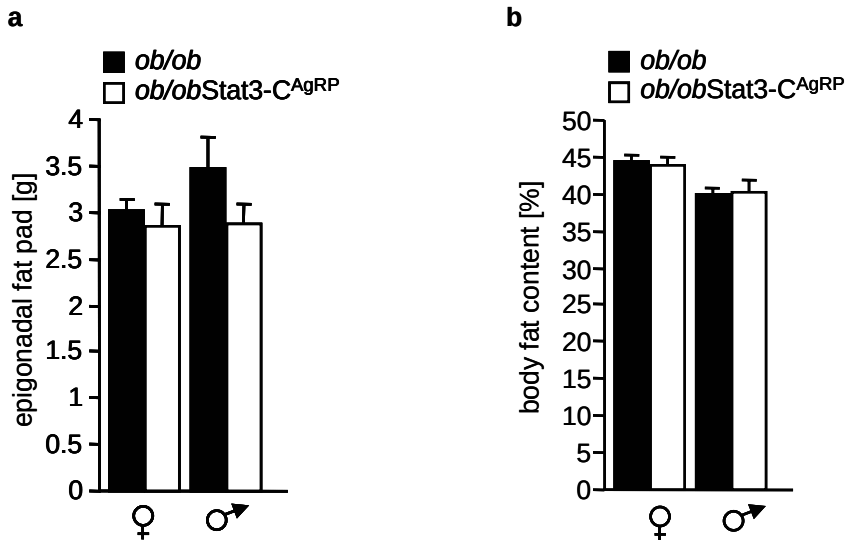


**Figure 31: Unaltered adiposity of *ob/ob*Stat3-C$^{AgRP}$ mice**

**(a)** Epigonadal fat pad weights and **(b)** average body fat content of control (*ob/ob*) and *ob/ob*Stat3-C$^{AgRP}$ mice at the age of 16 weeks measured by nuclear magnetic resonance (n = 5 to 7 of each genotype).

Moreover, glucose metabolism was compared in control and *ob/ob*Stat3-C$^{AgRP}$ mice to analyze whether expression of Stat3-C in AgRP neurons of *ob/ob* mice results in improved glucose metabolism, similar to the improvement observed in Stat3-C$^{AgRP}$ mice. To this end, blood glucose of control and *ob/ob*Stat3-C$^{AgRP}$ mice was determined. *Ob/ob*Stat3-C$^{AgRP}$ mice exhibited normal blood glucose levels in the fed and fasted condition, although fasted blood glucose levels were slightly reduced compared to those of control animals (Figure 32a). Serum insulin concentrations of *ob/ob*Stat3-C$^{AgRP}$ mice were comparable to those of control animals (Figure 32b). Glucose tolerance tests revealed a tendency for improved glucose tolerance in *ob/ob*Stat3-C$^{AgRP}$ mice (Figure 32c).

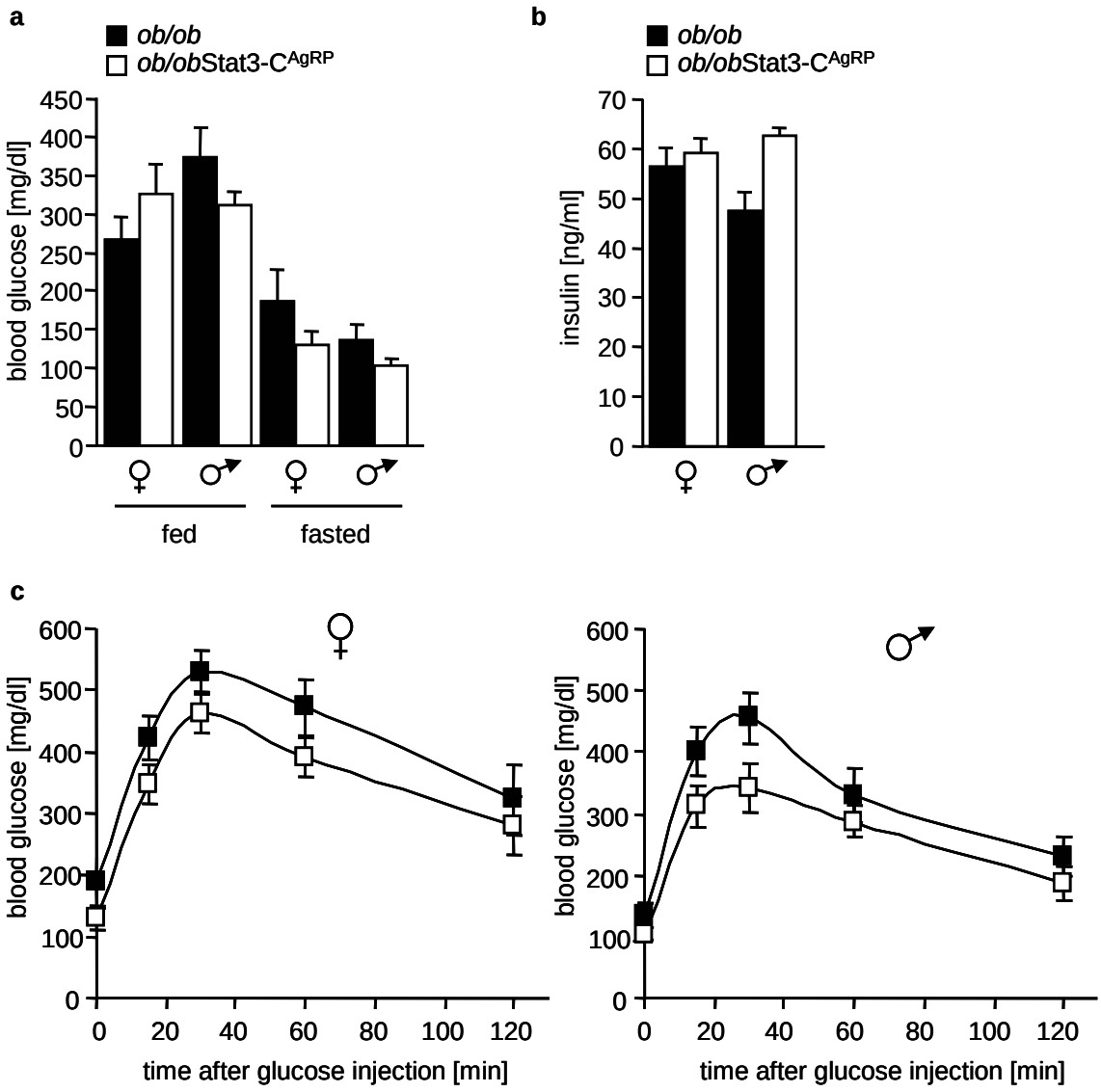


**Figure 32: Slightly improved glucose metabolism of *ob/ob*Stat3-C$^{AgRP}$ mice**

**(a)** Fed and fasted blood glucose concentrations of control (*ob/ob*) and *ob/ob*Stat3-C$^{AgRP}$ mice at the age of 9 and 12 weeks, respectively (n = 7 to 14 of each genotype). **(b)** Serum insulin concentrations of control *(ob/ob)* and *ob/ob*Stat3-C$^{AgRP}$ mice at the age of 8 weeks (n = 7 to 14 of each genotype). **(c)** Glucose tolerance tests of female (left panel) and male (right panel) control (*ob/ob*) and *ob/ob*Stat3-C$^{AgRP}$ mice at the age of 12 weeks (n = 8 to 12 of each genotype). ■ control (*ob/ob*) mice; □ *ob/ob*Stat3-C$^{AgRP}$ mice.

To investigate if the reduced body weight and adiposity of *ob/ob*Stat3-C$^{AgRP}$ mice was a result of reduced caloric intake, food intake of control and *ob/ob*Stat3-C$^{AgRP}$ mice was measured. As observed in Stat3-C$^{AgRP}$ animals, absolute food intake of both female and male *ob/ob*Stat3-C$^{AgRP}$ mice was comparable to that of control animals

(Figure 33a). Accordingly, when food intake was corrected for body weight, female *ob/ob*Stat3-C$^{AgRP}$ mice developed a relative hyperphagia, and also male *ob/ob*Stat3-C$^{AgRP}$ mice did not eat less than control mice (Figure 33b).

Taken together, reduced body weight and adiposity of *ob/ob*Stat3-C$^{AgRP}$ mice is not the result of reduced caloric intake.

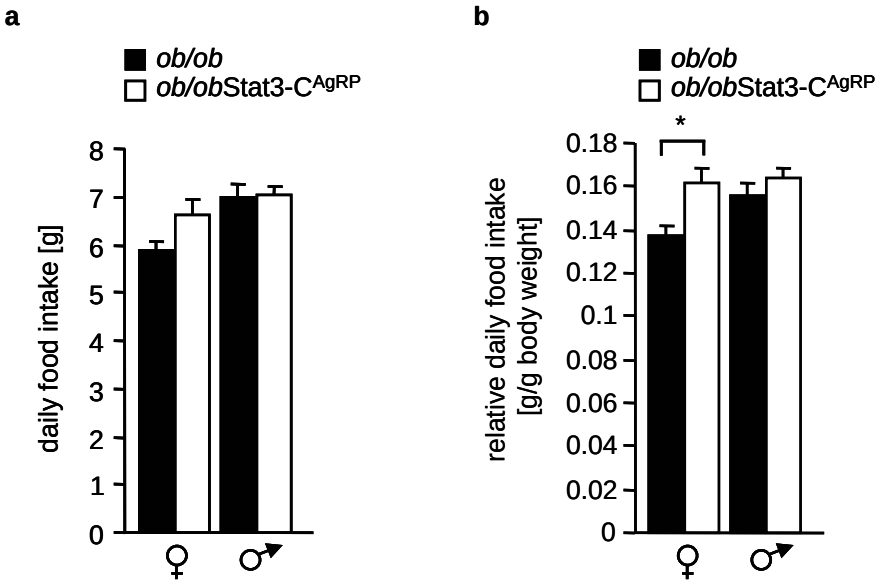


**Figure 33: Relative hyperphagia of *ob/ob*Stat3-C$^{AgRP}$ mice**

**(a)** Absolute and **(b)** relative (corrected for body weight) daily food intake of control (*ob/ob*) and *ob/ob*Stat3-C$^{AgRP}$ mice under NCD conditions at age of 9 weeks (n = 6 to 9 of each genotype).

Next, energy expenditure of *ob/ob*Stat3-C$^{AgRP}$ mice was determined by indirect calorimetrical analysis. This analysis revealed a small increase in oxygen consumption of *ob/ob*Stat3-C$^{AgRP}$ mice compared to control mice, which did not reach statistical significance (Figure 34a). As observed in Stat3-C$^{AgRP}$ mice, respiratory exchange ratio of *ob/ob*Stat3-C$^{AgRP}$ mice was not altered (Figure 34b).

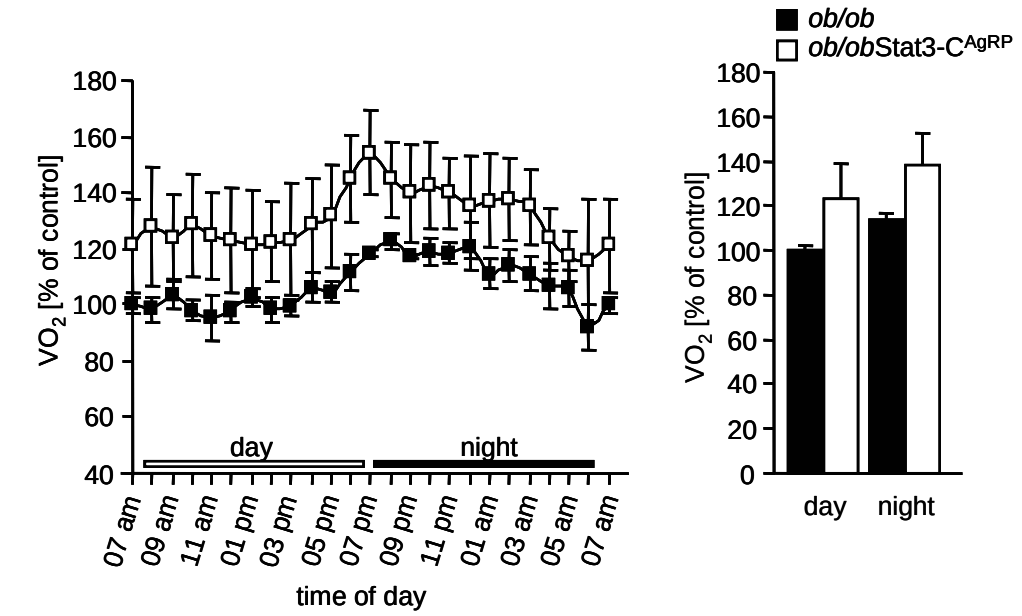


**b**

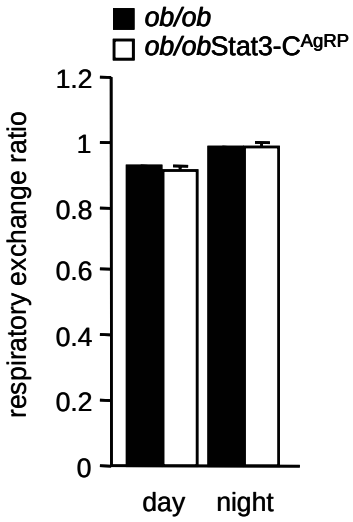


**Figure 34: Slightly increased metabolic rate of *ob/ob*Stat3-C$^{AgRP}$ mice**

**(a)** Oxygen consumption of 9 week old control (*ob/ob*) and *ob/ob*Stat3-C$^{AgRP}$ mice over time (left panel) and mean oxygen consumption of control (*ob/ob*) and *ob/ob*Stat3-C$^{AgRP}$ mice (right panel) (n = 3 to 4 of each genotype). **(b)** Mean respiratory exchange ratio of control (*ob/ob*) and *ob/ob*Stat3-C$^{AgRP}$ mice at the age of 9 weeks (n = 3 to 4 of each genotype). ■ control (*ob/ob*) mice; □ *ob/ob*Stat3-C$^{AgRP}$ mice.

To investigate, whether the leanness and the increase in energy expenditure of *ob/ob*Stat3-C$^{AgRP}$ mice resulted from enhanced locomotor activity as observed in Stat3-

$C^{AgRP}$ mice, basal locomotor activity of control and *ob/ob*Stat3-$C^{AgRP}$ mice was analyzed. Both female and male *ob/ob*Stat3-$C^{AgRP}$ mice exhibited a trend towards increased locomotor activity compared to control mice (Figure 35).

Taken together, expression of a constitutively active Stat3 protein selectively in AgRP neurons of *ob/ob* mice leads to an amelioration of the obese phenotype. This amelioration is not the result of reduced caloric intake, but a consequence of increased energy expenditure and locomotor activity, consistent with the phenotype observed in Stat3-$C^{AgRP}$ mice.

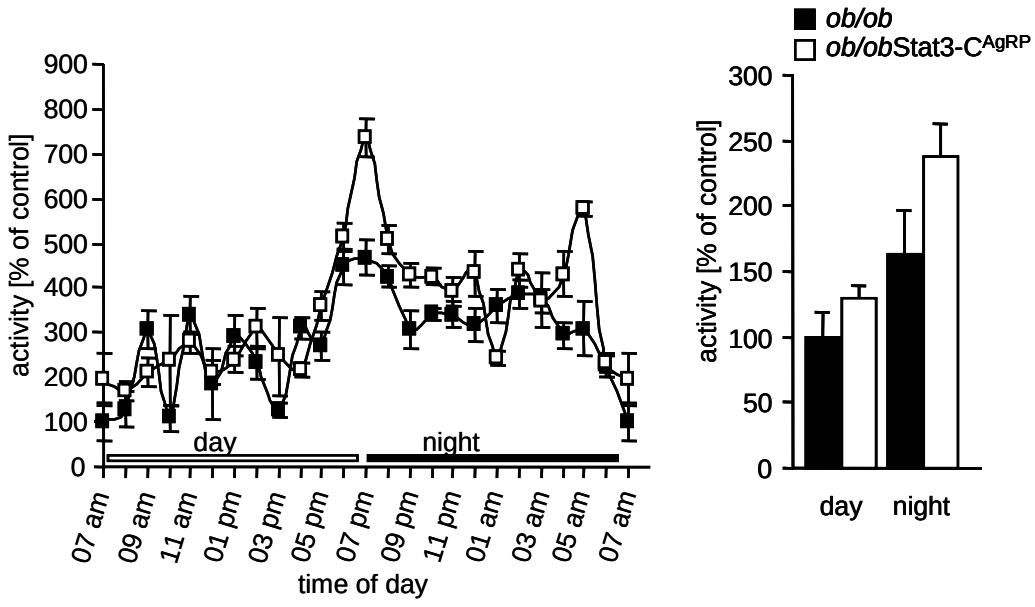


**Figure 35: Slightly increased locomotor activity of Stat3-$C^{AgRP}$ mice**

Basal locomotor activity control (*ob/ob*) and *ob/ob*Stat3-$C^{AgRP}$ mice over time (left panel) and mean basal locomotor activity of control (*ob/ob*) and *ob/ob*Stat3-$C^{AgRP}$ mice (right panel) at the age of 9 weeks (n = 3 to 4 of each genotype). ■ control (*ob/ob*) mice; □ *ob/ob*Stat3-$C^{AgRP}$ mice.

# 4 Discussion

## 4.1 Leptin in obesity

Obesity and associated insulin-resistant type 2 diabetes represent a steadily growing health burden in industrialized societies. To prevent or treat these diseases, it is critical to define the physiological principles for the precise regulation of energy homeostasis. The identification and sequencing of the mouse *obese* gene by J. Friedman's group in 1994 opened important new avenues in obesity research. Shortly after the discovery of leptin, defects concerning leptin or the leptin receptor were described in patients with severe obesity. However, only a very small number of all cases of obesity is associated with the absence of leptin or mutations in the leptin receptor gene. By contrast, in correlation with increased adipocyte size and number, most of the cases of obesity are associated with increased levels of circulating leptin (Considine et al., 1996b; Farooqi and O'Rahilly, 2005a; Maffei et al., 1996). Obesity in spite of high levels of circulating leptin indicates leptin resistance, i. e. the failure of high levels of leptin to suppress food intake and to decrease body weight and adiposity (for review, see (Myers et al., 2007)). Various mechanisms are involved in the development of leptin resistance, including alterations in the transport of leptin across the blood-brain barrier and most importantly alterations in intracellular leptin signaling (El-Haschimi et al., 2000; Munzberg et al., 2005). Lack or mutation of the leptin receptor on the other hand only accounts for the minority of all cases of obesity-related leptin resistance (Considine et al., 1996a).

## 4.2 Central leptin signaling

Several experiments over the last decade have highlighted the pivotal role of leptin for normal body weight and glucose homeostasis both in rodents and humans. Analyses of brain-restricted leptin receptor knockout mice as well as leptin receptor knockout mice with reconstitution of leptin receptor expression selectively in the brain have provided clear evidence that leptin action in the central nervous system accounts for most of leptin’s effects on energy and glucose homeostasis, if not for all (Cohen et

al., 2001; Kowalski et al., 2001). However, the leptin receptor is expressed in several regions of the central nervous system, and recent experiments with mice lacking the receptor in specific neuronal subpopulations have begun to shed light on the relative contribution of leptin signaling in individual regions of the central nervous system with respect to the regulation of energy and glucose homeostasis. Mice lacking the leptin receptor in POMC and AgRP neurons of the ARC and in neurons of the VMH have emphasized the significance of hypothalamic leptin signaling, in particular of leptin signaling in neurons of the ARC (Balthasar et al., 2004; Dhillon et al., 2006; van de Wall et al., 2007). Moreover, pharmacological studies showing that MC4R antagonists can blunt the acute anorectic effect of centrally applied leptin have underlined the importance of the melanocortin system in regulating leptin's effect at least concerning the regulation of food intake (da Silva et al., 2004). Furthermore, alterations in intracellular leptin signaling in neurons of the ARC were suggested to play a crucial role in the development of leptin resistance (El-Haschimi et al., 2000; Munzberg et al., 2004).

Taken together, leptin action in POMC- and AgRP-expressing neurons plays a key role in the regulation of energy homeostasis.

## 4.3 Activation of a constitutively active Stat3 protein in AgRP neurons

Although our understanding about leptin signaling in the ARC of the hypothalamus has improved significantly over the last years, the role of leptin signaling and particularly of leptin-evoked Stat3 signaling in AgRP neurons remains controversial. Therefore, the aim of this thesis was to study the role of Stat3 in AgRP expressing neurons. To this end, mice expressing a constitutively active version of the Stat3 protein (Stat3-C) selectively in AgRP neurons were generated. The Stat3-C protein was demonstrated to act as a constitutively active DNA-binding transcription factor *in vivo* without exhibiting any oncogenic effects. Furthermore, it was shown that Stat3-C is selectively expressed in AgRP neurons of Stat3-$C^{AgRP}$ mice. Therefore, mice overexpressing Stat3-C in AgRP neurons provide an adequate tool to study the role of Stat3 signaling in AgRP neurons *in vivo*. Moreover, overexpression of Stat3-C in leptin

deficient *ob/ob* mice serves as a second valuable model to study the role of leptin-evoked Stat3 activation in AgRP neurons.

### 4.3.1 Role of Stat3 in the regulation of AgRP expression

Much of the research on intracellular signaling pathways activated by the leptin receptor and their relative contributions to mediating different aspects of leptin action has focused on the leptin-stimulated activation of the Stat3 signaling pathway. Indeed, mice with mutated leptin receptors that do not bind Stat3, as well as mice lacking Stat3 specifically in the brain develop an obese phenotype (Bates et al., 2003; Gao et al., 2004), underlining the essential role of leptin-stimulated Stat3 activation in the regulation of energy homeostasis. Nevertheless, while Stat3 is directly responsible for the regulation of POMC expression (Xu et al., 2007), the role of leptin-stimulated activation of Stat3 in other distinct leptin-responsive neurons and particularly in the regulation of AgRP expression has remained a controversial issue.

Several observations suggest that leptin regulates AgRP expression directly via Stat3. First of all, phosphorylated Stat3 rapidly accumulates in AgRP neurons upon leptin administration (Hakansson and Meister, 1998). Furthermore, two Stat3-responsive elements exist in the *AgRP* promoter region (Brown et al., 2001). Indeed, overexpression of Stat3 in cultured cells inhibits AgRP transcription in reporter gene assays (Kitamura et al., 2006). Moreover, mice with a point mutation on the Stat3 binding site of the leptin receptor as well as pan-neuronal Stat3 knockout mice exhibit increased AgRP mRNA expression (Bates et al., 2003; Gao et al., 2004), but these experiments do not rule out whether Stat3 activation is directly involved in AgRP regulation. Alternatively, increased AgRP expression in those mice and in pan-neuronal Stat3 knockout mice may occur secondary to other disturbed signaling events.

On the other hand, several observations indicate that leptin regulates AgRP expression independently of Stat3 activation. The model of Stat3 as a direct regulator of AgRP expression *in vivo* suggests Stat3 to function as a transcriptional repressor, indicated by the reverse relationship of leptin signaling and AgRP expression. However, in most cases Stat3 functions as a transcriptional activator rather than a repressor (Aaronson and Horvath, 2002; Levy and Darnell, 2002). Importantly, AgRP overexpression in mice with disrupted leptin receptor-Stat3 signaling was much less

pronounced than in *db/db* mice (Bates et al., 2003). Furthermore, neuronal activity of AgRP neurons in mice with leptin receptor-Stat3 disruption was appropriately suppressed by leptin (Munzberg et al., 2007), indicating mechanisms other than Stat3-activation in the suppression of AgRP expression. Above all, AgRP neuron-restricted Stat3 gene inactivation has no effect on AgRP expression *in vivo* (Kaelin et al., 2006). Consistent with the data on AgRP neuron-specific Stat3 knockout mice, Stat3-$C^{AgRP}$ mice with AgRP neuron-restricted constitutive activation of Stat3 analyzed in this study exhibit unaltered expression of AgRP, thus providing evidence that neither the lack of Stat3 nor the constitutive activation of Stat3 lead to dysregulated AgRP expression *in vivo*.

Several studies suggest the PI3K pathway to be involved in the regulation of AgRP expression. Inhibition of the PI3K pathway blocks the inhibitory effect of leptin on food intake and PI3K signaling was shown to be directly required for leptin-mediated inhibition of AgRP expression (Morrison et al., 2005; Zhao et al., 2002). These data are consistent with the fact that the *AgRP* promoter contains two binding sites for the transcription factor FOXO and a report indicating that PI3K-mediated inhibition of FOXO-1 accounts for leptin's ability to regulate AgRP expression (Accili and Arden, 2004; Kitamura et al., 2006). Besides the involvement of the PI3K pathway, it was shown that fasting induced activation of AgRP expression is dependent on the presence of glucocorticoids and thus stimulated by the glucocorticoid rerceptor (Makimura et al., 2003).

### 4.3.2 Role of Stat3 in AgRP neurons in the regulation of energy homeostasis

Although the expression of AgRP is regulated by mechanisms independent of Stat3, Stat3-$C^{AgRP}$ mice reveal a crucial role for Stat3 in AgRP neurons in the regulation of energy homeostasis. Stat3-$C^{AgRP}$ mice do not exhibit altered levels of AgRP expression, but are leaner than control animals under NCD and exhibit a relative resistance to the development of diet-induced obesity. Consistent with the leanness observed in Stat3-$C^{AgRP}$ mice, expression of Stat3-C in AgRP neurons of leptin deficient *ob/ob* mice results in reduced body weight compared to control *ob/ob* mice. The leanness of Stat3-$C^{AgRP}$ and *ob/ob*Stat3-$C^{AgRP}$ mice underlines the critical role of Stat3 activation in AgRP neurons to maintain energy balance. Strikingly, the leanness of

Stat3-C$^{AgRP}$ and *ob/ob*Stat3-C$^{AgRP}$ mice is not a consequence of reduced food intake but occurs as a consequence of increased locomotor activity and energy expenditure. Hence, differential pathways activated by leptin within AgRP neurons apparently target different biological responses to result in negative energy balance, i.e. leptin-stimulated PI3K activation via inhibition of FOXO activity inhibits AgRP mRNA expression, thus regulating food intake (Kitamura et al., 2006). These data are consistent with the hypophagia observed in mice with acute ablation of AgRP/NPY-expressing neurons and also with the late onset hypophagia in AgRP knockout mice (Gropp et al., 2005; Luquet et al., 2005; Wortley et al., 2005). This thesis reveals a critical role for Stat3 activation in the stimulation of locomotor activity and energy expenditure independent of the direct regulation of food intake or AgRP mRNA expression in AgRP neurons. Thus, the experiments reveal an important novel mechanistic insight into the role of Stat3 specifically in AgRP neurons with respect to energy homeostasis.

### 4.3.3 Role of Stat3 in AgRP neurons in the regulation of glucose metabolism

Leptin regulates glucose homeostasis secondary to the control of energy balance, feeding and adiposity. On the other hand, there is also evidence for direct regulation of glucose metabolism by leptin (Schwartz et al., 1996a). Leptin administration to *ob/ob* mice results in improved glucose metabolism prior to effects on feeding and adiposity, presenting an evidence for the direct regulation of glucose metabolism by leptin. (Barzilai et al., 1997; Burcelin et al., 1999; Kamohara et al., 1997). Moreover, leptin administration to wild type and *ob/ob* mice regulates hepatic glucose flux (Liu et al., 1998). The direct regulation of glucose metabolism by leptin is mediated via the central nervous system, as central and peripheral administration of leptin have similar effects on glucose metabolism (Liu et al., 1998) and brain-specific expression of a leptin receptor transgene in *db/db* mice rescues the diabetic phenotype of *db/db* mice (Chua et al., 2004; Cohen et al., 2001; Kowalski et al., 2001).

The improved glucose metabolism observed in mice expressing a constitutively active Stat3 protein selectively in AgRP neurons most likely occurs as a consequence of reduced body weight and adiposity rather than of a direct effect of Stat3 activation in AgRP neurons. Thus, while NCD-fed Stat3-C$^{AgRP}$ mice exhibit unaltered blood glucose and insulin levels and unaltered glucose tolerance, Stat3-C$^{AgRP}$ mice under HFD

conditions exhibit reduced blood glucose and insulin levels and are more glucose tolerant than control animals. The amelioration of glucose metabolism in Stat3-$C^{AgRP}$ mice correlates with their leanness, which is much more pronounced under HFD conditions, indicating that Stat3-$C^{AgRP}$ mice develop a relative resistance to diet-induced obesity. Similarly, *ob/ob*Stat3-$C^{AgRP}$ mice, which exhibit only a slight reduction in body weight without reduced adiposity show almost no improvement of glucose metabolism compared to control *ob/ob* mice. In contrast, a direct effect of Stat3 signaling in AgRP neurons on glucose metabolism should result in improved glucose homeostasis in all three Stat3-C models. These observations are consistent with data on mice with disrupted leptin receptor-Stat3 signaling which indicate that leptin-evoked Stat3 signaling is involved in the regulation of glucose homeostasis via feeding and adiposity, whereas leptin receptor signals independent of Stat3 activation directly regulate glucose metabolism independently of effects on energy balance (Bates et al., 2005).

### 4.3.4 Role of Stat3 in AgRP neurons in the regulation of locomotor activity

Locomotor activity plays a substantial role in the regulation of energy homeostasis and is thought to represent a major factor in the prevalence of obesity. Nevertheless, whereas much research has focused on the control of energy intake in the past decade, the research on the regulation of energy expenditure, in particular on locomotor activity, has received far less attention. Early studies suggested the involvement of the hypothalamus in the regulation of locomotor activity, as chemical lesions of the hypothalamus in mice result in hypoactivity (Olney, 1969; Poon and Cameron, 1978). Studies on surgical hypothalamic lesions indicated distinct regions of the hypothalamus to play a role in the regulation of locomotor activity. Thus, surgical lesions of the VMH not only increase food intake and body weight, but also reduce locomotor activity (Tokunaga et al., 1991), whereas surgical lesions of the PVN result in obesity without affecting locomotor activity (Cox and Powley, 1981).

Other early studies suggested the involvement of leptin in the regulation of locomotor activity, as *ob/ob* mice are hypoactive (Mayer, 1953). The observation that unilateral restoration of leptin signaling in leptin receptor-deficient mice specifically in the ARC restores impaired locomotor activity to normal provides the first direct evidence for leptin-mediated regulation of locomotor activity in this neuronal site

(Coppari et al., 2005). Consistent with these observations, the study of Stat3-C$^{AgRP}$ and *ob/ob*Stat3-C$^{AgRP}$ mice revealed Stat3-dependent regulation of locomotor activity via AgRP neurons. In this thesis, the notion of the involvement of leptin signaling in the ARC in the regulation of locomotor activity is extended by two important findings. First, the neuronal population responsible for regulating locomotor activity within the ARC is directly defined as AgRP-expressing neurons. Second, Stat3 activation in this cell type is demonstrated to mediate the regulation of locomotor activity, consistent with the reduced locomotor activity of mice with a mutation of the Stat3 binding site of the leptin receptor (Bates et al., 2004). Taken together, the data on Stat3-C$^{AgRP}$ and *ob/ob*Stat3-C$^{AgRP}$ mice introduces a novel model according to which leptin-stimulated Stat3 activation in AgRP neurons directly regulates energy homeostasis and locomotor activity independent from regulating AgRP mRNA expression. This model is consistent with the recent finding that AgRP neuron-specific deletion of the leptin receptor results in reduced locomotor activity (van de Wall et al., 2007), but this study did not rule out the intracellular signaling molecules responsible for the stimulation of locomotor activity whithin AgRP neurons.

Analysis of central catecholamine concentrations in Stat3-C$^{AgRP}$ mice revealed a trend towards elevated dopamine content in the striatum and the frontal cortex, two regions receiving projections of various dopaminergic neurons (Lindvall and Bjorlund, 1983). This notion is supported by the decreased peripheral catecholamine concentrations of Stat3-C$^{AgRP}$ mice, as elevated central catecholamine concentrations were shown to decrease plasma catecholamine concentrations and thereby peripheral sympathetic activity (for review, see (Struthers and Dollery, 1985)). Dopaminergic neurons represent classical regulatory centers for locomotor behaviour, as blocking or stimulation of postsynaptic dopamine receptors reduces or increases locomotor activity, respectively (Arnt, 1987). Moreover, inhibition of dopamine transporters resulting in elevated synaptic dopamine concentration stimulates locomotor activity (Woolverton and Johnson, 1992) and dopamine-deficient animals are hypoactive (Zhou and Palmiter, 1995). Thus, increased dopamine levels in the striatum and frontal cortex potentially account for the increased locomotor activity of Stat3-C$^{AgRP}$ mice.

Different studies suggest the involvement of leptin in the regulation of dopamine release in distinct brain areas (Krugel et al., 2003; Roseberry et al., 2007), but the role for the ARC in this context remains unexplored. AgRP neurons may regulate the dopaminergic system via projections to MCH expressing neurons in the lateral

hypothalamus, as MCH neuronal projections regulate the dopaminergic system (Marsh et al., 2002; Smith et al., 2005). Nevertheless, the absence of detectable changes in MCH and hypocretin expression in Stat3-$C^{AgRP}$ mice indicates the existence of alternative pathways by which AgRP neurons control locomotor activity. Although the literature is sparse on how ARC neurons integrate the regulation of locomotor behaviour, some studies indicate a role for Y2, MSH and MC4R-signaling in control of striatal dopamine regulation and locomotor activity, consistent with the trend towards increased dopamine concentrations in this region observed in Stat3-$C^{AgRP}$ mice. (Adewale et al., 2007; Hsu et al., 2005; Sanchez et al., 2001; Sandyk, 1990; Singhal and Rastogi, 1982)

## 4.4 Perspectives

Overexpression of a constitutively active Stat3 protein in wild type mice revealed a crucial role for Stat3 in AgRP neurons in the regulation of energy homeostasis and particularly in the regulation of locomotor activity. Overexpression of the constitutively active Stat3 protein in leptin deficient mice further supports this finding. Future studies are needed to define the anatomical interaction of AgRP neurons with neuronal centers that control locomotor activity and the exact molecular mechanism in AgRP neurons leading to Stat3-dependent activation of locomotor activity in more detail. Nevertheless, Stat3-dependent regulation of locomotor activity provides a promising new target for the development of novel therapeutic approaches to the current obesity epidemic.

# 5 Summary

Over the last years, much of the research on obesity has focused on the study of leptin. This adipocyte-derived hormone circulates in proportion to fat mass and functions as an adiposity signal to decrease energy intake and increase energy expenditure in order to maintain energy homeostasis. Leptin signals informations on body energy stores to hypothalamic neurons located in the arcuate nucleus (ARC) of the hypothalamus. One of the leptin-regulated neuronal subtypes in the ARC are the orexigenic agouti-related peptide (AgRP)-producing neurons, which are directly inhibited by leptin. A key pathway downstream of the leptin receptor involves activation of the signal transducer and activator of transcription 3 (Stat3), but the role of Stat3 in the regulation of AgRP neurons remains controversial.

In this study, analysis of Stat3-$C^{AgRP}$ mice expressing a constitutively active version of the Stat3 protein (Stat3-C) selectively in AgRP neurons reveals a crucial role for Stat3 in AgRP neurons in the regulation of energy expenditure *in vivo*. Stat3-$C^{AgRP}$ mice are lean and develop a relative resistance to diet-induced obesity accompanied by improved glucose homeostasis. The lean phenotype of Stat3-$C^{AgRP}$ mice appears in the presence of unaltered AgRP expression and caloric intake as a consequence of increased energy expenditure evoked by elevated locomotor activity. Consistent with the phenotype observed in Stat3-$C^{AgRP}$ mice, expression of Stat3-C in AgRP neurons of leptin deficient *ob/ob* mice diminishes the obese phenotype of *ob/ob* mice as a result of increased energy expenditure and locomotor activity in the presence of unaltered food intake.

Analysis of brain catecholamines in Stat3-$C^{AgRP}$ mice revealed a trend towards elevated dopamine concentrations in the striatum and frontal cortex, which potentially account for the increased locomotor activity in those mice. Nevertheless, the anatomical interaction of AgRP neurons with neuronal centers that control locomotor activity and the exact molecular mechanism in AgRP neurons leading to Stat3-dependent activation of locomotor activity have to be defined further. Taken together, this thesis introduces a novel model according to which leptin-stimulated Stat3 activation in AgRP neurons directly regulates locomotor activity independent of the regulation of AgRP mRNA expression.

# 6 Zusammenfassung

Ein Schwerpunkt der Adipositasforschung der letzten Jahre konzentrierte sich auf die Untersuchung von Leptin. Das Hormon Leptin wird von Adipozyten proportional zur Fettmasse sezerniert und dient als „Fett-Signal", indem es die Kalorienzufuhr verringert und den Energieverbrauch erhöht, um ein Gleichgewicht im Energiehaushalt des Körpers zu erzielen. Leptin signalisiert Neuronen im Nucleus Arcuratus (ARC) des Hypothalamus den Zustand körpereigener Energiereserven. Die orexigenen AgRP (agouti-related peptide)-produzierenden Neuronen im ARC werden unmittelbar durch Leptin inhibiert. Ein Hauptsignalweg des Leptinrezeptors aktiviert Stat3 (signal transducer and activator of transcription 3), dessen Rolle in der Regulierung der AgRP Neuronen jedoch bisher ungeklärt blieb.

Die Analyse von Stat3-$C^{AgRP}$ Mäusen, die eine konstitutiv-aktive Form des Stat3 Proteins (Stat3-C) gezielt in AgRP Neuronen exprimieren, deckt in dieser Arbeit eine entscheidende Funktion von Stat3 in AgRP Neuronen in der Regulierung des Energieverbrauchs *in vivo* auf. Stat3-$C^{AgRP}$ Mäuse sind schlank und entwickeln eine relative Resistenz gegenüber Fettdiät-induzierter Adipositas bei gleichzeitiger Verbesserung der Glukosehomöostase. Dieser Phänotyp resultiert aus einem erhöhtem Energieverbrauch, der durch gesteigerte Bewegungsaktivität hervorgerufen wird. Die Expression von AgRP und die Kalorienzufuhr in Stat3-$C^{AgRP}$ Mäusen sind jedoch unverändert. In Übereinstimmung mit dem beobachteten Phänotyp der Stat3-$C^{AgRP}$ Mäuse weisen Leptin-defiziente *ob/ob* Mäuse mit AgRP-spezifischer Expression des Stat3-C Proteins reduzierte Fettleibigkeit aufgrund gesteigerten Energieverbrauchs und Bewegungsaktivität bei unveränderter Kalorienzufuhr auf.

Die Analyse von Katecholaminen im Gehirn von Stat3-$C^{AgRP}$ Mäusen ergab eine Tendenz zu erhöhter Dopaminkonzentration im Striatum und frontalen Kortex, die möglicherweise die gesteigerte Bewegungsaktivität der Mäuse verursacht. Die Interaktion von AgRP Neuronen mit neuronalen Zentren, die die Bewegungsaktivität regulieren und der exakte neuronale Mechanismus in AgRP Neuronen, der über die Aktivierung von Stat3 zu erhöhter Bewegungsaktivität führt, müssen jedoch weiter erforscht werden. Zusammengefasst präsentiert diese Arbeit ein neues Modell, nach dem die Aktivierung von Stat3 in AgRP Neuronen durch Leptin die Bewegungsaktivität unabhängig von der Expression von AgRP reguliert.

# 7 References

Aaronson, D. S., and Horvath, C. M. (2002). A road map for those who don't know JAK-STAT. Science *296*, 1653-1655.

Accili, D., and Arden, K. C. (2004). FoxOs at the crossroads of cellular metabolism, differentiation, and transformation. Cell *117*, 421-426.

Adewale, A. S., Macarthur, H., and Westfall, T. C. (2007). Neuropeptide Y-induced enhancement of the evoked release of newly synthesized dopamine in rat striatum: mediation by Y2 receptors. Neuropharmacology *52*, 1396-1402.

Ailhaud, G. (2000). Adipose tissue as an endocrine organ. Int J Obes Relat Metab Disord *24 Suppl 2*, S1-3.

Arnt, J. (1987). Behavioural studies of dopamine receptors: evidence for regional selectivity and receptor multiplicity. In Dopamine Receptors, I. Creese and C. M. Fraser, eds. (New York: Alan R. Liss), pp. 199 – 231.

Backer, J. M., Myers, M. G., Jr., Shoelson, S. E., Chin, D. J., Sun, X. J., Miralpeix, M., Hu, P., Margolis, B., Skolnik, E. Y., Schlessinger, J., and et al. (1992). Phosphatidylinositol 3'-kinase is activated by association with IRS-1 during insulin stimulation. Embo J *11*, 3469-3479.

Bado, A., Levasseur, S., Attoub, S., Kermorgant, S., Laigneau, J. P., Bortoluzzi, M. N., Moizo, L., Lehy, T., Guerre-Millo, M., Le Marchand-Brustel, Y., and Lewin, M. J. (1998). The stomach is a source of leptin. Nature *394*, 790-793.

Bagdade, J. D., Bierman, E. L., and Porte, D., Jr. (1967). The significance of basal insulin levels in the evaluation of the insulin response to glucose in diabetic and nondiabetic subjects. J Clin Invest *46*, 1549-1557.

Bagnol, D., Lu, X. Y., Kaelin, C. B., Day, H. E., Ollmann, M., Gantz, I., Akil, H., Barsh, G. S., and Watson, S. J. (1999). Anatomy of an endogenous antagonist: relationship between Agouti-related protein and proopiomelanocortin in brain. J Neurosci *19*, RC26.

Balthasar, N., Coppari, R., McMinn, J., Liu, S. M., Lee, C. E., Tang, V., Kenny, C. D., McGovern, R. A., Chua, S. C., Jr., Elmquist, J. K., and Lowell, B. B. (2004). Leptin receptor signaling in POMC neurons is required for normal body weight homeostasis. Neuron *42*, 983-991.

Banks, A. S., Davis, S. M., Bates, S. H., and Myers, M. G., Jr. (2000). Activation of downstream signals by the long form of the leptin receptor. J Biol Chem *275*, 14563-14572.

Banks, W. A., Kastin, A. J., Huang, W., Jaspan, J. B., and Maness, L. M. (1996). Leptin enters the brain by a saturable system independent of insulin. Peptides *17*, 305-311.

Barsh, G. S., Farooqi, I. S., and O'Rahilly, S. (2000). Genetics of body-weight regulation. Nature *404*, 644-651.

Barzilai, N., Wang, J., Massilon, D., Vuguin, P., Hawkins, M., and Rossetti, L. (1997). Leptin selectively decreases visceral adiposity and enhances insulin action. J Clin Invest *100*, 3105-3110.

Bates, S. H., Dundon, T. A., Seifert, M., Carlson, M., Maratos-Flier, E., and Myers, M. G., Jr. (2004). LRb-STAT3 signaling is required for the neuroendocrine regulation of energy expenditure by leptin. Diabetes *53*, 3067-3073.

Bates, S. H., Kulkarni, R. N., Seifert, M., and Myers, M. G., Jr. (2005). Roles for leptin receptor/STAT3-dependent and -independent signals in the regulation of glucose homeostasis. Cell Metab *1*, 169-178.

Bates, S. H., Stearns, W. H., Dundon, T. A., Schubert, M., Tso, A. W., Wang, Y., Banks, A. S., Lavery, H. J., Haq, A. K., Maratos-Flier, E., *et al.* (2003). STAT3 signalling is required for leptin regulation of energy balance but not reproduction. Nature *421*, 856-859.

Benoit, S. C., Air, E. L., Coolen, L. M., Strauss, R., Jackman, A., Clegg, D. J., Seeley, R. J., and Woods, S. C. (2002). The catabolic action of insulin in the brain is mediated by melanocortins. J Neurosci *22*, 9048-9052.

Bernardis, L. L., Awad, A., Fink, C., and Bellinger, L. L. (1992). Metabolic and neuroendocrine indices one month after lateral hypothalamic area lesions. Physiol Behav *52*, 133-139.

Billington, C. J., Briggs, J. E., Grace, M., and Levine, A. S. (1991). Effects of intracerebroventricular injection of neuropeptide Y on energy metabolism. Am J Physiol *260*, R321-327.

Birnbaum, M. J. (1992). The insulin-sensitive glucose transporter. Int Rev Cytol *137*, 239-297.

Bjorbaek, C., Buchholz, R. M., Davis, S. M., Bates, S. H., Pierroz, D. D., Gu, H., Neel, B. G., Myers, M. G., Jr., and Flier, J. S. (2001). Divergent roles of SHP-2 in ERK activation by leptin receptors. J Biol Chem *276*, 4747-4755.

Bjorbaek, C., El-Haschimi, K., Frantz, J. D., and Flier, J. S. (1999). The role of SOCS-3 in leptin signaling and leptin resistance. J Biol Chem *274*, 30059-30065.

Bjorbaek, C., Elmquist, J. K., Frantz, J. D., Shoelson, S. E., and Flier, J. S. (1998). Identification of SOCS-3 as a potential mediator of central leptin resistance. Mol Cell *1*, 619-625.

Bjorbak, C., Lavery, H. J., Bates, S. H., Olson, R. K., Davis, S. M., Flier, J. S., and Myers, M. G., Jr. (2000). SOCS3 mediates feedback inhibition of the leptin receptor via Tyr985. J Biol Chem *275*, 40649-40657.

Bjornholm, M., Munzberg, H., Leshan, R. L., Villanueva, E. C., Bates, S. H., Louis, G. W., Jones, J. C., Ishida-Takahashi, R., Bjorbaek, C., and Myers, M. G., Jr. (2007). Mice lacking inhibitory leptin receptor signals are lean with normal endocrine function. J Clin Invest *117*, 1354-1360.

Bornstein, S. R., Uhlmann, K., Haidan, A., Ehrhart-Bornstein, M., and Scherbaum, W. A. (1997). Evidence for a novel peripheral action of leptin as a metabolic signal to the adrenal gland: leptin inhibits cortisol release directly. Diabetes *46*, 1235-1238.

Bray, G. A. (2004). Medical consequences of obesity. J Clin Endocrinol Metab *89*, 2583-2589.

Broadwell, R. D., and Brightman, M. W. (1976). Entry of peroxidase into neurons of the central and peripheral nervous systems from extracerebral and cerebral blood. J Comp Neurol *166*, 257-283.

Broberger, C., De Lecea, L., Sutcliffe, J. G., and Hokfelt, T. (1998). Hypocretin/orexin- and melanin-concentrating hormone-expressing cells form distinct populations in the rodent lateral hypothalamus: relationship to the neuropeptide Y and agouti gene-related protein systems. J Comp Neurol *402*, 460-474.

Bromberg, J. F., Wrzeszczynska, M. H., Devgan, G., Zhao, Y., Pestell, R. G., Albanese, C., and Darnell, J. E., Jr. (1999). Stat3 as an oncogene. Cell *98*, 295-303.

Brown, A. M., Mayfield, D. K., Volaufova, J., and Argyropoulos, G. (2001). The gene structure and minimal promoter of the human agouti related protein. Gene *277*, 231-238.

Bruning, J. C., Gautam, D., Burks, D. J., Gillette, J., Schubert, M., Orban, P. C., Klein, R., Krone, W., Muller-Wieland, D., and Kahn, C. R. (2000). Role of brain insulin receptor in control of body weight and reproduction. Science *289*, 2122-2125.

Burcelin, R., Kamohara, S., Li, J., Tannenbaum, G. S., Charron, M. J., and Friedman, J. M. (1999). Acute intravenous leptin infusion increases glucose turnover but not skeletal muscle glucose uptake in ob/ob mice. Diabetes *48*, 1264-1269.

Burks, D. J., Font de Mora, J., Schubert, M., Withers, D. J., Myers, M. G., Towery, H. H., Altamuro, S. L., Flint, C. L., and White, M. F. (2000). IRS-2 pathways integrate female reproduction and energy homeostasis. Nature *407*, 377-382.

Cammisotto, P. G., Gelinas, Y., Deshaies, Y., and Bukowiecki, L. J. (2003). Regulation of leptin secretion from white adipocytes by free fatty acids. Am J Physiol Endocrinol Metab *285*, E521-526.

Campfield, L. A., Smith, F. J., Guisez, Y., Devos, R., and Burn, P. (1995). Recombinant mouse OB protein: evidence for a peripheral signal linking adiposity and central neural networks. Science *269*, 546-549.

Casola, S., Cattoretti, G., Uyttersprot, N., Koralov, S. B., Seagal, J., Hao, Z., Waisman, A., Egert, A., Ghitza, D., and Rajewsky, K. (2006). Tracking germinal center B cells expressing germ-line immunoglobulin gamma1 transcripts by conditional gene targeting. Proc Natl Acad Sci U S A *103*, 7396-7401.

Chehab, F. F., Lim, M. E., and Lu, R. (1996). Correction of the sterility defect in homozygous obese female mice by treatment with the human recombinant leptin. Nat Genet *12*, 318-320.

Cheung, C. C., Clifton, D. K., and Steiner, R. A. (1997). Proopiomelanocortin neurons are direct targets for leptin in the hypothalamus. Endocrinology *138*, 4489-4492.

Choudhury, A. I., Heffron, H., Smith, M. A., Al-Qassab, H., Xu, A. W., Selman, C., Simmgen, M., Clements, M., Claret, M., Maccoll, G., *et al.* (2005). The role of insulin receptor substrate 2 in hypothalamic and beta cell function. J Clin Invest *115*, 940-950.

Chretien, M., Benjannet, S., Gossard, F., Gianoulakis, C., Crine, P., Lis, M., and Seidah, N. G. (1979). From beta-lipotropin to beta-endorphin and 'pro-opio-melanocortin'. Can J Biochem *57*, 1111-1121.

Chua, S. C., Jr., Brown, A. W., Kim, J., Hennessey, K. L., Leibel, R. L., and Hirsch, J. (1991). Food deprivation and hypothalamic neuropeptide gene expression: effects of strain background and the diabetes mutation. Brain Res Mol Brain Res *11*, 291-299.

Chua, S. C., Jr., Liu, S. M., Li, Q., Sun, A., DeNino, W. F., Heymsfield, S. B., and Guo, X. E. (2004). Transgenic complementation of leptin receptor deficiency. II. Increased leptin receptor transgene dose effects on obesity/diabetes and fertility/lactation in lepr-db/db mice. Am J Physiol Endocrinol Metab *286*, E384-392.

Clegg, D. J., Wortman, M. D., Benoit, S. C., McOsker, C. C., and Seeley, R. J. (2002). Comparison of central and peripheral administration of C75 on food intake, body weight, and conditioned taste aversion. Diabetes *51*, 3196-3201.

Clement, K., Vaisse, C., Lahlou, N., Cabrol, S., Pelloux, V., Cassuto, D., Gourmelen, M., Dina, C., Chambaz, J., Lacorte, J. M., *et al.* (1998). A mutation in the human leptin receptor gene causes obesity and pituitary dysfunction. Nature *392*, 398-401.

Cohen, P., Zhao, C., Cai, X., Montez, J. M., Rohani, S. C., Feinstein, P., Mombaerts, P., and Friedman, J. M. (2001). Selective deletion of leptin receptor in neurons leads to obesity. J Clin Invest *108*, 1113-1121.

Coleman, D. L. (1978). Obese and diabetes: two mutant genes causing diabetes-obesity syndromes in mice. Diabetologia *14*, 141-148.

Considine, R. V., Considine, E. L., Williams, C. J., Hyde, T. M., and Caro, J. F. (1996a). The hypothalamic leptin receptor in humans: identification of incidental sequence polymorphisms and absence of the db/db mouse and fa/fa rat mutations. Diabetes *45*, 992-994.

Considine, R. V., Sinha, M. K., Heiman, M. L., Kriauciunas, A., Stephens, T. W., Nyce, M. R., Ohannesian, J. P., Marco, C. C., McKee, L. J., Bauer, T. L., and et al. (1996b). Serum immunoreactive-leptin concentrations in normal-weight and obese humans. N Engl J Med *334*, 292-295.

Coppack, S. W., Pinkney, J. H., and Mohamed-Ali, V. (1998). Leptin production in human adipose tissue. Proc Nutr Soc *57*, 461-470.

Coppari, R., Ichinose, M., Lee, C. E., Pullen, A. E., Kenny, C. D., McGovern, R. A., Tang, V., Liu, S. M., Ludwig, T., Chua, S. C., Jr., *et al.* (2005). The hypothalamic arcuate nucleus: a key site for mediating leptin's effects on glucose homeostasis and locomotor activity. Cell Metab *1*, 63-72.

Covey, S. D., Wideman, R. D., McDonald, C., Unniappan, S., Huynh, F., Asadi, A., Speck, M., Webber, T., Chua, S. C., and Kieffer, T. J. (2006). The pancreatic beta cell is a key site for mediating the effects of leptin on glucose homeostasis. Cell Metab *4*, 291-302.

Cowley, M. A., Smart, J. L., Rubinstein, M., Cerdan, M. G., Diano, S., Horvath, T. L., Cone, R. D., and Low, M. J. (2001). Leptin activates anorexigenic POMC neurons through a neural network in the arcuate nucleus. Nature *411*, 480-484.

Cox, J. E., and Powley, T. L. (1981). Intragastric pair feeding fails to prevent VMH obesity or hyperinsulinemia. Am J Physiol *240*, E566-572.

Cushman, S. W., and Wardzala, L. J. (1980). Potential mechanism of insulin action on glucose transport in the isolated rat adipose cell. Apparent translocation of intracellular transport systems to the plasma membrane. J Biol Chem *255*, 4758-4762.

Cushman, S. W., Wardzala, L. J., Simpson, I. A., Karnieli, E., Hissin, P. J., Wheeler, T. J., Hinkle, P. C., and Salans, L. B. (1984). Insulin-induced translocation of intracellular glucose transporters in the isolated rat adipose cell. Fed Proc *43*, 2251-2255.

da Silva, A. A., Kuo, J. J., and Hall, J. E. (2004). Role of hypothalamic melanocortin 3/4-receptors in mediating chronic cardiovascular, renal, and metabolic actions of leptin. Hypertension *43*, 1312-1317.

de Luca, C., Kowalski, T. J., Zhang, Y., Elmquist, J. K., Lee, C., Kilimann, M. W., Ludwig, T., Liu, S. M., and Chua, S. C., Jr. (2005). Complete rescue of obesity, diabetes, and infertility in db/db mice by neuron-specific LEPR-B transgenes. J Clin Invest *115*, 3484-3493.

Dhillon, H., Zigman, J. M., Ye, C., Lee, C. E., McGovern, R. A., Tang, V., Kenny, C. D., Christiansen, L. M., White, R. D., Edelstein, E. A.*, et al.* (2006). Leptin directly activates SF1 neurons in the VMH, and this action by leptin is required for normal body-weight homeostasis. Neuron *49*, 191-203.

Docherty, K., and Hutton, J. C. (1983). Carboxypeptidase activity in the insulin secretory granule. FEBS Lett *162*, 137-141.

Donahoo, W. T., Jensen, D. R., Yost, T. J., and Eckel, R. H. (1997). Isoproterenol and somatostatin decrease plasma leptin in humans: a novel mechanism regulating leptin secretion. J Clin Endocrinol Metab *82*, 4139-4143.

Dunn, S. L., Bjornholm, M., Bates, S. H., Chen, Z., Seifert, M., and Myers, M. G., Jr. (2005). Feedback inhibition of leptin receptor/Jak2 signaling via Tyr1138 of the leptin receptor and suppressor of cytokine signaling 3. Mol Endocrinol *19*, 925-938.

El-Haschimi, K., Pierroz, D. D., Hileman, S. M., Bjorbaek, C., and Flier, J. S. (2000). Two defects contribute to hypothalamic leptin resistance in mice with diet-induced obesity. J Clin Invest *105*, 1827-1832.

Elias, C. F., Aschkenasi, C., Lee, C., Kelly, J., Ahima, R. S., Bjorbaek, C., Flier, J. S., Saper, C. B., and Elmquist, J. K. (1999). Leptin differentially regulates NPY and POMC neurons projecting to the lateral hypothalamic area. Neuron *23*, 775-786.

Elias, C. F., Saper, C. B., Maratos-Flier, E., Tritos, N. A., Lee, C., Kelly, J., Tatro, J. B., Hoffman, G. E., Ollmann, M. M., Barsh, G. S.*, et al.* (1998). Chemically defined projections linking the mediobasal hypothalamus and the lateral hypothalamic area. J Comp Neurol *402*, 442-459.

Elmquist, J. K., Bjorbaek, C., Ahima, R. S., Flier, J. S., and Saper, C. B. (1998). Distributions of leptin receptor mRNA isoforms in the rat brain. J Comp Neurol *395*, 535-547.

Endo, T. A., Masuhara, M., Yokouchi, M., Suzuki, R., Sakamoto, H., Mitsui, K., Matsumoto, A., Tanimura, S., Ohtsubo, M., Misawa, H.*, et al.* (1997). A new protein containing an SH2 domain that inhibits JAK kinases. Nature *387*, 921-924.

Faouzi, M., Leshan, R., Bjornholm, M., Hennessey, T., Jones, J., and Munzberg, H. (2007). Differential accessibility of circulating leptin to individual hypothalamic sites. Endocrinology *148*, 5414-5423.

Farooqi, I. S., Jebb, S. A., Langmack, G., Lawrence, E., Cheetham, C. H., Prentice, A. M., Hughes, I. A., McCamish, M. A., and O'Rahilly, S. (1999). Effects of recombinant leptin therapy in a child with congenital leptin deficiency. N Engl J Med *341*, 879-884.

Farooqi, I. S., and O'Rahilly, S. (2005a). Monogenic obesity in humans. Annu Rev Med *56*, 443-458.

Farooqi, I. S., and O'Rahilly, S. (2005b). New advances in the genetics of early onset obesity. Int J Obes (Lond) *29*, 1149-1152.

Fekete, C., Kelly, J., Mihaly, E., Sarkar, S., Rand, W. M., Legradi, G., Emerson, C. H., and Lechan, R. M. (2001). Neuropeptide Y has a central inhibitory action on the hypothalamic-pituitary-thyroid axis. Endocrinology *142*, 2606-2613.

Fekete, C., Singru, P. S., Sanchez, E., Sarkar, S., Christoffolete, M. A., Riberio, R. S., Rand, W. M., Emerson, C. H., Bianco, A. C., and Lechan, R. M. (2006). Differential effects of central leptin, insulin, or glucose administration during fasting on the hypothalamic-pituitary-thyroid axis and feeding-related neurons in the arcuate nucleus. Endocrinology *147*, 520-529.

Flegal, K. M., Carroll, M. D., Ogden, C. L., and Johnson, C. L. (2002). Prevalence and trends in obesity among US adults, 1999-2000. Jama *288*, 1723-1727.

Fruhbeck, G., Gomez-Ambrosi, J., Muruzabal, F. J., and Burrell, M. A. (2001). The adipocyte: a model for integration of endocrine and metabolic signaling in energy metabolism regulation. Am J Physiol Endocrinol Metab *280*, E827-847.

Gao, Q., Wolfgang, M. J., Neschen, S., Morino, K., Horvath, T. L., Shulman, G. I., and Fu, X. Y. (2004). Disruption of neural signal transducer and activator of transcription 3 causes obesity, diabetes, infertility, and thermal dysregulation. Proc Natl Acad Sci U S A *101*, 4661-4666.

Ge, H., Huang, L., Pourbahrami, T., and Li, C. (2002). Generation of soluble leptin receptor by ectodomain shedding of membrane-spanning receptors in vitro and in vivo. J Biol Chem *277*, 45898-45903.

Gong, Y., Ishida-Takahashi, R., Villanueva, E. C., Fingar, D. C., Munzberg, H., and Myers, M. G., Jr. (2007). The long form of the leptin receptor regulates STAT5 and ribosomal protein S6 via alternate mechanisms. J Biol Chem *282*, 31019-31027.

Gropp, E., Shanabrough, M., Borok, E., Xu, A. W., Janoschek, R., Buch, T., Plum, L., Balthasar, N., Hampel, B., Waisman, A., *et al.* (2005). Agouti-related peptide-expressing neurons are mandatory for feeding. Nat Neurosci *8*, 1289-1291.

Hagan, J. J., Leslie, R. A., Patel, S., Evans, M. L., Wattam, T. A., Holmes, S., Benham, C. D., Taylor, S. G., Routledge, C., Hemmati, P., *et al.* (1999). Orexin A activates locus coeruleus cell firing and increases arousal in the rat. Proc Natl Acad Sci U S A *96*, 10911-10916.

Hakansson, M. L., and Meister, B. (1998). Transcription factor STAT3 in leptin target neurons of the rat hypothalamus. Neuroendocrinology *68*, 420-427.

Halaas, J. L., Gajiwala, K. S., Maffei, M., Cohen, S. L., Chait, B. T., Rabinowitz, D., Lallone, R. L., Burley, S. K., and Friedman, J. M. (1995). Weight-reducing effects of the plasma protein encoded by the obese gene. Science *269*, 543-546.

Harris, J. I. (1959). Studies on pituitary polypeptide hormones. III. The structure of alpha-melanocyte-stimulating hormone from pig pituitary glands. Biochem J *71*, 451-459.

Harris, M., Aschkenasi, C., Elias, C. F., Chandrankunnel, A., Nillni, E. A., Bjoorbaek, C., Elmquist, J. K., Flier, J. S., and Hollenberg, A. N. (2001). Transcriptional regulation of the thyrotropin-releasing hormone gene by leptin and melanocortin signaling. J Clin Invest *107*, 111-120.

Harvey, J., McKay, N. G., Walker, K. S., Van der Kaay, J., Downes, C. P., and Ashford, M. L. (2000). Essential role of phosphoinositide 3-kinase in leptin-induced K(ATP) channel activation in the rat CRI-G1 insulinoma cell line. J Biol Chem *275*, 4660-4669.

Haslam, D. W., and James, W. P. (2005). Obesity. Lancet *366*, 1197-1209.

He, W., Lam, T. K., Obici, S., and Rossetti, L. (2006). Molecular disruption of hypothalamic nutrient sensing induces obesity. Nat Neurosci *9*, 227-233.

Herrid, M., O'Shea, T., and McFarlane, J. R. (2007). Ontogeny of leptin and its receptor expression in mouse testis during the postnatal period. Mol Reprod Dev.

Hill, J. O., and Peters, J. C. (1998). Environmental contributions to the obesity epidemic. Science *280*, 1371-1374.

Hogan, B., Constantini, F., and Lacy, I. (1987). Manipulating the mouse embryo. Cold Spring Harbor Laboratory Press.

Hoggard, N., Mercer, J. G., Rayner, D. V., Moar, K., Trayhurn, P., and Williams, L. M. (1997). Localization of leptin receptor mRNA splice variants in murine peripheral tissues by RT-PCR and in situ hybridization. Biochem Biophys Res Commun *232*, 383-387.

Howe, L. R., Leevers, S. J., Gomez, N., Nakielny, S., Cohen, P., and Marshall, C. J. (1992). Activation of the MAP kinase pathway by the protein kinase raf. Cell *71*, 335-342.

Hsu, R., Taylor, J. R., Newton, S. S., Alvaro, J. D., Haile, C., Han, G., Hruby, V. J., Nestler, E. J., and Duman, R. S. (2005). Blockade of melanocortin transmission inhibits cocaine reward. Eur J Neurosci *21*, 2233-2242.

Inoue, H., Nojima, H., and Okayama, H. (1990). High efficiency transformation of Escherichia coli with plasmids. Gene *96*, 23-28.

Inoue, H., Ogawa, W., Asakawa, A., Okamoto, Y., Nishizawa, A., Matsumoto, M., Teshigawara, K., Matsuki, Y., Watanabe, E., Hiramatsu, R., *et al.* (2006). Role of hepatic STAT3 in brain-insulin action on hepatic glucose production. Cell Metab *3*, 267-275.

Jegou, S., Boutelet, I., and Vaudry, H. (2000). Melanocortin-3 receptor mRNA expression in pro-opiomelanocortin neurones of the rat arcuate nucleus. J Neuroendocrinol *12*, 501-505.

Joseph, S. A., Pilcher, W. H., and Bennett-Clarke, C. (1983). Immunocytochemical localization of ACTH perikarya in nucleus tractus solitarius: evidence for a second opiocortin neuronal system. Neurosci Lett *38*, 221-225.

Kaelin, C. B., Gong, L., Xu, A. W., Yao, F., Hockman, K., Morton, G. J., Schwartz, M. W., Barsh, G. S., and MacKenzie, R. G. (2006). Signal transducer and activator of transcription (stat) binding sites but not stat3 are required for fasting-induced transcription of agouti-related protein messenger ribonucleic acid. Mol Endocrinol *20*, 2591-2602.

Kaelin, C. B., Xu, A. W., Lu, X. Y., and Barsh, G. S. (2004). Transcriptional regulation of agouti-related protein (Agrp) in transgenic mice. Endocrinology *145*, 5798-5806.

Kahn, B. B., and Flier, J. S. (2000). Obesity and insulin resistance. J Clin Invest *106*, 473-481.

Kamohara, S., Burcelin, R., Halaas, J. L., Friedman, J. M., and Charron, M. J. (1997). Acute stimulation of glucose metabolism in mice by leptin treatment. Nature *389*, 374-377.

Kastin, A. J., and Pan, W. (2000). Dynamic regulation of leptin entry into brain by the blood-brain barrier. Regul Pept *92*, 37-43.

Keith, B. J., and Paxinos, G. (1997). The Mouse Brain in Stereotaxic Coordinates. Academic Press.

Kitamura, T., Feng, Y., Kitamura, Y. I., Chua, S. C., Jr., Xu, A. W., Barsh, G. S., Rossetti, L., and Accili, D. (2006). Forkhead protein FoxO1 mediates Agrp-dependent effects of leptin on food intake. Nat Med *12*, 534-540.

Kloek, C., Haq, A. K., Dunn, S. L., Lavery, H. J., Banks, A. S., and Myers, M. G., Jr. (2002). Regulation of Jak kinases by intracellular leptin receptor sequences. J Biol Chem *277*, 41547-41555.

Kokoeva, M. V., Yin, H., and Flier, J. S. (2005). Neurogenesis in the hypothalamus of adult mice: potential role in energy balance. Science *310*, 679-683.

Konner, A. C., Janoschek, R., Plum, L., Jordan, S. D., Rother, E., Ma, X., Xu, C., Enriori, P., Hampel, B., Barsh, G. S., *et al.* (2007). Insulin Action in AgRP-Expressing Neurons Is Required for Suppression of Hepatic Glucose Production. Cell Metab *5*, 438-449.

Kowalski, T. J., Liu, S. M., Leibel, R. L., and Chua, S. C., Jr. (2001). Transgenic complementation of leptin-receptor deficiency. I. Rescue of the obesity/diabetes phenotype of LEPR-null mice expressing a LEPR-B transgene. Diabetes *50*, 425-435.

Krugel, U., Schraft, T., Kittner, H., Kiess, W., and Illes, P. (2003). Basal and feeding-evoked dopamine release in the rat nucleus accumbens is depressed by leptin. Eur J Pharmacol *482*, 185-187.

Kulkarni, R. N., Wang, Z. L., Wang, R. M., Hurley, J. D., Smith, D. M., Ghatei, M. A., Withers, D. J., Gardiner, J. V., Bailey, C. J., and Bloom, S. R. (1997). Leptin rapidly suppresses insulin release from insulinoma cells, rat and human islets and, in vivo, in mice. J Clin Invest *100*, 2729-2736.

Lacaze-Masmonteil, T., de Keyzer, Y., Luton, J. P., Kahn, A., and Bertagna, X. (1987). Characterization of proopiomelanocortin transcripts in human nonpituitary tissues. Proc Natl Acad Sci U S A *84*, 7261-7265.

Lam, T. K., Gutierrez-Juarez, R., Pocai, A., and Rossetti, L. (2005). Regulation of blood glucose by hypothalamic pyruvate metabolism. Science *309*, 943-947.

Larhammar, D. (1996). Structural diversity of receptors for neuropeptide Y, peptide YY and pancreatic polypeptide. Regul Pept *65*, 165-174.

Lee, G. H., Proenca, R., Montez, J. M., Carroll, K. M., Darvishzadeh, J. G., Lee, J. I., and Friedman, J. M. (1996). Abnormal splicing of the leptin receptor in diabetic mice. Nature *379*, 632-635.

Levy, D. E., and Darnell, J. E., Jr. (2002). Stats: transcriptional control and biological impact. Nat Rev Mol Cell Biol *3*, 651-662.

Levy, J. R., Gyarmati, J., Lesko, J. M., Adler, R. A., and Stevens, W. (2000). Dual regulation of leptin secretion: intracellular energy and calcium dependence of regulated pathway. Am J Physiol Endocrinol Metab *278*, E892-901.

Li, C., Ioffe, E., Fidahusein, N., Connolly, E., and Friedman, J. M. (1998). Absence of soluble leptin receptor in plasma from dbPas/dbPas and other db/db mice. J Biol Chem *273*, 10078-10082.

Licinio, J., Caglayan, S., Ozata, M., Yildiz, B. O., de Miranda, P. B., O'Kirwan, F., Whitby, R., Liang, L., Cohen, P., Bhasin, S.*, et al.* (2004). Phenotypic effects of leptin replacement on morbid obesity, diabetes mellitus, hypogonadism, and behavior in leptin-deficient adults. Proc Natl Acad Sci U S A *101*, 4531-4536.

Lindvall, O., and Bjorlund, A. (1983). Dopamine and norepinephrine-containing neuron systems: their anatomy in the rat brain. In Chemical Neuroanatomy, P. C. Emson, ed. (New York: Raven Press), pp. 229 – 255.

Liu, L., Karkanias, G. B., Morales, J. C., Hawkins, M., Barzilai, N., Wang, J., and Rossetti, L. (1998). Intracerebroventricular leptin regulates hepatic but not peripheral glucose fluxes. J Biol Chem *273*, 31160-31167.

Loftus, T. M., Jaworsky, D. E., Frehywot, G. L., Townsend, C. A., Ronnett, G. V., Lane, M. D., and Kuhajda, F. P. (2000). Reduced food intake and body weight in mice treated with fatty acid synthase inhibitors. Science *288*, 2379-2381.

Lollmann, B., Gruninger, S., Stricker-Krongrad, A., and Chiesi, M. (1997). Detection and quantification of the leptin receptor splice variants Ob-Ra, b, and, e in different mouse tissues. Biochem Biophys Res Commun *238*, 648-652.

Luoh, S. M., Di Marco, F., Levin, N., Armanini, M., Xie, M. H., Nelson, C., Bennett, G. L., Williams, M., Spencer, S. A., Gurney, A., and de Sauvage, F. J. (1997). Cloning and characterization of a human leptin receptor using a biologically active leptin immunoadhesin. J Mol Endocrinol *18*, 77-85.

Luquet, S., Perez, F. A., Hnasko, T. S., and Palmiter, R. D. (2005). NPY/AgRP neurons are essential for feeding in adult mice but can be ablated in neonates. Science *310*, 683-685.

Lutticken, C., Wegenka, U. M., Yuan, J., Buschmann, J., Schindler, C., Ziemiecki, A., Harpur, A. G., Wilks, A. F., Yasukawa, K., Taga, T., and et al. (1994). Association of transcription factor APRF and protein kinase Jak1 with the interleukin-6 signal transducer gp130. Science *263*, 89-92.

Maffei, M., Halaas, J., Ravussin, E., Pratley, R. E., Lee, G. H., Zhang, Y., Fei, H., Kim, S., Lallone, R., Ranganathan, S., and et al. (1995). Leptin levels in human and rodent: measurement of plasma leptin and ob RNA in obese and weight-reduced subjects. Nat Med *1*, 1155-1161.

Maffei, M., Stoffel, M., Barone, M., Moon, B., Dammerman, M., Ravussin, E., Bogardus, C., Ludwig, D. S., Flier, J. S., Talley, M., and et al. (1996). Absence of mutations in the human OB gene in obese/diabetic subjects. Diabetes *45*, 679-682.

Makimura, H., Mizuno, T. M., Isoda, F., Beasley, J., Silverstein, J. H., and Mobbs, C. V. (2003). Role of glucocorticoids in mediating effects of fasting and diabetes on hypothalamic gene expression. BMC Physiol *3*, 5.

Makimura, H., Mizuno, T. M., Mastaitis, J. W., Agami, R., and Mobbs, C. V. (2002). Reducing hypothalamic AGRP by RNA interference increases metabolic rate and decreases body weight without influencing food intake. BMC Neurosci *3*, 18.

Manson, J. E., Willett, W. C., Stampfer, M. J., Colditz, G. A., Hunter, D. J., Hankinson, S. E., Hennekens, C. H., and Speizer, F. E. (1995). Body weight and mortality among women. N Engl J Med *333*, 677-685.

Mantzoros, C. S., Flier, J. S., and Rogol, A. D. (1997). A longitudinal assessment of hormonal and physical alterations during normal puberty in boys. V. Rising leptin levels may signal the onset of puberty. J Clin Endocrinol Metab *82*, 1066-1070.

Marks, D. L., Boucher, N., Lanouette, C. M., Perusse, L., Brookhart, G., Comuzzie, A. G., Chagnon, Y. C., and Cone, R. D. (2004). Ala67Thr polymorphism in the Agouti-related peptide gene is associated with inherited leanness in humans. Am J Med Genet A *126*, 267-271.

Marsh, D. J., Weingarth, D. T., Novi, D. E., Chen, H. Y., Trumbauer, M. E., Chen, A. S., Guan, X. M., Jiang, M. M., Feng, Y., Camacho, R. E.*, et al.* (2002). Melanin-concentrating hormone 1 receptor-deficient mice are lean, hyperactive, and hyperphagic and have altered metabolism. Proc Natl Acad Sci U S A *99*, 3240-3245.

Masuzaki, H., Ogawa, Y., Sagawa, N., Hosoda, K., Matsumoto, T., Mise, H., Nishimura, H., Yoshimasa, Y., Tanaka, I., Mori, T., and Nakao, K. (1997). Nonadipose tissue production of leptin: leptin as a novel placenta-derived hormone in humans. Nat Med *3*, 1029-1033.

Matkovic, V., Ilich, J. Z., Skugor, M., Badenhop, N. E., Goel, P., Clairmont, A., Klisovic, D., Nahhas, R. W., and Landoll, J. D. (1997). Leptin is inversely related to age at menarche in human females. J Clin Endocrinol Metab *82*, 3239-3245.

Mayer, J. (1953). Decreased activity and energy balance in the hereditary obesity-diabetes syndrome of mice. Science *117*, 504-505.

McMinn, J. E., Wilkinson, C. W., Havel, P. J., Woods, S. C., and Schwartz, M. W. (2000). Effect of intracerebroventricular alpha-MSH on food intake, adiposity, c-Fos induction, and neuropeptide expression. Am J Physiol Regul Integr Comp Physiol *279*, R695-703.

Mei, Z., Grummer-Strawn, L. M., Pietrobelli, A., Goulding, A., Goran, M. I., and Dietz, W. H. (2002). Validity of body mass index compared with other body-composition screening indexes for the assessment of body fatness in children and adolescents. Am J Clin Nutr *75*, 978-985.

Minth, C. D., Bloom, S. R., Polak, J. M., and Dixon, J. E. (1984). Cloning, characterization, and DNA sequence of a human cDNA encoding neuropeptide tyrosine. Proc Natl Acad Sci U S A *81*, 4577-4581.

Mizuno, T. M., Bergen, H., Funabashi, T., Kleopoulos, S. P., Zhong, Y. G., Bauman, W. A., and Mobbs, C. V. (1996). Obese gene expression: reduction by fasting and stimulation by insulin and glucose in lean mice, and persistent elevation in acquired (diet-induced) and genetic (yellow agouti) obesity. Proc Natl Acad Sci U S A *93*, 3434-3438.

Mizuno, T. M., and Mobbs, C. V. (1999). Hypothalamic agouti-related protein messenger ribonucleic acid is inhibited by leptin and stimulated by fasting. Endocrinology *140*, 814-817.

Montague, C. T., Farooqi, I. S., Whitehead, J. P., Soos, M. A., Rau, H., Wareham, N. J., Sewter, C. P., Digby, J. E., Mohammed, S. N., Hurst, J. A.*, et al.* (1997). Congenital leptin deficiency is associated with severe early-onset obesity in humans. Nature *387*, 903-908.

Morris, B. J. (1989). Neuronal localisation of neuropeptide Y gene expression in rat brain. J Comp Neurol *290*, 358-368.

Morrison, C. D., Morton, G. J., Niswender, K. D., Gelling, R. W., and Schwartz, M. W. (2005). Leptin inhibits hypothalamic Npy and Agrp gene expression via a mechanism that requires phosphatidylinositol 3-OH-kinase signaling. Am J Physiol Endocrinol Metab *289*, E1051-1057.

Mountjoy, K. G., Mortrud, M. T., Low, M. J., Simerly, R. B., and Cone, R. D. (1994). Localization of the melanocortin-4 receptor (MC4-R) in neuroendocrine and autonomic control circuits in the brain. Mol Endocrinol *8*, 1298-1308.

Munzberg, H., Bjornholm, M., Bates, S. H., and Myers, M. G., Jr. (2005). Leptin receptor action and mechanisms of leptin resistance. Cell Mol Life Sci *62*, 642-652.

Munzberg, H., Flier, J. S., and Bjorbaek, C. (2004). Region-specific leptin resistance within the hypothalamus of diet-induced obese mice. Endocrinology *145*, 4880-4889.

Munzberg, H., Jobst, E. E., Bates, S. H., Jones, J., Villanueva, E., Leshan, R., Bjornholm, M., Elmquist, J., Sleeman, M., Cowley, M. A., and Myers, M. G., Jr. (2007). Appropriate inhibition of orexigenic hypothalamic arcuate nucleus neurons independently of leptin receptor/STAT3 signaling. J Neurosci *27*, 69-74.

Myers, M. G., Cowley, M. A., and Munzberg, H. (2007). Mechanisms of Leptin Action and Leptin Resistance. Annu Rev Physiol.

Naka, T., Narazaki, M., Hirata, M., Matsumoto, T., Minamoto, S., Aono, A., Nishimoto, N., Kajita, T., Taga, T., Yoshizaki, K., *et al.* (1997). Structure and function of a new STAT-induced STAT inhibitor. Nature *387*, 924-929.

Niswender, K. D., Morton, G. J., Stearns, W. H., Rhodes, C. J., Myers, M. G., Jr., and Schwartz, M. W. (2001). Intracellular signalling. Key enzyme in leptin-induced anorexia. Nature *413*, 794-795.

Obici, S., Feng, Z., Karkanias, G., Baskin, D. G., and Rossetti, L. (2002a). Decreasing hypothalamic insulin receptors causes hyperphagia and insulin resistance in rats. Nat Neurosci *5*, 566-572.

Obici, S., Feng, Z., Morgan, K., Stein, D., Karkanias, G., and Rossetti, L. (2002b). Central administration of oleic acid inhibits glucose production and food intake. Diabetes *51*, 271-275.

Ollmann, M. M., Wilson, B. D., Yang, Y. K., Kerns, J. A., Chen, Y., Gantz, I., and Barsh, G. S. (1997). Antagonism of central melanocortin receptors in vitro and in vivo by agouti-related protein. Science *278*, 135-138.

Olney, J. W. (1969). Brain lesions, obesity, and other disturbances in mice treated with monosodium glutamate. Science *164*, 719-721.

Overton, J. M., and Williams, T. D. (2004). Behavioral and physiologic responses to caloric restriction in mice. Physiol Behav *81*, 749-754.

Pages, N., Orosco, M., Rouch, C., Yao, O., Jacquot, C., and Bohuon, C. (1993). Refeeding after 72 hour fasting alters neuropeptide Y and monoamines in various cerebral areas in the rat. Comp Biochem Physiol Comp Physiol *106*, 845-849.

Pelleymounter, M. A., Cullen, M. J., Baker, M. B., Hecht, R., Winters, D., Boone, T., and Collins, F. (1995). Effects of the obese gene product on body weight regulation in ob/ob mice. Science *269*, 540-543.

Pilkis, S. J., and Granner, D. K. (1992). Molecular physiology of the regulation of hepatic gluconeogenesis and glycolysis. Annu Rev Physiol *54*, 885-909.

Plum, L., Ma, X., Hampel, B., Balthasar, N., Coppari, R., Munzberg, H., Shanabrough, M., Burdakov, D., Rother, E., Janoschek, R., *et al.* (2006). Enhanced PIP3 signaling in POMC neurons causes KATP channel activation and leads to diet-sensitive obesity. J Clin Invest *116*, 1886-1901.

Poitout, V., Hagman, D., Stein, R., Artner, I., Robertson, R. P., and Harmon, J. S. (2006). Regulation of the insulin gene by glucose and fatty acids. J Nutr *136*, 873-876.

Polonsky, K. S., Given, B. D., Hirsch, L., Shapiro, E. T., Tillil, H., Beebe, C., Galloway, J. A., Frank, B. H., Karrison, T., and Van Cauter, E. (1988). Quantitative study of insulin secretion and clearance in normal and obese subjects. J Clin Invest *81*, 435-441.

Poon, T. K., and Cameron, D. P. (1978). Measurement of oxygen consumption and locomotor activity in monosodium glutamate-induced obesity. Am J Physiol *234*, E532-534.

Pralong, F. P., Roduit, R., Waeber, G., Castillo, E., Mosimann, F., Thorens, B., and Gaillard, R. C. (1998). Leptin inhibits directly glucocorticoid secretion by normal human and rat adrenal gland. Endocrinology *139*, 4264-4268.

Qu, D., Ludwig, D. S., Gammeltoft, S., Piper, M., Pelleymounter, M. A., Cullen, M. J., Mathes, W. F., Przypek, R., Kanarek, R., and Maratos-Flier, E. (1996). A role for melanin-concentrating hormone in the central regulation of feeding behaviour. Nature *380*, 243-247.

Rahmouni, K., Haynes, W. G., and Mark, A. L. (2002). Cardiovascular and sympathetic effects of leptin. Curr Hypertens Rep *4*, 119-125.

Roseberry, A. G., Painter, T., Mark, G. P., and Williams, J. T. (2007). Decreased vesicular somatodendritic dopamine stores in leptin-deficient mice. J Neurosci *27*, 7021-7027.

Rossi, M., Kim, M. S., Morgan, D. G., Small, C. J., Edwards, C. M., Sunter, D., Abusnana, S., Goldstone, A. P., Russell, S. H., Stanley, S. A., *et al.* (1998). A C-terminal fragment of Agouti-related protein increases feeding and antagonizes the effect of alpha-melanocyte stimulating hormone in vivo. Endocrinology *139*, 4428-4431.

Saiki, R. K., Bugawan, T. L., Horn, G. T., Mullis, K. B., and Erlich, H. A. (1986). Analysis of enzymatically amplified beta-globin and HLA-DQ alpha DNA with allele-specific oligonucleotide probes. Nature *324*, 163-166.

Saiki, R. K., Scharf, S., Faloona, F., Mullis, K. B., Horn, G. T., Erlich, H. A., and Arnheim, N. (1985). Enzymatic amplification of beta-globin genomic sequences and restriction site analysis for diagnosis of sickle cell anemia. Science *230*, 1350-1354.

Sainsbury, A., Rohner-Jeanrenaud, F., Cusin, I., Zakrzewska, K. E., Halban, P. A., Gaillard, R. C., and Jeanrenaud, B. (1997). Chronic central neuropeptide Y infusion in normal rats: status of the hypothalamo-pituitary-adrenal axis, and vagal mediation of hyperinsulinaemia. Diabetologia *40*, 1269-1277.

Sakurai, T., Amemiya, A., Ishii, M., Matsuzaki, I., Chemelli, R. M., Tanaka, H., Williams, S. C., Richarson, J. A., Kozlowski, G. P., Wilson, S., *et al.* (1998). Orexins and orexin receptors: a family of hypothalamic neuropeptides and G protein-coupled receptors that regulate feeding behavior. Cell *92*, 1 page following 696.

Saladin, R., De Vos, P., Guerre-Millo, M., Leturque, A., Girard, J., Staels, B., and Auwerx, J. (1995). Transient increase in obese gene expression after food intake or insulin administration. Nature *377*, 527-529.

Sambrook, J., E:F:, F., and Maniatis, T. (1989). Molecular Cloning. Cold Spring Harbor Laboratory Press.

Sanchez, M. S., Barontini, M., Armando, I., and Celis, M. E. (2001). Correlation of increased grooming behavior and motor activity with alterations in nigrostriatal and mesolimbic catecholamines after alpha-melanotropin and neuropeptide glutamine-isoleucine injection in the rat ventral tegmental area. Cell Mol Neurobiol *21*, 523-533.

Sandyk, R. (1990). MIF-induced augmentation of melatonin functions: possible relevance to mechanisms of action of MIF-1 in movement disorders. Int J Neurosci *52*, 59-65.

Silver, L. M. (1995). Mouse genetics: concepts and practice. Oxford University Press.

Schwartz, M. W., Baskin, D. G., Bukowski, T. R., Kuijper, J. L., Foster, D., Lasser, G., Prunkard, D. E., Porte, D., Jr., Woods, S. C., Seeley, R. J., and Weigle, D. S. (1996a). Specificity of leptin action on elevated blood glucose levels and hypothalamic neuropeptide Y gene expression in ob/ob mice. Diabetes *45*, 531-535.

Schwartz, M. W., Peskind, E., Raskind, M., Boyko, E. J., and Porte, D., Jr. (1996b). Cerebrospinal fluid leptin levels: relationship to plasma levels and to adiposity in humans. Nat Med *2*, 589-593.

Schwartz, M. W., and Porte, D., Jr. (2005). Diabetes, obesity, and the brain. Science *307*, 375-379.

Schwartz, M. W., Seeley, R. J., Campfield, L. A., Burn, P., and Baskin, D. G. (1996c). Identification of targets of leptin action in rat hypothalamus. J Clin Invest *98*, 1101-1106.

Schwartz, M. W., Seeley, R. J., Woods, S. C., Weigle, D. S., Campfield, L. A., Burn, P., and Baskin, D. G. (1997). Leptin increases hypothalamic pro-opiomelanocortin mRNA expression in the rostral arcuate nucleus. Diabetes *46*, 2119-2123.

Schwartz, M. W., Sipols, A. J., Marks, J. L., Sanacora, G., White, J. D., Scheurink, A., Kahn, S. E., Baskin, D. G., Woods, S. C., Figlewicz, D. P., and et al. (1992). Inhibition of hypothalamic neuropeptide Y gene expression by insulin. Endocrinology *130*, 3608-3616.

Schwartz, M. W., Woods, S. C., Porte, D., Jr., Seeley, R. J., and Baskin, D. G. (2000). Central nervous system control of food intake. Nature *404*, 661-671.

Seeley, R. J., Yagaloff, K. A., Fisher, S. L., Burn, P., Thiele, T. E., van Dijk, G., Baskin, D. G., and Schwartz, M. W. (1997). Melanocortin receptors in leptin effects. Nature *390*, 349.

Seibler, J., Zevnik, B., Kuter-Luks, B., Andreas, S., Kern, H., Hennek, T., Rode, A., Heimann, C., Faust, N., Kauselmann, G., *et al.* (2003). Rapid generation of inducible mouse mutants. Nucleic Acids Res *31*, e12.

Seidell, J. C. (1997). Time trends in obesity: an epidemiological perspective. Horm Metab Res *29*, 155-158.

Shimada, M., Tritos, N. A., Lowell, B. B., Flier, J. S., and Maratos-Flier, E. (1998). Mice lacking melanin-concentrating hormone are hypophagic and lean. Nature *396*, 670-674.

Shintani, M., Nishimura, H., Yonemitsu, S., Masuzaki, H., Ogawa, Y., Hosoda, K., Inoue, G., Yoshimasa, Y., and Nakao, K. (2000). Downregulation of leptin by free fatty acids in rat adipocytes: effects of triacsin C, palmitate, and 2-bromopalmitate. Metabolism *49*, 326-330.

Shutter, J. R., Graham, M., Kinsey, A. C., Scully, S., Luthy, R., and Stark, K. L. (1997). Hypothalamic expression of ART, a novel gene related to agouti, is up-regulated in obese and diabetic mutant mice. Genes Dev *11*, 593-602.

Singhal, R. L., and Rastogi, R. B. (1982). MIF-1: effects on norepinephrine, dopamine and serotonin metabolism in certain discrete brain regions. Pharmacol Biochem Behav *16*, 229-233.

Sipols, A. J., Baskin, D. G., and Schwartz, M. W. (1995). Effect of intracerebroventricular insulin infusion on diabetic hyperphagia and hypothalamic neuropeptide gene expression. Diabetes *44*, 147-151.

Smith, D. G., Tzavara, E. T., Shaw, J., Luecke, S., Wade, M., Davis, R., Salhoff, C., Nomikos, G. G., and Gehlert, D. R. (2005). Mesolimbic dopamine super-sensitivity in melanin-concentrating hormone-1 receptor-deficient mice. J Neurosci *25*, 914-922.

Spanswick, D., Smith, M. A., Groppi, V. E., Logan, S. D., and Ashford, M. L. (1997). Leptin inhibits hypothalamic neurons by activation of ATP-sensitive potassium channels. Nature *390*, 521-525.

Stahl, N., and Yancopoulos, G. D. (1994). The tripartite CNTF receptor complex: activation and signaling involves components shared with other cytokines. J Neurobiol *25*, 1454-1466.

Stanley, B. G., Kyrkouli, S. E., Lampert, S., and Leibowitz, S. F. (1986). Neuropeptide Y chronically injected into the hypothalamus: a powerful neurochemical inducer of hyperphagia and obesity. Peptides *7*, 1189-1192.

Starr, R., Willson, T. A., Viney, E. M., Murray, L. J., Rayner, J. R., Jenkins, B. J., Gonda, T. J., Alexander, W. S., Metcalf, D., Nicola, N. A., and Hilton, D. J. (1997). A family of cytokine-inducible inhibitors of signalling. Nature *387*, 917-921.

Strubbe, J. H., and Mein, C. G. (1977). Increased feeding in response to bilateral injection of insulin antibodies in the VMH. Physiol Behav *19*, 309-313.

Struthers, A. D., and Dollery, C. T. (1985). Central nervous system mechanisms in blood pressure control. Eur J Clin Pharmacol *28 Suppl*, 3-11.

Sul, H. S., Latasa, M. J., Moon, Y., and Kim, K. H. (2000). Regulation of the fatty acid synthase promoter by insulin. J Nutr *130*, 315S-320S.

Swart, I., Jahng, J. W., Overton, J. M., and Houpt, T. A. (2002). Hypothalamic NPY, AGRP, and POMC mRNA responses to leptin and refeeding in mice. Am J Physiol Regul Integr Comp Physiol *283*, R1020-1026.

Tartaglia, L. A. (1997). The leptin receptor. J Biol Chem *272*, 6093-6096.

Tartaglia, L. A., Dembski, M., Weng, X., Deng, N., Culpepper, J., Devos, R., Richards, G. J., Campfield, L. A., Clark, F. T., Deeds, J., *et al.* (1995). Identification and expression cloning of a leptin receptor, OB-R. Cell *83*, 1263-1271.

Tobe, K., Suzuki, R., Aoyama, M., Yamauchi, T., Kamon, J., Kubota, N., Terauchi, Y., Matsui, J., Akanuma, Y., Kimura, S., *et al.* (2001). Increased expression of the sterol regulatory element-binding protein-1 gene in insulin receptor substrate-2(-/-) mouse liver. J Biol Chem *276*, 38337-38340.

Tokunaga, K., Matsuzawa, Y., Fujioka, S., Kobatake, T., Keno, Y., Odaka, H., Matsuo, T., and Tarui, S. (1991). PVN-lesioned obese rats maintain ambulatory activity and its circadian rhythm. Brain Res Bull *26*, 393-396.

Vaisse, C., Halaas, J. L., Horvath, C. M., Darnell, J. E., Jr., Stoffel, M., and Friedman, J. M. (1996). Leptin activation of Stat3 in the hypothalamus of wild-type and ob/ob mice but not db/db mice. Nat Genet *14*, 95-97.

van de Wall, E., Leshan, R., Xu, A. W., Balthasar, N., Coppari, R., Liu, S. M., Jo, Y. H., Mackenzie, R. G., Allison, D. B., Dun, N. J., *et al.* (2007). Collective and Individual Functions of Leptin Receptor Modulated Neurons Controlling Metabolism and Ingestion. Endocrinology.

van den Top, M., Lee, K., Whyment, A. D., Blanks, A. M., and Spanswick, D. (2004). Orexigen-sensitive NPY/AgRP pacemaker neurons in the hypothalamic arcuate nucleus. Nat Neurosci *7*, 493-494.

Walker, C. G., Bryson, J. M., Bell-Anderson, K. S., Hancock, D. P., Denyer, G. S., and Caterson, I. D. (2005). Insulin determines leptin responses during a glucose challenge in fed and fasted rats. Int J Obes (Lond) *29*, 398-405.

Walker, C. G., Bryson, J. M., Phuyal, J. L., and Caterson, I. D. (2002). Dietary modulation of circulating leptin levels: site-specific changes in fat deposition and ob mRNA expression. Horm Metab Res *34*, 176-181.

Welt, C. K., Chan, J. L., Bullen, J., Murphy, R., Smith, P., DePaoli, A. M., Karalis, A., and Mantzoros, C. S. (2004). Recombinant human leptin in women with hypothalamic amenorrhea. N Engl J Med *351*, 987-997.

White, D. W., Kuropatwinski, K. K., Devos, R., Baumann, H., and Tartaglia, L. A. (1997). Leptin receptor (OB-R) signaling. Cytoplasmic domain mutational analysis and evidence for receptor homo-oligomerization. J Biol Chem *272*, 4065-4071.

WHO: www.who.int

Williams, G., Harrold, J. A., and Cutler, D. J. (2000). The hypothalamus and the regulation of energy homeostasis: lifting the lid on a black box. Proc Nutr Soc *59*, 385-396.

Williams, T. D., Chambers, J. B., Gagnon, S. P., Roberts, L. M., Henderson, R. P., and Overton, J. M. (2003). Cardiovascular and metabolic responses to fasting and thermoneutrality in Ay mice. Physiol Behav *78*, 615-623.

Wilson, B. D., Bagnol, D., Kaelin, C. B., Ollmann, M. M., Gantz, I., Watson, S. J., and Barsh, G. S. (1999). Physiological and anatomical circuitry between Agouti-related protein and leptin signaling. Endocrinology *140*, 2387-2397.

Wilson, K. R., Todorovic, A., Proneth, B., and Haskell-Luevano, C. (2006). Overview of endogenous and synthetic melanocortin peptides. Cell Mol Biol (Noisy-le-grand) *52*, 3-20.

Woods, S. C., Lotter, E. C., McKay, L. D., and Porte, D., Jr. (1979). Chronic intracerebroventricular infusion of insulin reduces food intake and body weight of baboons. Nature *282*, 503-505.

Woolverton, W. L., and Johnson, K. M. (1992). Neurobiology of cocaine abuse. Trends Pharmacol Sci *13*, 193-200.

Wortley, K. E., Anderson, K. D., Yasenchak, J., Murphy, A., Valenzuela, D., Diano, S., Yancopoulos, G. D., Wiegand, S. J., and Sleeman, M. W. (2005). Agouti-related protein-deficient mice display an age-related lean phenotype. Cell Metab *2*, 421-427.

Xu, A. W., Ste-Marie, L., Kaelin, C. B., and Barsh, G. S. (2007). Inactivation of signal transducer and activator of transcription 3 in proopiomelanocortin (Pomc) neurons

causes decreased pomc expression, mild obesity, and defects in compensatory refeeding. Endocrinology *148*, 72-80.

Yasukawa, H., Misawa, H., Sakamoto, H., Masuhara, M., Sasaki, A., Wakioka, T., Ohtsuka, S., Imaizumi, T., Matsuda, T., Ihle, J. N., and Yoshimura, A. (1999). The JAK-binding protein JAB inhibits Janus tyrosine kinase activity through binding in the activation loop. Embo J *18*, 1309-1320.

Yaswen, L., Diehl, N., Brennan, M. B., and Hochgeschwender, U. (1999). Obesity in the mouse model of pro-opiomelanocortin deficiency responds to peripheral melanocortin. Nat Med *5*, 1066-1070.

Zhang, E. E., Chapeau, E., Hagihara, K., and Feng, G. S. (2004). Neuronal Shp2 tyrosine phosphatase controls energy balance and metabolism. Proc Natl Acad Sci U S A *101*, 16064-16069.

Zhang, Y., Proenca, R., Maffei, M., Barone, M., Leopold, L., and Friedman, J. M. (1994). Positional cloning of the mouse obese gene and its human homologue. Nature *372*, 425-432.

Zhao, A. Z., Huan, J. N., Gupta, S., Pal, R., and Sahu, A. (2002). A phosphatidylinositol 3-kinase phosphodiesterase 3B-cyclic AMP pathway in hypothalamic action of leptin on feeding. Nat Neurosci *5*, 727-728.

Zhou, Q. Y., and Palmiter, R. D. (1995). Dopamine-deficient mice are severely hypoactive, adipsic, and aphagic. Cell *83*, 1197-1209.

# 8 Acknowledgements

I sincerely thank Prof. Dr. Jens C. Brüning for giving me the opportunity to join his research group and providing me with this interesting project.

I would like to thank Prof. Dr. Thomas Langer, Prof. Dr. Siegfried Roth and Dr. Ursula Lichtenberg for agreeing to form my thesis committee.

I thank all the members of the Brüning lab for creating a friendly and productive environment, for help with experiments and for discussions.
In particular I thank Sigrid Irlenbusch for helping with ELISAs, Brigitte Hampel for cutting sections and Eva Rother, Linda Koch and Bengt Belgardt for proofreading the manuscript.

Außerdem möchte ich meiner Familie für Ihre Unterstützung während des gesamten Studiums danken.

# 9 Erklärung

Ich versichere, daß ich die von mir vorgelegte Dissertation selbständig angefertigt, die benutzten Quellen und Hilfsmittel vollständig angegeben und die Stellen der Arbeit – einschließich Tabellen, Karten und Abbildungen -, die anderen Werken im Wortlaut oder dem Sinn nach entnommen sind, in jedem Einzelfall als Entlehnung kenntlich gemacht habe; daß diese Dissertation noch keiner anderen Fakultät oder Universität zur Prüfung vorgelegen hat; daß sie – abgesehen von unten angegebenen Teilpublikationen – noch nicht veröffentlicht ist sowie, daß ich eine solche Veröffentlichung vor Abschluß des Promotionsverfahrens nicht vornehmen werde. Die Bestimmungen dieser Promotionsordnung sind mir bekannt. Die von mir vorgelegte Dissertation ist von Prof. Dr. Jens C. Brüning betreut worden.

Köln, Februar 2008 Andrea Mesaros

**Teilpublikationen**

Mesaros, A., Koralov, S.B., Rother, E., Wunderlich, F.T., Ernst, M.B., Barsh, G.S., Rajewsky, K., and Brüning, J.C. (2008). Activation of Stat3 Signaling in AgRP Neurons Promotes Locomotor Activity. Cell Metab. *in press; March 2008*.

# 10 Curriculum Vitae

**Persönliche Daten**


| | |
|---|---|
| Name | Andrea Mesaros |
| Adresse | Immermannstrasse 40, 50931 Köln |
| Email | mesaros@gmx.de |
| Geburtstag | 18.11.1978 |
| Geburtsort | Bergisch Gladbach |
| Nationalität | deutsch |


**Schulische Ausbildung**

| | |
|---|---|
| 1985 – 1989 | Gemeinschaftsgrundschule Heiligenhaus |
| 1989 – 1998 | Paul Klee Gymnasium Overath mit dem Abschluss der Allgemeinen Hochschulreife |

**Studium**

| | |
|---|---|
| 1998 – 2004 | Studium der Biologie an der Mathematisch-Naturwissenschaftlichen Fakultät der Universität zu Köln |
| 2003 | Diplomprüfungen im Hauptfach Genetik und in den Nebenfächern Biochemie und Zoologie |
| 2003 – 2004 | Diplomarbeit in der Abteilung Mausgenetik und Metabolismus des Instituts für Genetik der Universität zu Köln zum Thema: „Tetrazyklin-regulierte Überexpression von PLRG1“ |
| seit 04/2004 | Promotion in der Abteilung Mausgenetik und Metabolismus des Instituts für Genetik der Universtät zu Köln |

**Publikationen**

| | |
|---|---|
| 2006 | Krones-Herzig, A., Mesaros, A., Metzger, D., Ziegler, A., Lemke, U., Brüning, JC., Herzig, S. 2006. Signal-dependent control of gluconeogenic key enzyme genes through coactivator-associated arginine methyltransferase 1. *J Biol. Chem*. 281(6):3025-9. |